Synthesis and investigation of smart nanoparticles

by
Yolandé Koen

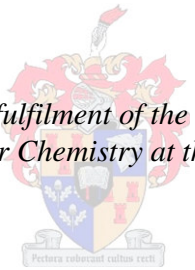

Thesis presented in partial fulfilment of the requirements for the degree Master of Science in Polymer Chemistry at the University of Stellenbosch

Supervisor: Prof R.D. Sanderson
Co-supervisor: Dr. J.B. McLeary
Faculty of Science
Department of Chemistry and Polymer Science

December 2010

DECLARATION

By submitting this dissertation electronically, I declare that the entirety of the work contained therein is my own, original work, and that I have not previously in its entirety or in part submitted it for obtaining any qualification.

December 2010

ABSTRACT

The use of various ‘smart materials’ (briefly meaning materials that respond to a change in their environment) is currently of interest to both academics and industry. The primary aim of the current study was to entrap photochromic (PC) dyes in miniemulsions, as a means to improve their fatigue resistance, thus synthesizing smart nanoparticles. In the coatings industry the use of aqueous systems is becoming a common requirement for health and environmental reasons.

Miniemulsion entrapment allows the direct dispersion of PC dyes into aqueous systems while allowing for the opportunity to tailor-make the host matrix in order to obtain a suitable PC response and improved fatigue resistance.

The optimal instrument set-up required to establish the PC response of films of the so-called smart nanoparticles (i.e. PC miniemulsions) was determined. A UV-Vis instrument with a chip-type UV LED mounted inside for activation of the samples provided PC response results. A tungsten lamp with filter provided deactivation of the samples.

A stable butyl methacrylate (BMA) miniemulsion formulation was established by conducting a design of experiments. A chromene and spironapthoxazine (SNO) PC dye were entrapped in the BMA miniemulsion. A hindered amine light stabiliser (HALS) was also entrapped with the SNO dye in the BMA miniemulsion to further improve the fatigue resistance. The following PC properties of the smart nanoparticles films were evaluated: colourability, thermal decay rate, half-life and fatigue resistance. To compare results with conventional systems, a BMA solution polymer was prepared. The SNO dye and different concentrations of the HALS were mixed with the BMA solution polymer.

In comparison to the SNO smart nanoparticles the chromene smart nanoparticles films had lower colourability, but better fatigue resistance.

Incorporating HALS at levels of 0.5–2% in the BMA miniemulsion with PC dye did not lead to any significant improvement in fatigue resistance, yet films of the BMA solution polymer showed some improvement.

SNO dye incorporated at 1% gave similar colourability in both miniemulsion and in solution polymer, yet the fatigue resistance of the films of the PC miniemulsions was much better.

OPSOMMING

Die gebruik van verskeie “slim materiale’ (kortliks beskryf as materiale wat reageer op `n verandering in hul omgewing) is tans van belang vir beide akademici en die industrie. Die hoofdoel van hierdie studie was om miniemulsietegnologie te gebruik om fotochromiese (FC) kleurstowwe vas te vang, vir die sintese van slim nanopartikels, om sodoende die weerstand teen afgematheid te verbeter. In die verfindustrie word die gebruik van waterbasissisteme meer algemeen weens gesondheids- en omgewingsredes.

Die gebruik van miniemulsie sisteme om materiale vas te vang maak dit moontlik om FC kleurstowwe direk in waterbasissisteme te meng. Die sintese van `n unieke gasheer matriks word benodig om die optimum FC verandering te toon en weerstand teen afgematheid te verbeter.

Om die FC verandering van die sogenaamde slim nanopartikel films (d.w.s. FC miniemulsies) te ondersoek was `n gepaste instrumentele opstelling nodig. Dit is vasgestel dat `n UV-Vis instrument waarin `n skyfie-tipe UV LED gemonteer is vir aktivering van die monsters, reproduseerbare resultate gegee het. Die monsters is gedeaktiveer deur gebruik te maak van `n tungsten lig met ‘n filter.

`n Eksperimentele ontwerp is toegepas om `n stabiele butielmetakrielaat (BMA) miniemulsie formulasie te verkry. `n ‘Chromene’ en ‘spironapthoxazine’ (SNO) FC kleurstof is in die BMA miniemulsie vasgevang tesame met `n verhinderde amien ligstabiliseerder (VALS) om die weerstand teen afgematheid verder te verbeter. Die volgende FC eienskappe van die slim nanopartikels is gemeet: kleurintensiteit, tempo van termiese verwering, half-lewe en weerstand teen afgematheid. `n BMA polimeeroplossing is berei om resultate mee te vergelyk. Die SNO kleurstof en verskillende konsentrasies van die VALS is met die BMA polimeeroplossing gemeng.

In vergelyking met die slim SNO nanopartikels het die intelligente chromene nanopartikelfilms `n swakker kleurintensiteit gehad, maar `n hoër weerstand teen afgematheid.

Die gebruik van 0.5–2% VALS in die BMA miniemulsie met FC kleurstof het minimale verbetering in weerstand teen afgematheid getoon, maar daar was wel `n beduidende verbetering in die geval van films met FC kleurstof in `n BMA polimeeroplossing.

Byvoeging van 1% SNO kleurstof in `n BMA miniemulsie of polimeeroplossing het dieselfde kleurintensiteit gelewer, maar die weerstand teen afgematheid van die FC miniemulsie was baie beter.

ACKNOWLEDGEMENTS

I would like to express my gratitude to the following people and institutions:

My promoter, Prof R. Sanderson, for giving me the opportunity to study under his guidance and all the polymer knowledge he taught me during completion of supplementary honours subjects.

My co-promoter, Dr J.B. McLeary, for the guidance, endless support and encouragement. I truly appreciate everything you did for me.

Plascon, for the financial support through all the years I completed the honours subjects and my MSc.

Victoria Leyland from James Robinson for the generous donation of the photochromic dye used in this study.

Mohammed Jaffer from UCT for TEM images.

Ullie Deutchlander from US Laser Research Institute, for his invaluable assistance with modifying measuring equipment.

To everyone who helped reading and editing the thesis thank you, especially to Dr. C. Terblanche and Dr. M. Hurndall.

To my family and friends, I am forever in dept to you for the support and encouragement you gave me even through times when I could not spend much time with you. I appreciate each one of you!

Over and above, all I would like to give thanks to the Great I AM without whom I would have never made it as far as I have. Toda YHWH.

LIST OF CONTENTS

LIST OF FIGURES

LIST OF TABLES

LIST OF ABBREVIATIONS

AFM	Atomic force microscopy
AIBN	2,2'-azobis(isobutyronitrile)
BA	Butyl acrylate
BMA	Butyl methacrylate
DOE	Design of experiments
FRA	Free radical adduct
HALS	Hindered amine light stabiliser
Irr.	Irradiation
LASER	Light amplification by the stimulated emission of radiation
LEDs	Light-emitting diodes
MA	Methyl acrylate
MC	Merocyanine
MMA	Methyl methacrylate
MW	Molecular weight
MWD	Molecular weight distribution
PC	Photochromic
PiB	Polyisobutadiene
PMMA	Polymethyl methacrylate
PP	Palatinate purple
PS	Particle size
PSt	Polystyrene
PSD	Particle size distribution
PT	Photosol 7-106
RAFT	Reversible addition fragmentation chain transfer
SEC	Size-exclusion chromatography
SDS	Sodium dodecyl sulphate
SO	Spirooxazine
SNO	Spironapthoxazine
SP	Spiropyran
Sty	Styrene
TEM	Transmission electron microscopy
THF	Tetrahydrofuran

T_g	Glass transition temperature
TLC	Thin layer chromatography
TSC	Total solids content
Tungst.	Tungsten
UV	Ultra violet
Vis	Visible

LIST OF SYMBOLS

ϕcol	Colouration quantum yield
c	Concentration
k*f*	Decay constant
$t_{½}$	Half-life
$A_{o(}\lambda)$	Intial absorbance at a specific wavelength
λ_{max}	Maximum wavelength
ε	Molar absorption coefficient
ΔA_0	Maximum absorbance during photostationary state minus the minimum absorbance during the bleached state
l	Pathlength
K	Proportionality constant
Φ	Quantum yield

1 Introduction and objectives

1.1 Introduction

The term '*smart materials'* (like the term '*nanotechnology*') is currently a very common catchword. These materials are used in application areas such as medical, engineering, military and coatings industries. But what does this term actually mean? What qualifies a material as being smart? There is currently great confusion about the term; and it is frequently used as a commercial selling tool without the materials adhering to all the criteria used to define it.[1]

A smart material can be defined as any material that has the intelligence to respond instantaneously in a distinct and predictable manner when it senses a change to its external or internal environment and activates its function according to this change.[2-4] The stimulus causing a response can include changes in stress, strain, light, temperature, chemical composition (including pH), electric field, magnetic field, hydrostatic pressure, different types of radiation, or any combination of these. The activation by stimuli can cause a change in the distribution of stresses and strains, or a change in colour, refractive index or volume. The response that a smart material shows should preferably be reversible upon removal of the stimuli.[1,5]

Indicators responding to a pH change as the stimulus and activating its function through a colour change is a very common use of smart materials.[1] Although smart material activation was first observed in the 1880s, research into this field only commenced in the early 1960s. Extensive research has been carried out into smart materials, but commercialisation has been limited. This is ascribed to high raw material and production costs, and the availability of these materials.[6]

In the medical industry smart materials are used for the controlled release of drugs;[7-9] luminescent sensors, to monitor the health of specimens;[10] 'smart tattoos', as functional implantable glucose sensors;[11] pressure sensitive materials for the detection of underfoot pressure;[12] and breath monitors.[13]

In the engineering industry electric responsive smart materials can improve the movement of robotics[14] and smart cuttings tools where sensitive materials are incorporated to improve process safety in the cutting industry.[15]

The military are equipped with smart skin T-shirts that sense when a soldier has been injured and will monitor the severity of the injuries to make an intelligent decision to stabilise the injury or signal the urgency for a medical team to react.[3]

Encyclopaedia Britannica defines a *coating* as "any mixture of film-forming materials plus pigments, solvents, and other additives, which, when applied to a surface and cured or dried, yields a thin film that is functional and often decorative". The first *smart coating* was studied in 1984 by Svensson and GranqVist[16] for application in electrochromic smart windows. Since then many investigations to produce smart windows have been undertaken[16-25], and many patents have been issued.[1] Other common uses for smart coatings are to produce self-cleaning coatings,[26]anti-corrosive coatings,[27-29]self-healing coatings,[4-5] antibacterial coatings,[30]high temperature resistant coatings,[30-32] and light or temperature sensitive coatings.[4,33-40] As is evident from the applications, many fascinating uses for smart coatings have been found over the last few years.

The focus of the present study is on smart coatings, and in particular coatings that are light sensitive. Materials that display this property of light sensitivity are generally termed photochromic (PC).

1.2 Photochromic materials

T.L. Phipson made one of the first observations of the PC phenomenon in 1881 when he saw that a black gatepost turned white during the night. The black coating that the gatepost was painted with contained a zinc based PC pigment (comparable to the compound now known as lithopone).[41]

Today PC coatings are used for various optical-transmission materials, such as ophthalmic lenses and smart windows, on packaging and labels, for novelty items (toys, clothes, mobile phone covers), and for optical data storage, to name but a few.[42-44]

Many inorganic and organic compounds exhibit the ability to respond to exposure to light.[41,45] Inorganic materials exhibiting PC properties include metal oxides, alkaline earth metals, mercury compounds, and transition metal compounds. Although inorganic PC compounds offer high sensitivity towards colouring and discolouration, as well as superior stability against photodegradation, they are very dull and provide a very limited colour range.[46] Some of these inorganic materials are also very difficult to use in combination with any other materials besides inorganic glass.[47]

Organic PC dyes provide the freedom to formulate to almost any colour imaginable as they provide an extensive variety of hues. They are compatible with a broad range of resins and other organic compounds, making them useful for a multitude of applications. Organic PC dyes do however have limitations due to aggregation effects, thermal instability and photochemical degradation.[48] They tend to loose colour intensity upon repeated intermittent exposure to light (termed cyclability) or continuous exposure to light (termed fatigue) as the irreversible formation of uncoloured or weakly coloured species increases.[49] To overcome these limitations PC dyes can be formulated with additives, such as hindered amine light stabilisers (HALS), antioxidants, ultra violet (UV) absorbers, singlet oxygen quenchers, thermal stabilisers and clays as stabilisers for the higher-energy coloured form species, and by excluding oxygen from the system (e.g. via entrapment into polymer particles) to increase the PC dye lifetime and stability.[46,49-50]

PC dyes are not compatible with aqueous systems when directly dispersed into a polymeric binder. However, entrapment in emulsions creates the potential to incorporate these dyes into aqueous systems, thereby opening a wide range of new application possibilities.[51]

1.3 Objectives

The objectives of this study were the following:

1. Carry out a literature study to identify the most widely used PC compounds, the current concerns associated with these compounds, and possible means of solving the problems associated with these concerns.
2. Establish appropriate measuring techniques, and the reproducibility of these measurements, to determine the properties of the PC compounds.
3. Establish a stable miniemulsion formulation suitable to entrap the PC dyes.

4. Entrap the selected PC dyes into the identified miniemulsion and evaluate the PC properties of films prepared from the samples.
5. Investigate the use of light stabilising additives in the miniemulsions with PC compounds to improve the fatigue resistance of the dyes.
6. Compare the fatigue resistance of films of the PC miniemulsions, with and without light stabilising additive, with films of a conventional system where dyes and additives are mixed into a solution polymer.

1.4 Layout of thesis

Chapter 1 – Introduction

In chapter one a general introduction to smart materials, and specifically PC materials, is given, and the objectives of the study are stated.

Chapter 2 – Literature review

Chapter two will explain the concept of photochromism in more detail. The different organic chemical families displaying PC properties will be identified and some limitations in their properties discussed. A historical overview of different means investigated to increase the PC lifetime of organic compounds in various systems will be given. General terminologies used to characterise PC properties will be defined, and various applicable analytical techniques, instrumental set-ups and light sources used to evaluate PC properties will be reviewed.

Chapter 3 – Experimental set-ups required to characterise photochromic materials

Various sample preparation techniques for obtaining optically clear and uniform latex films (for measuring the PC response) are described. The evaluation of various experimental set-ups, in terms of activation and deactivation sources, to measure the PC response is described. The repeatability of measurements is also reported.

Chapter 4 – Synthesis and evaluation of smart nanoparticles

The stability and physical properties of a butyl methacrylate (BMA) miniemulsion system to be used to entrap the PC compound in was studied in terms of varying the solids content and initiator and surfactant concentrations, to identify an optimum starting formulation. A process to entrap the PC compounds and an additive into the identified optimised

miniemulsion is described. The resulting smart nanoparticles are evaluated for their PC efficiency and lifetime, and compared to that of the case where a dye and additive are dispersed in a solution polymer.

Chapter 5 – Conclusions

In the final chapter the main findings from the previous chapters are summarised and conclusions are made to the original objectives. Recommendations are made for future studies.

References

(1) Harvey, J. A. In *Mechanical engineers' handbook*; 3rd ed.; Kutz, M., Ed.; John Wiley & Sons: New Jersey, 2006, 418.
(2) Addington, D. M.; Schodek, D. L. *Smart Materials and New Technologies for the Architecture and Design Professions*; Elsevier: Amsterdam; London, 2005.
(3) Akhras, G. *Canadian Military Journal* **2000**, *1*, 25.
(4) Challener, C. *Journal of Coatings Technology* **2008**, *5*, 38.
(5) Feng, W.; Patel, S. H.; Young, M.-Y.; Zunino III, J. L.; Xanthos, M. *Advances in Polymer Technology* **2007**, *26*, 1.
(6) Ruffin, P. B. *Paper presented at the conference:* Quantum sensing and nanophotonic devices, San Jose, CA, USA, 2004; p 177.
(7) Liu, S.; Zhang, Z.; Han, M.-Y. *Advanced Materials* **2005**, *17*, 1862.
(8) Cui, F.; He, C.; Yin, L.; Qian, F.; He, M. et al. *Biomacromolecules* **2007**, *8*, 2845.
(9) Wienforth, F.; Landrock, A.; Schindler, C.; Siegert, J.; Kirch, W. *Journal of Clinical Pharmacology* **2007**, *47*, 653.
(10) Bencic, T. J.; Eldridge, J. I. *Paper presented at the conference:* Advanced sensor technologies for nondestructive evaluation and structural health monitoring, San Diego, CA, USA, 2005; p 88.
(11) Brown, J. Q.; Srivastava, R.; McShane, M. J. *Biosensors and Bioelectronics* **2005**, *21*, 212.
(12) Brady, S.; Lau, K. T.; Megill, W.; Wallace, G. G.; Diamond, D. *Synthetic Metals* **2005**, *154*, 25.
(13) Brady, S.; Diamond, D.; Lau, K.-T. *Sensors and Actuators A: Physical* **2005**, *119*, 398.
(14) Rasmussen, L. *Paper presented at the conference:* Electroactive polymer actuators and devices, San Diego, California, USA, 2007; p 652423.
(15) Luthje, H.; Bandorf, R.; Biehl, S.; Stint, B. *Sensors and Actuators A: Physical* **2004**, *116*, 133.
(16) Svensson, J. S. E. M.; Granqvist, C. G. *Paper presented at the conference:* The International Society for Optical Engineering **1984**, 30.
(17) Yi, X.; Li, Y.; Chen, S.; Wang, S.; Lai, J. et al. *International Journal of Nanoscience* **2005**, *4*, 99.
(18) Li, X.; Chen, S.; Wang, S.; Lai, J.; Chen, C. et al. *Paper presented at the conference:* Smart Materials III, Sydney, Australia, 2004; p 256.
(19) Ke, X.; Yan, X.; Song, S.; Li, D.; Yang, J. J. et al. *Optical Materials* **2007**, *29*, 1375.
(20) Nunes, S. C.; de Zea Bermudez, V.; Silva, M. M.; Smith, M. J.; Ostrovskii, D. et al. *Journal of Material Chemistry* **2007**, *17*, 4239.
(21) Agnihotry, S.; Saxena, T.; Deepa, M.; Verma, A.; Swati, S. et al. *Ionics* **2004**, *10*, 226.
(22) Vinodh, M. S.; Mohan, S.; Subaskar, P.; Bhojraj, H.; Narayanamurthy, H. et al. *Paper presented at the conference:* Smart Materials, Structures, and Systems, 2003; p 780.

(23) Manning, T. D.; Parkin, I. P.; Clark, R. J. H.; Sheel, D.; Pemble, M. E. et al. *Journal of Materials Chemistry* **2002**, *12*, 2936.
(24) Perennes, F.; Twardowski, P.; Gesbert, D.; Meyrueis, P.; Co., E. A. et al. *Paper presented at the conference:* The International Society for Optical Engineering, 1992; p 368.
(25) Babulanam, S. M.; Estrada, W.; Hakim, M. O.; Yatsuya, S.; Andersson, A. M. et al. *Paper presented at the conference:* The International Society for Optical Engineering **1987**, 64.
(26) M. Thieme, R. F., S. Schmidt, F. Simon, A. Hennig, H. Worch, K. Lunkwitz, D. Scharnweber, *Advanced Engineering Materials* **2001**, *3*, 691.
(27) Riaz, U.; Ashraf, S. M.; Ahmad, S. *Progress in Organic Coatings* **2007**, *59*, 138.
(28) Pereira da Silva, J. E.; Cordoba de Torresi, S. I.; Torresi, R. M. *Corrosion Science* **2005**, *47*, 811.
(29) Kendig, M.; Hon, M. *Corrosion* **2004**, *60*, 1024.
(30) Bohannon, J. *Science* **2005**, *309*, 376.
(31) Nicholls, J. *Journal of the Minerals, Metals and Materials Society* **2000**, *52*, 28.
(32) Hosoda, H.; Miyazaki, S.; Hanada, S. *Intermetallics* **2000**, *8*, 1081.
(33) Ma, Y.; Zhu, B.; Wu, K. *Journal of Coatings Technology* **2000**, *69*, 67.
(34) Ma, Y. P.; Xu, J. Y.; Zhu, B. R.; Wu, K. R. *Journal of Coatings Technology* **2003**, *75*, 43.
(35) Lucht, B. L.; Euler, W. B. *FATIPEC Congress* **2004**, *2*, 557.
(36) Higgins, S. *Chemica Oggi* **2003**, *1*, 63.
(37) Postle, S. R.; Kingston, S. B. US 4 444 939, 1984.
(38) Crano, J. C.; Flood, T.; Knowles, D.; Kumar, A.; Van Gemert, B. *Pure and Applied Chemistry* **1996**, *68*, 1395.
(39) Klukowska, A.; Posset, U.; Schottner, G.; Wis, M. L.; Salemi-Delvaux, C. et al. *Material Science* **2002**, *20*, 95.
(40) Parry, H.; Corns, N.; Towns, A. New uses for photochromics; James Robinson; 20 September 2004; http://www.james-robinson.ltd.uk.
(41) Brown, G. H. *Photochromism*; John Wiley & Sons: Canada, 1971.
(42) Avellaneda, C. O.; Bulhoes, L. *Solid State Ionics* **2003**, *165*, 117.
(43) McArdle, C. B. *Applied Photochromic Polymer Systems*; Blackie & Son: London, 1992.
(44) Zimehl, R.; Textor, T.; Bahners, T.; Schollmeyer, E. *Progress in Colloid and Polymer Science* **2004**, *125*, 49.
(45) Balcomb, J. D. *Passive solar buildings*; MIT Press: Cambridge, Mass., 1992.
(46) Mennig, M.; Fries, K.; Lindenstruth, M.; Schmidt, H. *Thin Solid Films* **1999**, *351*, 230.
(47) Kamada, M.; Suefuku, S. US 5 208 132, 1993.
(48) Arunkumar, E., Forbes, C.C., Smith, B.D. *European Journal of Organic Chemistry* **2005**, *2005*, 4051.
(49) Reid, P. I.; Waters, B. R. GB 4503177, 1985.
(50) Crano, J. C.; Robert, J. G. *Organic Photochromic and Thermochromic Compounds*; Marcel Dekker: New York, 1999.
(51) Han, M.; Lee, E.; Kim, E. *Optical Materials* **2002**, 579.

2 Literature review

2.1 The concept of photochromism

The word photochromism originates from the Greek words "phos" meaning "light" and "chroma" meaning colour.[1] Photochromism can be defined as a reversible transformation of chemical species A (also known as the mother species) into its isomer species B (also known as the daughter species), induced in one or both directions by absorption of electromagnetic radiation between the two forms. Species A and B will have different energy absorption spectra and energy content (Figure 2.1).[2-3]

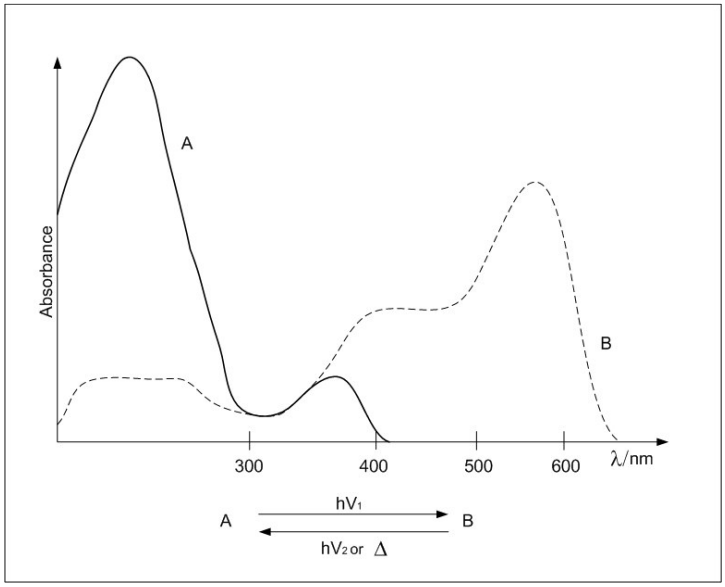

Figure 2.1. Photochromism of a unimolecular system.[4]

Species A is defined as the thermally stable species. It is usually colourless or a pale yellow and is activated at lower wavelengths, typically in the UV region (300–400nm), although it could also be in the visible region (400–700nm), to form species B. The latter is generally coloured and has at least one absorption band appearing at a longer wavelength than the bands of species A.[2,5] This is known as positive photochromism, and the reverse reaction can either occur thermally (recognised as Type T photochromism) or photochemically (know as Type P photochromism), or as a combination of the two. Conversions where λ_{max} of species A is larger than λ_{max} of species B are known as negative or inverse photochromism.[4]

The most common organic PC systems involve unimolecular reactions. A system that, for example, involves a photocycloaddition reaction or an electron transfer process, as shown in Figure 2.2, is referred to as bimolecular.[4,6]

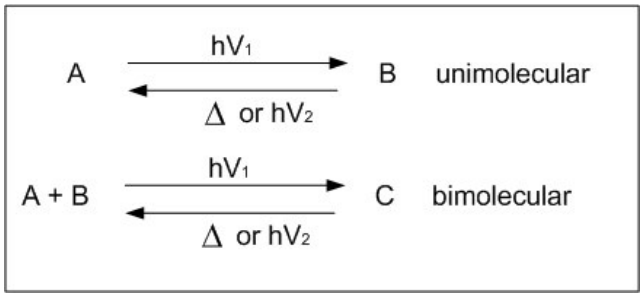

Figure 2.2. Unimolecular and bimolecular photochromism. [3]

In a unimolecular PC system the concentration of species B (the coloured species) will be low relative to the concentration of species A. As the sample is irradiated (t_1) the concentration of species B will increase until it reaches the photostationary state (i.e. where equilibrium between A →B is reached). When the excitation irradiation is switched off (t_2) species B will revert back to species A. The rate will depend on the chemical structure of the dye, the matrix into which it is incorporated, and the temperature.[7]

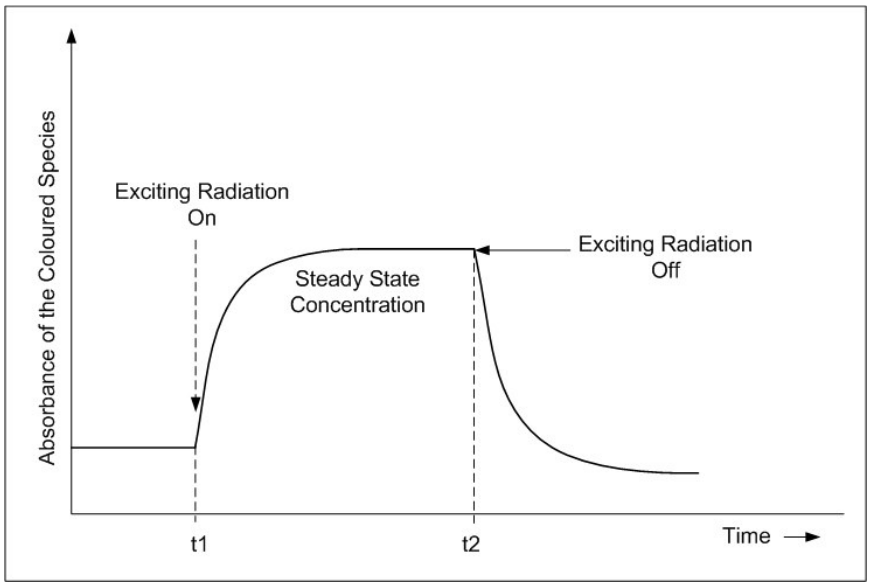

Figure 2.3. PC dye absorbance during activation and deactivation.[8]

PC properties can be affected by polar groups on the dye structure, complexation and protonation. Interactions with the dye and host matrix reduce the dye mobility, and

decrease the thermal decolouration rate. Polar groups on the dye can form covalent bonds with the matrix, stabilising the open form of the dye and causing slower fading kinetics than would otherwise be observed if the dye was only physically entrapped.[7] The effect of the matrix is most significant between solution and polymer phases where differences in free volume are the most pronounced. The open and closed forms of a PC dye can differ in polarity, hence the polarity of the matrix can preferentially stabilise either the open or the closed form of the dye.[9] In the case of the spirooxazines (SOs) the closed form is less polar than the open merocyanine (MC) form and will be favoured in a less polar environment.[7]

Temperature plays an important role in photokinetics as many PC compounds are also thermochromic. In polymer systems temperature plays an important role in the mobility of the matrix.[9] Properties such as chain mobility (i.e. rigidity), free volume, polymer polarity and crystallinity are important when evaluating photokinetics in a polymer matrix.[10] Rigid polymer matrices with high glass transition temperature (T_g) values (polymethyl methacrylate, PMMA, 175°C) provide more steric hindrance than soft polymer matrices with lower T_g values (polyisobutadiene, PiB, 76°C), leading to a decrease in the colouration and fading rates.[11] In general, polymers used above their T_g act as solutions where mobility is high, displaying single exponential kinetics. Below T_g steric hindrance greatly influence mobility, resulting in more complex kinetics. In a similar fashion a polymer with higher crystallinity than another polymer with similar polarity (such as Nylon-6 vs. polyethylene terephthalate) can also cause steric hindrance and a decrease in kinetic rates. [9]

The spectrum of the coloured species is sensitive to environmental factors such as temperature, solvent and concentration,[6] which can cause a change in the position, shape and intensity of absorption bands.[9] In general, as the temperature decreases from room temperature to temperatures well below room temperature the equilibrium between the various coloured species is changed and longer wavelength bands are observed at $\lambda_{max.}$ The influence of the solvent on the shift of the MC band specifically depends on the nature of the oxygen in the MC group to form the ketone-like or zwitterionic structure. If the oxygen forms the ketone-like structure the visible λ_{max} will shift to shorter wavelengths (i.e. red), the extinction coefficient will decrease, and the half-width will increase as the polarity of the solvent increases, changing the equilibrium between the two forms, i.e. positive solvatochromism. If the oxygen is in the ionic form the opposite occurs, resulting in

negative solvatochromism.[6,9] Solvatochromism is only present in solutions. The polarity of polymer matrices also affects kinetics. The PC process is non-destructive but the closed form is not always fully converted to the open form. As samples switch between the open and closed forms side reactions can occur. These side reactions cause the formation of products that are unable to return to the closed ring form. Fatigue resistance depends on the nature of the PC dye's structure.[1,9] This is further discussed in Section 2.2.

2.2 Families of organic photochromic compounds

Table 2.1 depicts the major families of organic PC compounds and their respective open and closed forms. The chemical processes involved to convert the majority of species to their respective open forms can be described by six mechanisms: (1) heterocyclic/homolytic bond cleavage, (2) cis-trans-isomerisation, (3) valence tautomerism, (4) electron transfer systems, (5) pericyclic reactions and (6) triplet-triplet absorption.[4]

Table 2.1. The major families of organic PC compounds

Closed form	**Activation/ deactivation**	**Open form(s)**
1. Spiropyrans		
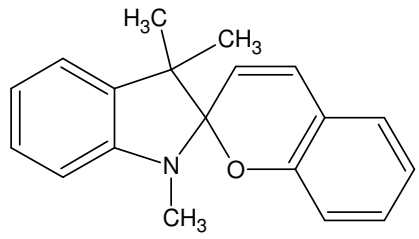	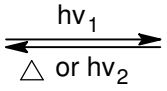	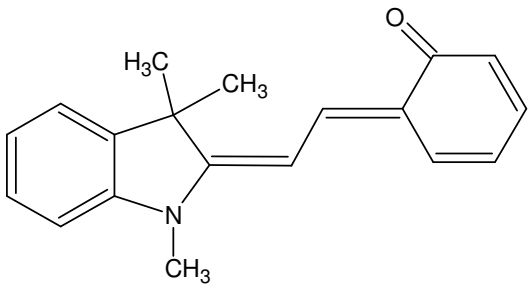
2. Spirooxazines		
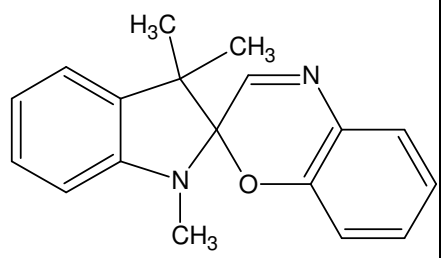	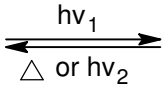	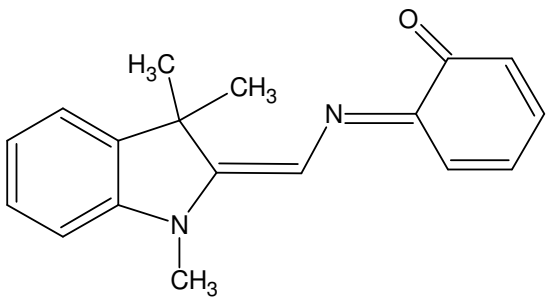

Closed form	**Activation/ deactivation**	**Open form(s)**
3. Chromenes		
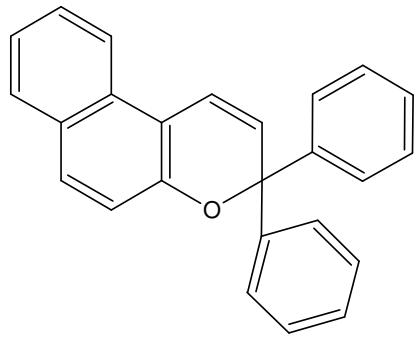	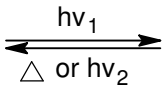	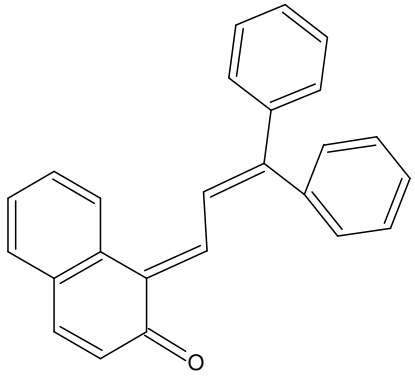
4. Fulgides and fulgimides		
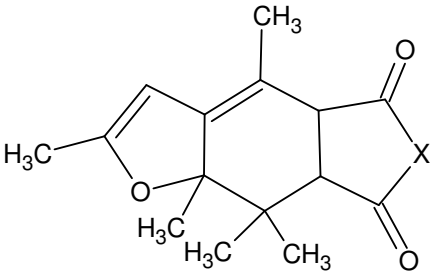	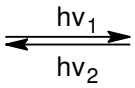	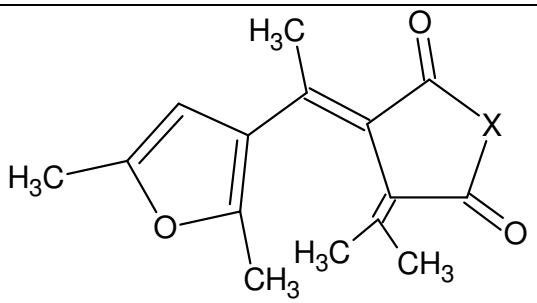
5. Diarylethene and related compounds		
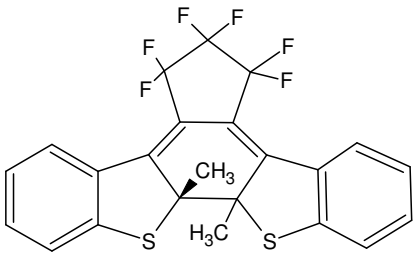	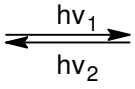	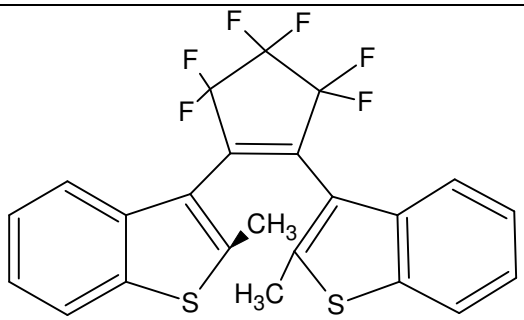
6. Spirodihydro-indolizines		
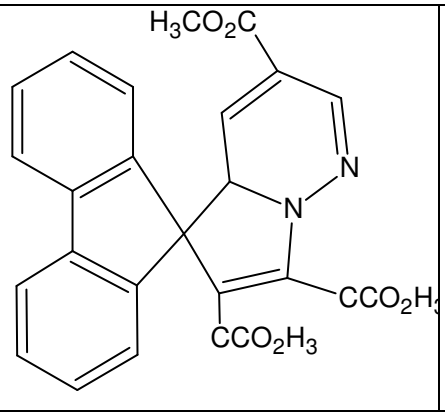	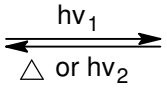	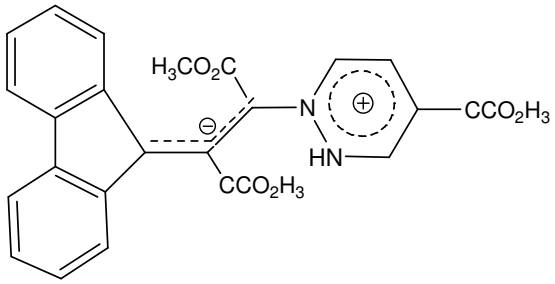

Closed form	**Activation/ deactivation**	**Open form(s)**
7. Azo compounds		
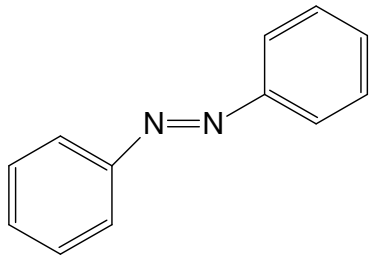	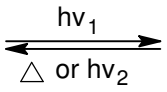	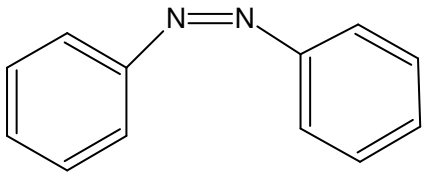
8. Polycylic aromatic compounds		
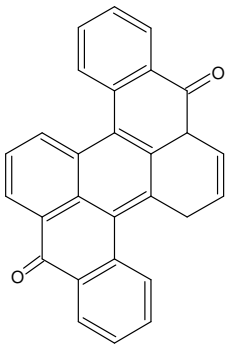	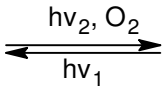	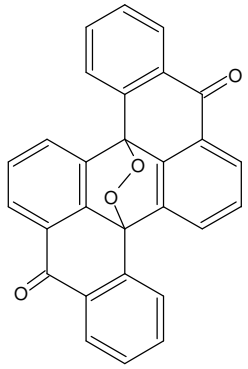
9. Anils and related compounds		
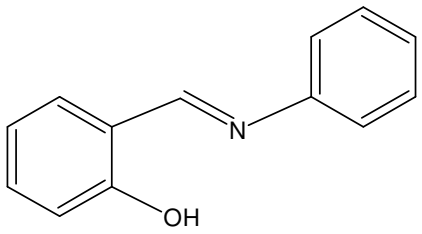	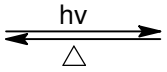	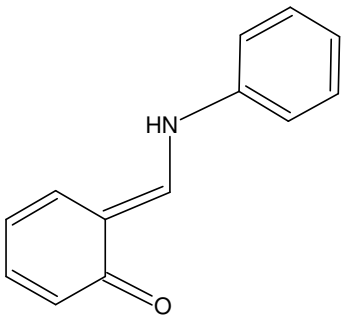
10. Polycyclic quinones		
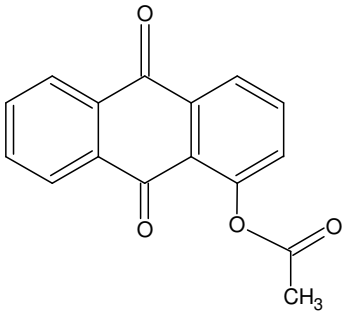	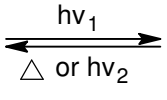	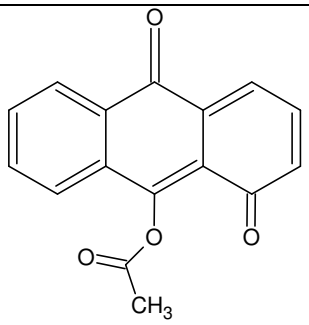

Closed form	Activation/ deactivation	Open form(s)
11. Perimidinespirocyclohexadienones		
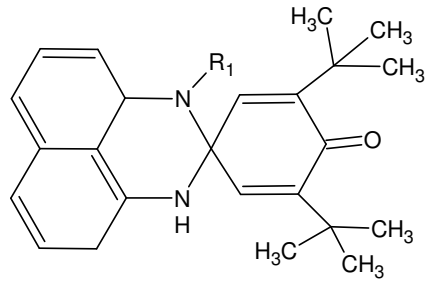	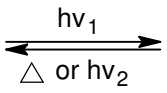	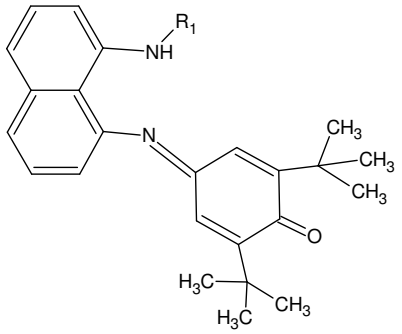
12. Viologens		
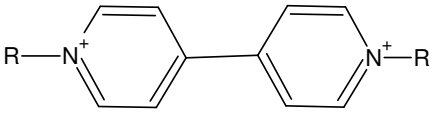	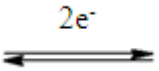	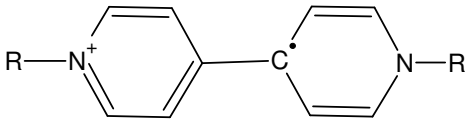
13. Trimethanes		
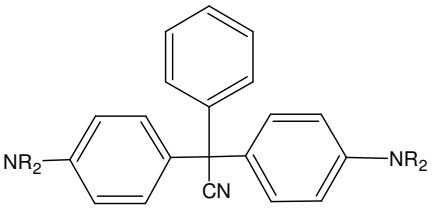	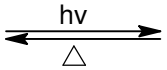	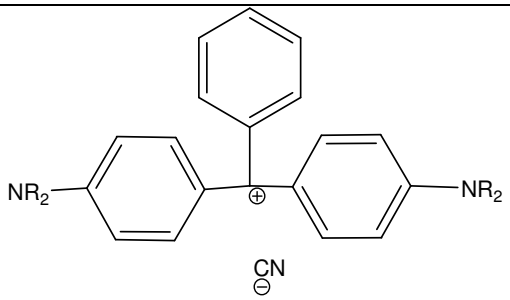

Sources: References 1, 4 and 12.

Of the large variety of organic PC compounds of different classes, an indolino spironapthoxazine (SNO) PC compound was used in the first commercial plastic PC lens in 1982, under the tradename Photolite™.[13] Several references indicate that SO compounds outperform most PC compounds from a fatigue resistance point of view and that they also have high photoresponse rates, high colourability, good optical durability and good photostability.[13-17] SOs are very similar in structure to spiropyrans (SPs), the only difference being the replacement of the carbon in the pyran ring with a nitrogen to form an oxazine ring. This significantly improves resistance to photodegradation,[9,11] which is a very important property to consider for industrial applications; poor fatigue resistance is often the main problem faced during the commercialisation of PC systems.[18-19]

2.2.1 Formation of the open merocyanine form

SOs like SPs undergo thermal and photochemical reversible transformations from the closed SO to the open MC form.[7,20-21] SO compounds undergo heterolytic cleavage of the CO_{spiro}–bond, which has been reported to occur in approximately 700fs. Subsequently, the intermediate product 'X' is believed to form in the orthogonal plane of the parent species. The intermediate product 'X' has a lifetime of approximately 470fs, after which isomerisation to the coplanar form takes place to produce the metastable MC.[22] MCs absorb in the visible region of the light spectrum at around 600nm due to their highly conjugated π-electron cloud. In SOs the change is observed from a colourless (or weakly coloured) solution to an intense violet solution.[23-24] The two benzene rings in the structure of the SO form are in the orthogonal plane and in the MC form coplanar. This change in configuration from the SO to MC form requires some space for movement around the pi-orbitals, and is referred to as the sweep volume. In order for the forwards or backwards reaction to take place without any restriction, the free volume in the system needs to be greater than the sweep volume required. If the free volume is smaller than the sweep volume, the kinetics of the isomerisation will be retarded. SO will thus not easily undergo isomerisation reactions in strictly constrained environments since it requires a certain degree of available free volume.[25]

Eight different isomers of the MC form are theoretically possible. The isomers that are in a cis configuration around the central β-bond on the methine bridge are however high energy isomers and therefore not stable. The trans isomers represent the lower energy form and are subsequently more stable.[15,25] From the four possible trans configurations it is the TTC and CTC isomers (see Figure 2.4) that are the most stable due to electrostatic interactions between the central hydrogen and the carbonyl oxygen. The TTT and the CTT forms are less stable due to H–H repulsion between the central hydrogen and the closest hydrogen on the naphthalene ring.[15]

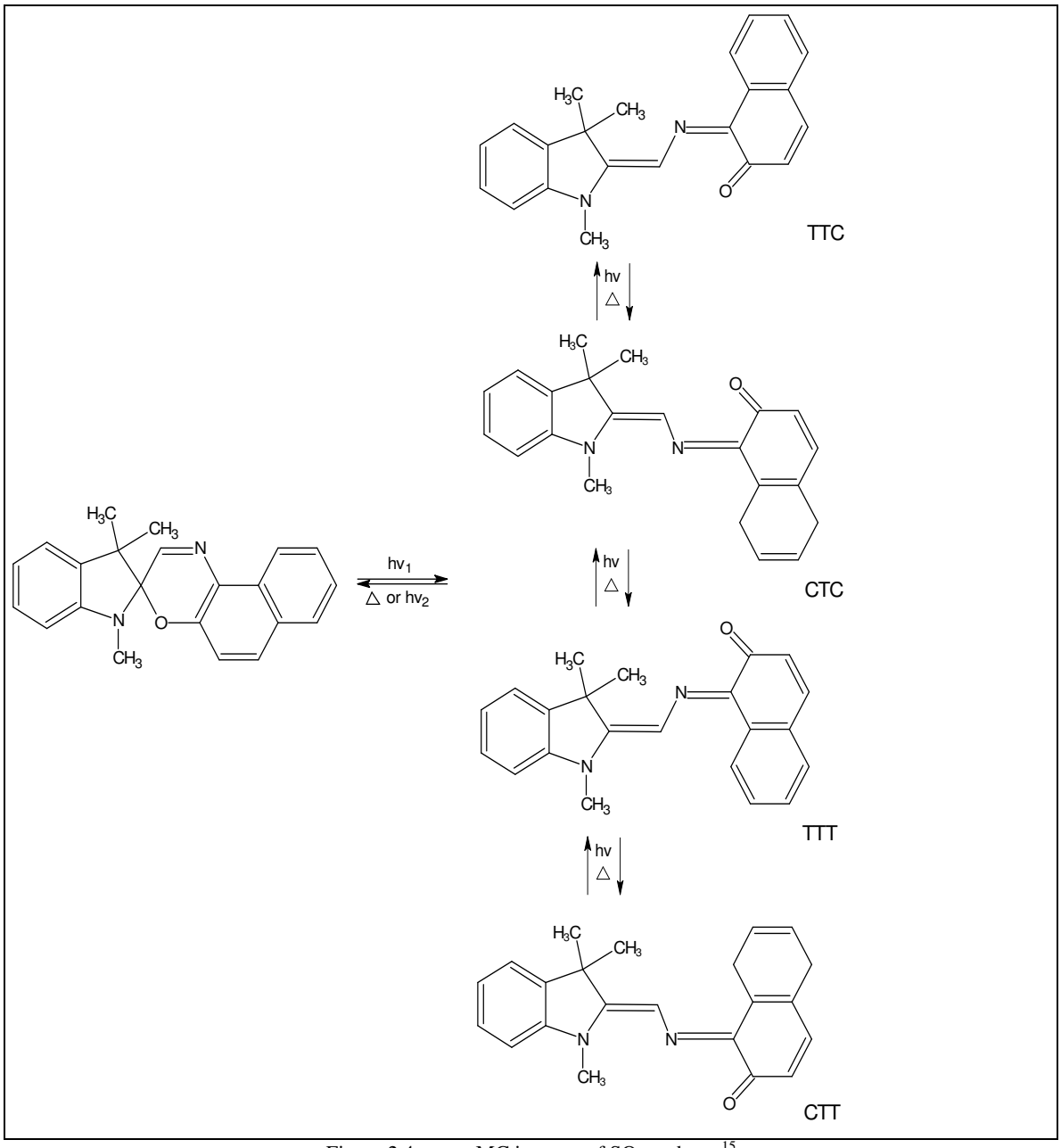

Figure 2.4. MC isomers of SO products.[15]

2.2.2 Decrease of the photochromic dye lifetime

There are two main pathways by which SO products can be degraded, namely oxidation and radical attack (see Figure 2.5). Both degradation pathways lead to the formation of highly coloured red species that do not show PC activity. Oxidative degradation can even take place in matrices that are oxygen deficient, such as polymer matrices. The open MC form is readily attacked by free radicals on the $C_5'=C_6'$ double bond at position $6'$, to form free radical adducts (FRAs) that cannot return to the ring closed SO form.[2,9,26-27]

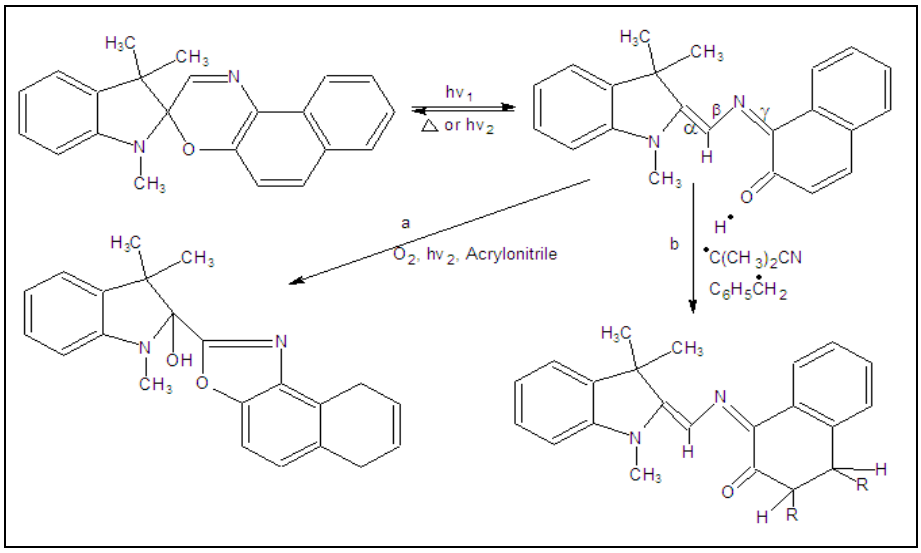

Figure 2.5. Degradation processes in SO compounds (a) via oxidation and (b) via radical attack.[26]

2.3 Improvements of photochromic dye properties

In the next section various means used in literature to improve the properties of PC dyes will be reviewed. This include modification of the PC dye structure, dispersion in polymer matrices, copolymerisation with polymers, incorporation into sol-gels, entrapment in polymeric dispersions (macroemulsions and miniemulsions specifically) and the incorporation of additives.

2.3.1 Modification of the photochromic dye structure

PC fatigue resistance is highly dependent on the chemical structure of the PC dye. It has already been established that SO displays the highest degree of fatigue resistance compared to other PC compounds. However, by modifying the dye structure further improvements can be made.[13] Li et al.[12] describe the connection of bis-spiro compounds (SP and SNO) with a phosphoryl group (see example in Figure 2.6), which can act as an antioxidant and photostabiliser. The fatigue resistance of the bis-spiro groups connected with a phosphoryl group was studied in methanol. Results showed that the bis-spiro compounds are more fatigue resistant than the parent molecules, possibly due to the intramolecular interactions of the two MC groups on the molecules.[12]

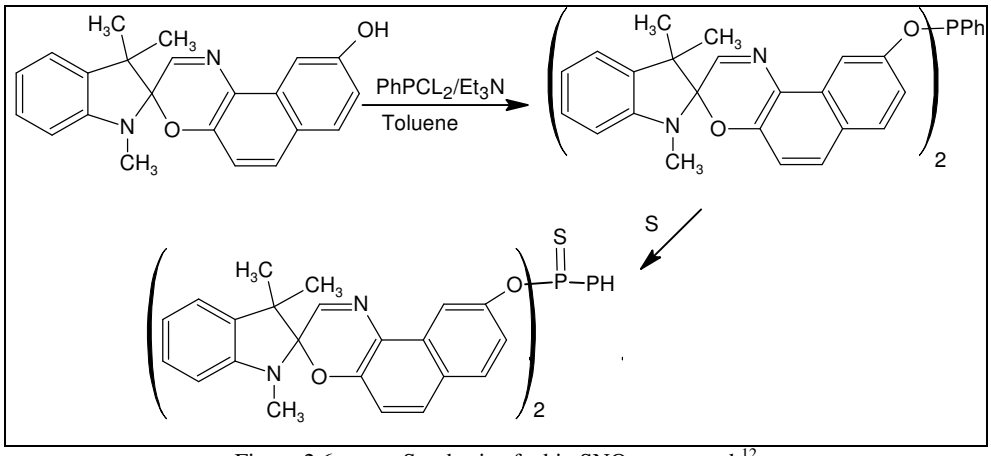

Figure 2.6. Synthesis of a bis-SNO compound.[12]

2.3.2 Dispersion in polymer matrices

Fatigue resistance can be related to the ability of the PC dyes to move within the host matrix. The higher the free volume of the matrix the more movement is possible and the faster the degradation. The matrix properties required to minimise fatigue are therefore in contradiction with the requirement not to influence the PC response of the dye.[28-29] Sriprom et al.[30] confirm that the switching kinetics for the lower T_g PMA are much faster than for higher T_g PMMA. Polymer matrices with higher free volumes are preferred in order to minimise the effect on PC kinetics while fatigue resistance is improved by the incorporation of additives.[28] Rauzy et al.[31] observed that an increase of a PC SP compound up to a certain concentration decreased the T_g of the PMMA matrix. The dye acts as an impurity to the system and functions as a plasticiser up to a certain concentration. The same effect is evident with SO compounds, an increased dye concentration should therefore increase the PC response rate.[31]

2.3.3 Copolymerisation with polymers

PC monomers can be covalently bound to polymer chains by copolymerisation.[28] Attachment to the polymer matrix has the advantage over compounds simply dispersed in a polymer matrix because bonding prevents leaching of the photochrome which would otherwise lead to a stepwise reduction in PC properties. The copolymerised compound allows better compatibility with the polymer matrix, to prevent separation of the phases. The PC kinetics can be fine tuned by modifications of the copolymerised dye polymer structure[30,32]. Lyubimov et al.[32] showed that copolymerised SP molecules have bi-

exponential decolouration kinetics in comparison to the linear kinetics of dye dispersed into a matrix. Sriprom et al.[30] copolymerised SP compounds with methyl methacrylate (MMA) and methyl acrylate (MA) using the reversible addition fragmentation chain transfer (RAFT) process and also produced block copolymers, PMMA-b-poly (MA-co-SP) and polystyrene (PSt)-b-poly (MA-co-SP). In this study the covalent bonding of SP compounds decreased the fading rates compared to when SP was mixed in the specific polymer matrices. The block copolymers allowed fine tuning of the PC switching via the MA moiety, while including a harder matrix via the PMMA and PSt blocks. Similar results were obtained by Such et al.[33] for SO copolymerised with n-butyl acrylate (n-BA) and incorporated into a rigid matrix, because the lower T_g moiety allows for fast switching kinetics.

2.3.4 Incorporation into sol-gels

Sol-gels are porous inorganic–organic hybrid materials that offer tailormade microenvironments in terms of the matrices' flexibility and polarity, using processing temperatures as low as room temperature.[8,34] Sol-gels offer an advantage over polymeric encapsulation/entrapment because of the limited stability of polymers upon UV irradiation.[35] By incorporating PC dyes into sol-gel matrices self-aggregation, crystallisation, diffusion and interaction with degradation products are prevented. This leads to enhanced colourability and greater stabilisation of the PC dye.[7,36] Numerous articles report the synthesis of various sol-gel compositions.[7,35-40] Dyes can either be physically entrapped or covalently bound in sol-gel matrices. The latter causes a slower PC response due to restricted mobility of the moiety, but improved fatigue resistance. Faster PC responses are observed when dyes are only physically entrapped in soft, non-polar matrices.[7] Improvements in colourability and photostability in sol-gel matrices by the incorporation of fluoroalkylsilane and bisphenol A as additives have been reported.[41]

2.3.5 Entrapment in polymeric dispersions

Various organic and inorganic materials have been entrapped to obtain lower viscosity dispersions.[42-43] Other hydrophobic materials have also been incorporated since they are not compatible with aqueous systems and can subsequently not be incorporated directly

into polymeric binders.[44] These materials include oil-soluble dyes, PC dyes, titanium dioxide, magnetite particles, carbon black, and many others.[45]

The reduction of volatile organic compounds is gaining increased attention and in the coatings industry the use of aqueous systems (as opposed to solvent-based systems) is becoming a general requirement for health and environmental reasons.[46] Miniemulsion encapsulation allows the direct dispersion of PC compounds into aqueous systems while allowing the opportunity to tailor-make the host matrix to obtain a suitable PC response and improve fatigue resistance.[47] The same restrictions for dispersing dyes into polymer matrices apply to entrapment with regards to suitable host matrices in terms of free volume. Rigid matrices such as polyesters are not suitable. Fatigue resistance can also be improved in these systems by incorporating additives.[28]

Han et al.[47] studied the miniemulsion entrapment of diarylethenes in PSt. At high dye concentrations in a polymer these dyes can form aggregates, giving an opaque film and reducing colour efficiency. By microentrapment, aggregation is prevented and higher dye loadings are possible, which improves PC efficiency. Han et al. experimented with different types of initiators and found that the initiator had a large influence on the morphology of the particles and their ability to encapsulate the dye. A non-ionic initiator 2,2'-azobis(isobutyronitrile) (AIBN) was reported to deliver spherical entrapped nanoparticles.[47]

The successful preparation of PMMA microspheres containing SO,[48] MMA miniemulsions containing functionalised SP,[49] 2,2'-n-isopropyl acrylamide shell and styrene (Sty) core emulsion particles with SP entrapped in the core,[50] and a crosslinked polypyrrole shell with a linear polypyrrole core entrapping a pyrene dye[51] have been reported. In these studies it was mainly the successful switching PC response of the entrapped dyes that was determined.

To the best of the author’s knowledge there are no reports on the fatigue resistance of miniemulsion entapped PC dyes.

2.3.5.1 Conventional and miniemulsion polymerisation

Emulsion polymerisation is widely used to disperse pigments in aqueous systems. There are different ways to synthesize these aqueous dispersions, such as macroemulsion polymerisation (i.e. conventional emulsion polymerisation), microemulsion polymerisation and miniemulsion polymerisation. The different systems vary in their formulations, kinetics and the mechanistic process.[52]

Figure 2.7 illustrates the different mechanistic processes involved in conventional and miniemulsion polymerisation.

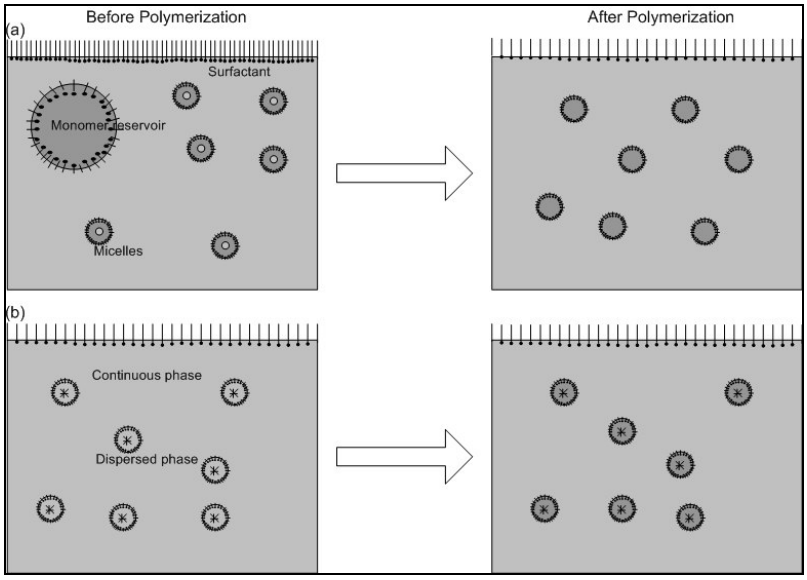

Figure 2.7. Comparison of (a) conventional emulsion and (b) miniemulsion polymerisation.[53]

In conventional emulsion polymerisation surfactant stabilised monomer reservoirs (typically 5−10microns) coexist with surfactant micelles. The initiator forms radicals which nucleate particles within the monomer-swollen micelles. Monomer diffuses through the continuous phase to the particles where it is polymerised. Particles grow until all monomer reservoirs are depleted, and some shrinkage occurs after growth. Particles larger than 100nm are typically formed.[53] The particles size depends on kinetic parameters, including temperature, initiator concentration, nucleation rate and stability of the nanoparticles.[53-54]

Unlike conventional emulsion polymerisation, the latex particle size (PS) in a miniemulsion corresponds to the initial size of the monomer droplet.[54] This is very useful

for encapsulation/entrapment processes which require homogeneous, stable monomer droplets, which are transformed into the final latex particle without much kinetic exchange.[53] With miniemulsion polymerisation direct oil-in-water emulsification is obtained by applying high shear to the heterogeneous monomer and aqueous phase.[55] The particle size distribution (PSD) initially established is a function of the sonication applied. After efficient dispersion the PS is affected by the amount of monomer and water, the monomer solubility and the surfactant concentration.[53] In miniemulsion polymerisation monomer can diffuse from unnucleated droplets to nucleated droplets. This process is called Ostwald ripening, which occurs due to droplet pressure differences between unnucleated droplets and nucleated droplets.

To minimise Ostwald ripening an ultra-hydrophobe can be incorporated into the monomer phase to obtain similar effective pressure (i.e. osmotic pressure combats droplet pressure) in all the monomer droplets, hindering the monomer from diffusing.[53] Hexadecane is used as a model hydrophobe compound which is homogeneously dispersed in the monomer droplets and is incorporated at a minimum molar ratio of 1.25 to the monomer content.[53] The amount of hydrophobe does not affect the PS, but only the pressure difference between the droplet and osmotic pressure.[53] Hydrophobic dyes, plasticisers or other additives are also useful as hydrophobic compounds to prevent Ostwald ripening.[53] Standard practice in colloidal stabilisation is to incorporate the correct surfactant type and concentration, and this is also applicable in miniemulsion polymerisation. Using adequate costabiliser and homogenisation, the steady state of the miniemulsion is quickly reached during sonication.[53] Polymerisation now occurs by radical entry into the pre-existing monomer droplets without the formation of new particles. Other hydrophobic species (such as dyes) can therefore be incorporated into the monomer phase prior to agitation and be encapsulated/entrapped within polymer particles with high efficiency.[53]

2.3.6 Incorporation of additives

Many different types of additives have been used to prevent degradation and increase the PC response of dye species over time. Additives that have the best effect on improving the lifetime of PC dyes are HALS, anti-oxidants, and UV absorbers.[2] Use of triplet state quenchers and thermal stabilisers can also lead to some improvements in fatigue resistance.[22,28] The addition of organonickel, HALS and phenol-based stabilisers in

polymer matrices containing SOs has been found to increase the lifetime of the PC moiety.[2,5,56] In their patent, Fries et al.[57] describe the incorporation of PC dye in a sol-gel matrix and recommend the use of antioxidants such as phenols, hydroquinones, pyrocatechols and aromatic amines. These antioxidants can be used alone or in combination with UV absorbers such as benzophenone and its derivatives, and other natural compounds such as urocanic acid and ergosterol. Kamada et al.[58] describe the dispersion of a PC compound in a hindered amine to form an oily product which was mixed with water. The oil droplets were encapsulated into polymer matrices such as a polyamide, polyurethane or PSt using conventional techniques such as interfacial and in-situ polymerisation. The walls of the microcapsules could be crosslinked to increase surface hardness. In PC miniemulsions, stabilising agents were incorporated to improve the PC lifetime of the liquid sample.[59-60]

To the best of the author's knowledge, in miniemulsion systems the use of additives such as HALS and antioxidants to improve the PC film has not been reported.

2.4 Application of photochromic dyes in coating systems

PC dyes are widely used for ophthalmic purposes.[61] Dyes in sol-gel matrices are of particular interest for this application due to their high scratch resistance. They are therefore often used for decorating glass items.[62] PC coatings are used on novel consumer products such as mobile phone covers and perfume packaging.[28] In the decorative coatings market water-based systems are becoming increasingly important due to health and environmental concerns associated with organic solvents.[63] Commercially available PC dyes can be "tricked" into water-based systems by first dissolving the dye in a low alkyl alcohol solvent (e.g. ethanol). In coatings systems low pH conditions should be avoided and the dyes should not be added in excessively high concentrations in order to avoid aggregation.[64] PC compounds entrapped in polymeric dispersions can be directly incorporated into polymeric binders. An acrylic polymer has been used to disperse PC glass beads.[57]A coalescing agent was incorporated to assist with film formation of the dried coating without cracks. PC miniemulsions can potentially open new application areas in the decorative coatings market. These could include indoor water-based paint that changes colour as the light intensity changes during the day.

2.5 Characterisation of photochromic properties

In order to characterise PC dispersions it is necessary to first consider different methods of sample preparation, analytical instrumentation, and light source requirements. PC dispersions are generally characterised using spectroscopic instrumentation. Commonly measured PC parameters and rules for adherence to the Beer–Lambert law also need to be considered.

2.5.1 Sample preparation

The correct sample preparation is required before PC compounds can be characterised. Sample preparation for spectroscopic measurements of transparent liquids is simple, but sample preparation for measurements of dispersions requires more careful attention.

2.5.1.1 The photochromic dye

To measure PC properties the compound should be placed in an environment that represents the form of its end use as closely as possible.[2] The properties of PC dyes can easily be evaluated by dissolving the sample in a suitable solvent such as THF, toluene or xylene.[65] This solution is placed into a cuvette and analysed using a spectroscopic instrument.

2.5.1.2 The photochromic latex

Su et al.[49] describe the characterisation of SP nanoparticles prepared as a miniemulsion in water. Scattering of light by nanoparticles causes an increase in the unirradiated curve from the high to the low wavelengths. Upon UV irradiation, absorption of the PC dyes can be observed in aqueous media. In order to determine the PC properties of dyes entrapped in a miniemulsion the form of a dried film of the sample best represents the state of the end use. Such films can be used to obtain data from UV-Vis, ellipsometric spectrometry, flash photolysis or colourimetric analysis.

Various means of preparing thin films of below 40nm[66] to films of up to 170µm[67] thick have been reported in literature. The most common means of preparing films is via spin coating,[50,68] and solvent casting in a mould.[67,69] Vacuum thermal deposition or gravity-deposition,[70-71] Langmuir-Blodgett film preparation, and dipping methods[41,72] are also

used, but apply more to polymer solutions rather than to nanoparticles. Films for absorption measurements can be prepared on substrates such as glass, quartz, silica or fused silica,[37,73] or in a petri dish.[69] Films can be analysed on the substrates themselves or removed and the free film analysed.[67] Films are usually dried either in air or vacuum at specific temperatures and for specific time periods, depending on the nature of the matrix.[36,41,69] In order to obtain optically clear films it is important that the substrate on which the sample is placed be thoroughly clean. Klukowska et al.[7] have described a method for the cleaning of glass slides: wash them in a sodium hydroxide solution, wash with deionised water, place the glass slides in an ultrasonic bath, again wash with deionised water, and dry using compressed air. Samples can also be filtered through, for example, 0.2µm Millipore filters[74-75] before casting them onto the substrate.

a) Spin coating

Several references describe the preparation of ultrathin films by spin coating.[7,34,36,50,73-74] The three most important parameters that influence a sample's film thickness are the solute concentration, solution viscosity and the spin rate.[66] The faster the spin rate, the higher the mechanical forces the sample experiences and the less contact time there is between the sample molecules. Film thicknesses in the nanometer to micrometer range can be obtained using spin coating. Spin coating is performed by dripping a solution of the sample in the middle of a spinning substrate. The solute concentration, sample volume and spinning rate can influence the uniformity of the film formed.[76] The film thickness and uniformity of very thin films can be measured by atomic force microscopy (AFM)[77] or ellipsometry.[78] Using these techniques, a variation of 20nm in 40nm thick films can be measured at a distance 2cm away from the centre.[66] To improve the uniformity of the film, solvents with different volatility[78]and slip additives such as BYK-301 (as used by Koppetsch[8]) can be incorporated.

b) Solvent casting

Solvent casting can be used to obtain a free film of a sample. The polymer and PC dye are dissolved in a solvent such as toluene and poured into a petri dish. The solvent is left to evaporate, after which further drying is enforced in an oven. A sample is then cut from this dried film and the free film mounted in a holder for analysis. The film thickness of samples can be varied by changing the solute concentration. Film thicknesses of 1−170µm, measured using a film thickness gauge, have been reported.[67,69]

2.5.2 Spectroscopic instrumentation

Two spectroscopic techniques used to determine PC kinetics are reviewed here, namely UV-Vis analysis and laser flash photolysis.

2.5.2.1 UV-Vis analysis

Absorption spectra are the most established means of studying the kinetic properties of PC systems.[68] UV-Vis measurements are easily performed via transmission spectroscopy for liquid samples or clear solid films, where data adhere to the Beer–Lambert law. For opaque films, powders and other solids, specular reflectance or diffuse reflectance measurements are used.[79] Specular reflectance can be used for very highly reflective samples with extremely smooth (mirror like) surfaces. Diffuse reflectance is used on uneven surfaces such as powders and solids, such as microspheres,[48] as well as paint films.[80] Standard transmittance spectrophotometers can be equipped with accessories, such as the praying mantis accessory, to enable reflectance measurements.[81] Both specular and diffuse reflectance set-ups require a mirror assembly to direct radiation onto the sample and from the sample to the detector system. Reflectance spectra can be converted to absorbance spectra using the Kubelka-Munk function for easy comparison with spectra from standard transmission spectroscopy.[81]

According to literature, transmission UV-Vis spectroscopy has often been used to characterise the PC properties of dye compounds and thin films.[2,25,29,72,82] In this study the use of three different measurement techniques were investigated; they differed in the way that the instrumentation was set up.

Option A: An outside light source (a means of activating/deactivating) was used to pre-irradiate samples, and a standard UV-Vis instrument was used for monitoring the absorbance.
Option B: An existing UV-Vis instrument was modified to monitor absorbance during the activation or deactivation process.
Option C: An instrument specifically designed to monitor absorbance during the activation or deactivation process was built.

More detailed descriptions of how these options have been used in literature follows.

Option A:

Tan et al.[69] describe the measurements performed on PPMA films of 1mm thickness and a 2wt% loading of the PC compounds. Absorption measurements at the λ_{max} were taken immediately before and after 30s of irradiation, at 365nm, with a 12W ultraviolet lamp. Koppetsch[8] describes measurements of dye degradation on spin coated Ormosil coatings, at 350nm, using a Rayonet photochemical reactor lamp 2.5cm away from the sample, using various filters to cut off wavelengths below 300nm. Samples of $1cm^2$ were irradiated for 30s and with a 5s delay, secured into a cuvette holder, to monitor the absorption at λ_{max}, using a Shimadzu UV-2100 spectrophotometer (see Figure 2.8). Fading kinetics could also be measured by irradiation of the sample for 1min in the cuvette holder with a hand-held TLC lamp set to a long wavelength to form the MC, while covering the slits of the instrument to prevent damage. For these measurements there was a 4s delay between irradiation and data collection. Data collection was carried out over the temperature range from 5–30ºC. A refrigeration unit was connected to the cuvette holders and the temperature of the slides measured with thermocouples.

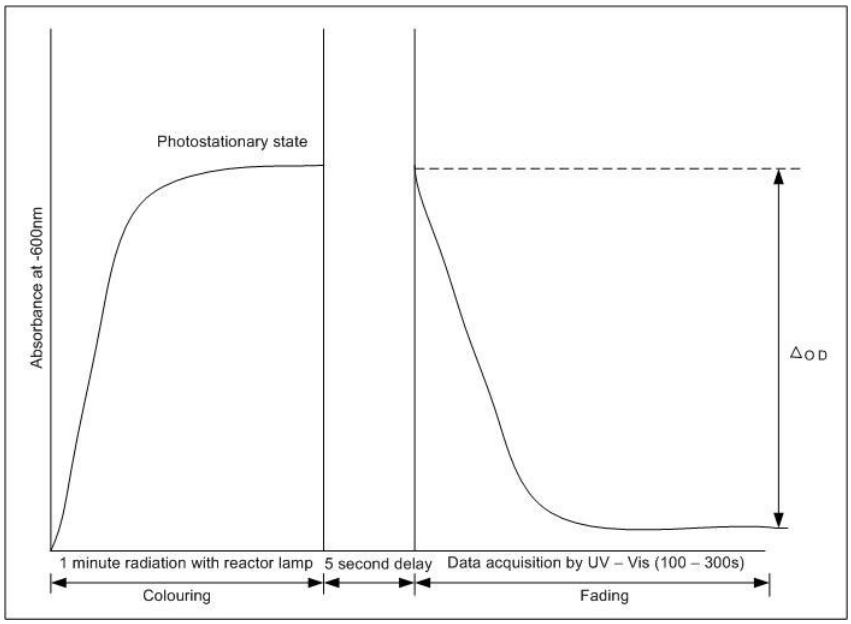

Figure 2.8. Activation/deactivation measurement of PC film.[8]

There are several reports describing this process of obtaining data by pre-irradiating the samples before acquiring the absorbance data with a standard UV instrument with some time delay.[29,35,72,83-84] There are also a few reports describing the use of external irradiation and quantifying the PC change using other techniques, such as colourimetery.[7,36]

Option B:

Lee et al.[74] describe the modification of a Hewlett Packard 8453 spectrophotometer, photodiode array type (PDA), λ = 190–1100nm, to measure the activation and deactivation of spin coated SP compounds in PMMA and a chalcone epoxy polymer. For this set-up a 1kW high-pressure mercury lamp equipped with a liquid optical cable and a bandpass filter (UG11, Oriel Co.) was used to observe the activation of the films. The light intensity at the exposed film area was recorded to be 1.15mW/cm^2 for the wavelength range 280–390 nm. To observe the deactivation process the samples were irradiated with white light of 1mW/cm^2 intensity. Both the excitation and deactivation light sources were deflected onto the sample at a 45º angle to the monitoring beam of the UV-Vis instrument.

Choi et al.[75] describe the measurements of a solution of a bifunctional copolymer containing SP and chalcone linkages that was cast onto a quartz plate and dried in a vacuum oven (80ºC) overnight. The activation and deactivation light sources were also positioned at a 45º angle to the monitoring beam of the UV-Vis instrument, in this case by using reflection mirrors. The instrument used was a Hewlett Packard 8453 spectrophotometer (PDA type, λ = 190–1100nm). The activation source was a 1kW high-pressure mercury lamp fitted with a liquid optical cable. The light intensity measured at the sample surface was 1.15mW/cm^2 for the wavelength range 250–390 nm. In this set-up the white light was produced using a He-Ne laser at 633nm with an intensity of 6.88mW/cm^2 at the sample surface. See Figure 2.9.

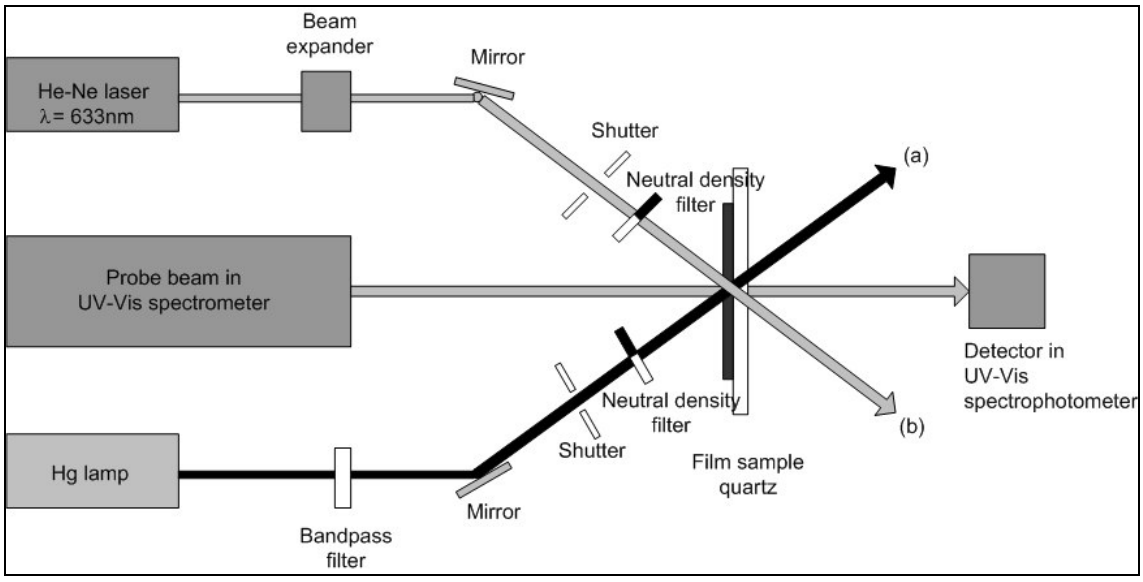

Figure 2.9. Optical set-up for investigating photochromism of solid samples.[75]

There are further reports of the use of the latter type of set-up,[16,85] optionally equipped with additional accessories such as a cryostat for cuvette holders.[86] The latter allows temperature control, and therefore measurement of the kinetics of PC compounds in solution, which is otherwise not possible.

Option C:

Crano and Guglielmetti[2] suggest utilising a triangular optical bench to construct an instrument to measure PC properties at room temperature. Infrared is cut off by using a copper sulphate solution and neutral density filters are used to control the intensity of the irradiation which is supplied via a xenon lamp. A shutter assembly that incorporates focussing lenses is placed in front of the sample compartment, which consists of a holder in a temperature controlled water bath (see Figure 2.10).

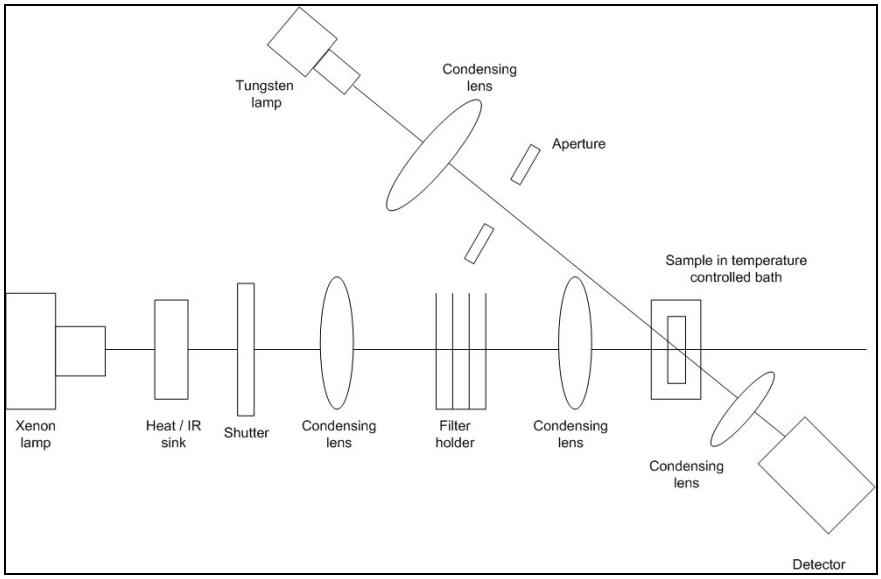

Figure 2.10. Triangular optical bench. [2]

To measure the optical density of the sample a tungsten lamp set-up is mounted on a separate optical bench and placed in such a manner to allow measurement of the absorbance at an angle to the first optical bench. A bandpass filter and silicone detector are used to complete the monitoring set-up.

More recently, using the suggestion of Crano and Gugliemeyti, Parry et al.[61] assembled an instrument for analysing SO and chromene PC compounds produced by James Robinson Ltd (UK), under the Reversacol brandname. Using an optical bench, a xenon lamp with

specific filters was used to activate the sample secured in a holder. The temperature in the holder is controlled using a waterbath to ensure no distortions from heat generated by the incident light conditioning beam. The spectrophotometer analysing beam is set at an angle to the sample, from where the reflectance or absorbance is recorded by the spectrophotometer (photomultiplier) and sent to an electronics control box linked to a computer. This instrument allows measurements to be recorded while the PC activation or deactivation process is taking place of a solid or liquid sample that is either clear or opaque. See Figure 2.11.

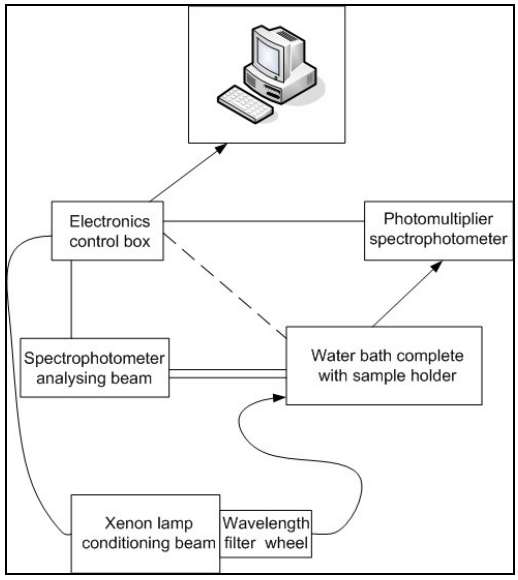

Figure 2.11. Schematic representation of the instrumental set-up used by James Robinson Ltd. [61]

2.5.2.2 Laser flash photolysis

In solutions and other matrices with sufficient free volume, PC compounds show ultrafast kinetic dynamics. Transient absorption measurements, incorporating laser activation and detections, are required to accurately determine these kinetic parameters. Technology has now evolved from nanosecond and picosecond measurements, down to even femtosecond transition measurements.[87-88] To resolve the time profile of such short-lived transitions, two very short optical pulses are required. One pulse is used for excitation (pump) and the other for monitoring (probe). The two pulses are usually provided by a single laser, and follow different optical paths to arrive at the sample position. By changing the optical path length the interval time of the pump and probe pulse can be varied. The time resolution obtainable with laser flash photolysis depends greatly on the duration of the pulse provided by the laser. Typical pulses used for femtosecond resolution are obtained by a mode-locked

Ti:sapphire laser system, where the shortest pulse duration obtainable is 4fs.[89-91] Other flash photolysis set-ups incorporate a XeCl excimer laser with a 8ns pulse duration,[8] a Nd:YAG laser with a 3ns pulse duration,[87] and a mode-locked Nd:phosphate glass laser with a 8ps pulse duration.[88] Femtosecond analysis of SOs indicate that the primary photoproduct is formed within 100–300fs.[92]

2.5.3 Light source requirements for spectroscopic measurements

Different light sources can be used for the activation and deactivation of PC compounds to obtain the desired status. For the closed species A to convert to the open species B, activation at lower wavelengths is used. Typically, these wavelengths will be in the UV region 300–400nm, but they could also be in the visible region 400–700nm. For the activation of SO, in particular, only UV-A light is required (wavelength 315–380nm).[2] Light sources typically used for activation in this region are handheld UV TLC lamps (365nm),[69] mercury lamps,[74-75] xenon lamps,[82,84] and lasers such as a Nd:YAG (354.7nm) and a XeCl excimer laser (308nm).[2,87,93] Filters or monochromators can be used with arc lamps (such as xenon and mercury lamps) to select specific wavelengths of interest, and typically cut off irradiation below 300nm.[6,34,94]

Deactivation of PC species by irradiation is enforced via white light irradiation. Choi et al.[75] used a He-Ne laser at 633nm with an intensity of 6.88mW/cm^2 to produce white light and Crano and Guglielmetti [2] used a 450W Xe lamp as a bleaching light source.

2.5.3.1 Light source parameters

Several factors pertaining to the light source, besides the specific wavelength (spectral output), need to be considered for the activation or deactivation of PC materials. The light source should have sufficient intensity and intrinsic stability, and the lifetime of the source is important in quantitative spectroscopic measurements.[95]

Spectral output

A deuterium lamp is a typical UV source used in spectrophotometers with a continuum output from 180–400nm and some lines at 486 and 656nm. For a deuterium lamp to

produce irradiation it requires the cathode to be heated. This heat will strike an arc that emits heat, and will continue to produce a discharge.[95]

A mercury arc produces a higher intensity than a deuterium lamp. A mercury lamp emits a line spectrum with the intensity focussed at 365, 436 and 546nm.[95-96]

A xenon lamp has a continuum spectral output between 190 and 750nm (25% of the intensity). It also has a few intense spectral lines at 780 and 1000nm (70% of the intensity), with a decreasing continuum down to 2.6µm.[95]

A tungsten filament lamp is most commonly used for visible light irradiation in spectrophotometers. The tungsten lamp has the highest intensity at 1000nm, and which drops to a wavelength of about 300nm, which is the minimum wavelength with useful intensity. A tungsten lamp requires a transformer to supply power and the voltage of the supply should be controlled. At higher voltages the luminance and colour temperature increases, which increases the brightness of the wavelengths in the visible region.[95-96]

Figure 2.12 illustrates the spectral output lines for deuterium, mercury, xenon and quartz (tungsten) lamps.

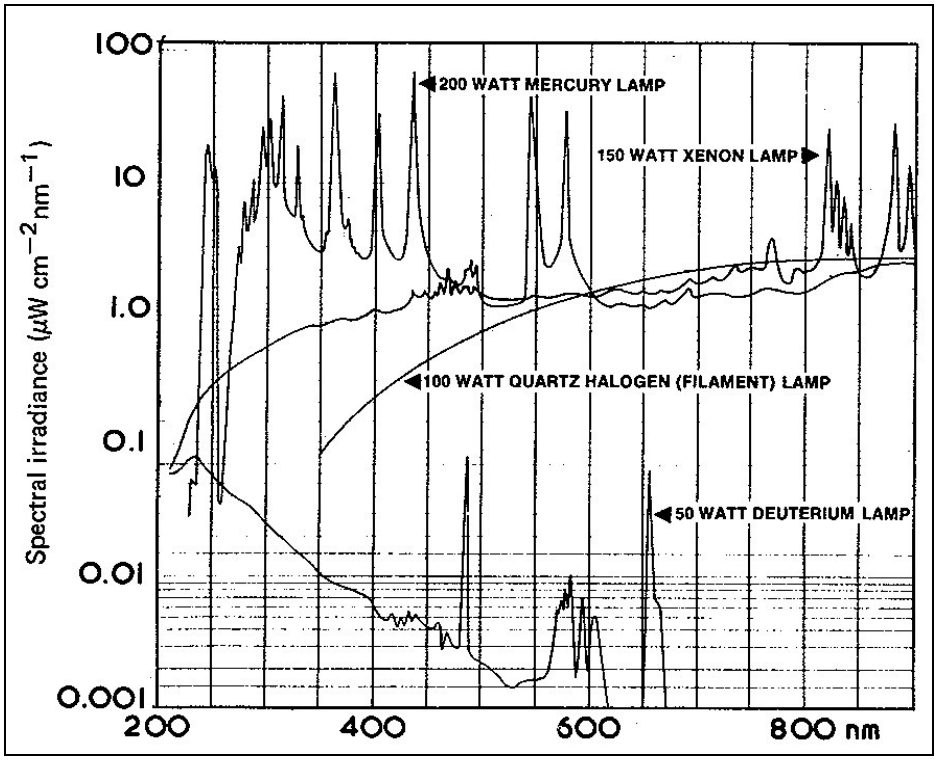

Figure 2.12. Spectral lines of mercury, xenon, quartz and deuterium light sources. [95]

Light from a laser (**l**ight **a**mplification by the **s**timulated **e**mission of **r**adiation) is produced when an atom or molecule that is excited (i.e. has an excess of energy) is stimulated to emit the energy.[97] Lasers usually emit a single wavelength or a very narrow range of wavelengths. Each source is characteristic for a specific spectral output. The spectral output depends on the nature of the material emitting the laser, the optical system, and the means by which the laser is energised. Materials used in laser technology can be solid-state (Nd:YAG), liquid (dye – rhodamine 6G) or gas (He-Ne, CO_2). He-Ne lasers are commonly known outside the laser industry. The most commonly used spectral output line for He-Ne lasers is at 632.8nm, but under different optics this gas mixture can produce lines at either 543nm or infrared light up to 3393nm.[98]

Light-emitting diodes (LEDs) are most often semiconductors. Their operation is based on a negatively charged n-region and a positively charged p-region. A certain voltage is required across the two semiconductors to create a flow of electrons from the negative to the positive region. Each negative electron pairing with a positive electron allows a decrease in total energy (dependent on the type of semiconductors used), which can be released in the form of electromagnetic radiation. LEDs can emit radiation from the UV (365nm) region up to the long wavelength visible (red ~625nm) region, depending on the type of semiconductors used.[99] See Figure 2.13 for spectral profiles of LEDs.

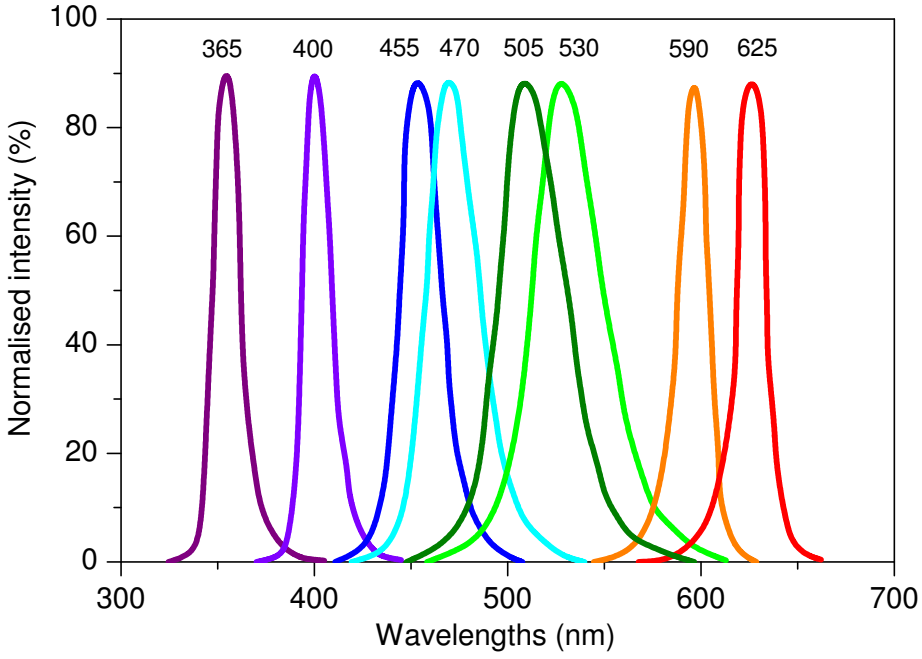

Figure 2.13. Spectral profiles of light emitting diodes.[99]

Table 2.2 gives a summary of the other important parameters to consider when evaluating light sources for quantitative spectroscopic measurements.

Table 2.2. Summary of the properties different light sources

	Arc lamps (deuterium, mercury, xenon)	**Filament lamps (tungsten)**	**Lasers**	**LEDs**
Wavelength (spectral output and width)	Deuterium: continuum 180–400nm; line 486–656nm Mercury: line (365, 436, 546nm dominate) Xenon: continuum 190–750nm, line 780–1000nm	Continuum from 300–1000nm	Dependent on material, very narrow bandwidth	Dependent on material, 20–70nm bandwidth
Intensity	High intensity	Lower than arc lamps, increases from 300 to 1000nm.	0.5–10mW	<10mW–250mW max
Warm-up time	Long	Long	Long	Fast
Irradiation stability	Not stable (flickering)	Very stable	Relatively stable	Very stable
Operating temperature	High	High	High	Low
Lifespan	Very short	Short	Long	Very long
Multiple/ fast switching on/off	No	No	No	Yes

In the present study experiments were carried out to determine which light source is most efficient for the specific measurements of interest. This will be described in Chapter 3.

2.5.4 Photochromic kinetic parameters

There are several parameters that should be reported when determining PC properties. These parameters and their measurement are defined in Sections 2.5.4.1–2.5.4.5.

2.5.4.1 Colourability

The term colourability refers to the tendency of the uncoloured species A to convert to the coloured species B upon irradiation. The intensity of the irradiation should be sufficient in order to produce a high quantum yield.[100-101] Colourability is often used to describe how efficient a PC material is in terms of the strength of the observed colour and the fatigue resistance. These are two very important parameters, in various applications.[16,86]

The absorbance of species A in a very dilute solution at a given wavelength $A_o(\lambda)$ before irradiation is given as the product of the proportionality constant (*k*, which includes the incident photo flux), the colouration quantum yield (ϕcol), the molar absorption coefficient (ε_B) and the concentration of A (c_A):

$$A_o(\lambda) = k\ \phi col\ \varepsilon_B\ c_A \qquad (1)$$

The colouration efficiency is given by the absorbance $A_o(\lambda)$ at the maximum wavelength of the activated form B immediately after irradiation.[4]

A detailed study on the colourability of a species would require measurements of the quantum yield at all activating wavelengths. This is not a simple task, since both thermal and photochemical reversibility may occur. In order to simplify measurements slightly it can be assumed that the establishment of species B in a well stirred mixture will obey Beer's law.[4] Flash photolysis techniques give the combination of the product of the ϕcol and the ε_B, and not the individual terms. The assumption that A is almost completely converted to B at extremely low temperatures, or in very high intensity experiments, allows ε_B to be obtained. [102]

However, fatigue also occurs, and during degradation other non-oxidative processes occur simultaneously with the dominating photo-oxidation process. Degradation increases the difficulty in obtaining quantum yields and rate constants for individual processes. To obtain quantitative data, continuous irradiation methods are preferable.[102]

In Figure 2.14 the sample is irradiated up to t_1, after which the irradiation light source is switched off. Curves a'_1 and b'_1 are monitored at the irradiation wavelength and curves a_1 and b_1 are monitored at the maximum absorption of the open form of the sample. The thermal rate constant k_{BA} can be extracted from the deactivation curves (b_1 and $b`_1$ from $t_1 \rightarrow \infty$) and $\phi$col and $\varepsilon_B$ from the activation curves ($a_1$ and $a`_1$ from $0 \rightarrow t_1$). The portion of

incident photoflux that is absorbed by the unactivated sample A can be calculated from the absorbance data at the irradiation wavelength.[4]

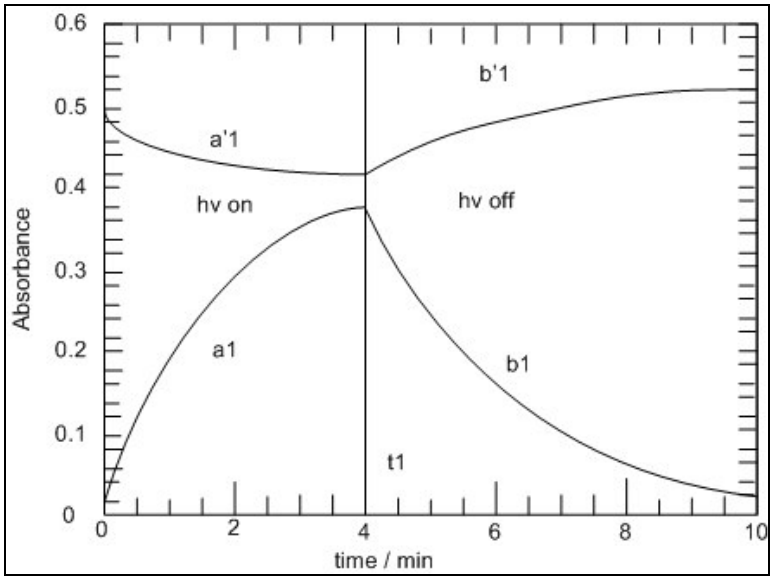

Figure 2.14. Activation/deactivation curves for kinetic determinations of PC properties.[4]

In order to conduct comparative studies related to colourability, fixed experimental conditions must be used. Parameters such as the excitation source, the distance of the filters from the source, temperature, time of irradiation, the sample matrix, and concentration of PC species are important. Using these fixed parameters, colourability can be given by ΔA_0 (maximum absorbance during photostationary state – minimum absorbance during bleached state). Half-life and degradation values can be established similarly.[29,35]

2.5.4.2 Half-life

Using the fixed parameters, as described in Section 2.5.4.1, the half-life ($t_{½}$) can be given as the time necessary for ΔA_0 to reach half of its original value at the wavelength of maximum absorption of the sample after one cycle of irradiation.[4,11] The thermal decay constant (k*f*) can be obtained by fitting a mono-exponential curve to the thermal deactivation curves of the samples. Using k*f* the half-life of the thermal decay process can be given by[103]:

$$t_{½} = \frac{\ln 2}{kf} \qquad (2)$$

The half-life of a sample can be from seconds to minutes, depending on the physical nature of the sample, i.e. if it is in solution or in a solid matrix (where it is sterically hindered).[7]

2.5.4.3 Number of cycles

During the activation and subsequent deactivation cycles, PC species B does not always revert back to an equal quantitative amount of A from which it was formed. This is due to the formation of byproducts.[4] If the amount of degradation during one cycle is given as *x* then the fraction of *y* after *n* cycles would be:

$$y = (1 - x)^n \quad (3)$$

For very low *x* and very large *n*:

$$y = 1 - nx \quad (4)$$

Thus, for $x = 0.001$ the yield is 99.9%, after 10^3 cycles, and 63% of A is lost. After 10^4 cycles almost all of A will be lost.

The number of cycles that a specific system can undergo before loosing a certain percentage of its original ΔA_0 value must be measured using fixed parameters, and monitoring ΔA_0 at the wavelength of maximum absorption of the sample.[4]

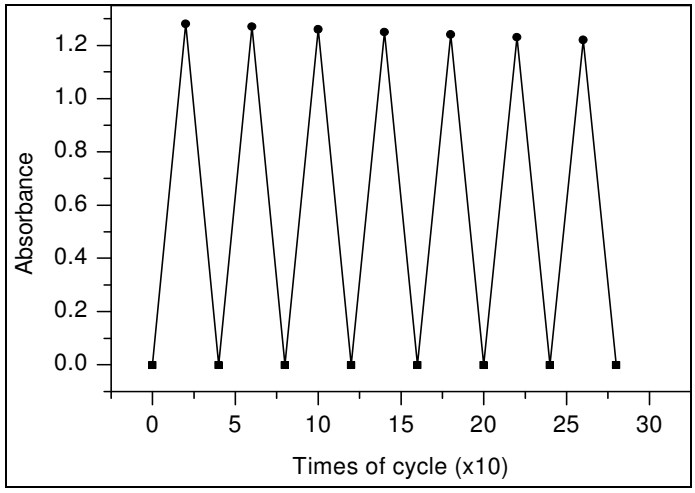

Figure 2.15. Photoinduced absorption changes of a PC dye at λ_{max}.[4] UV irradiation started at each ■, up to each •, after which thermal decay in the dark was observed.

2.5.4.4 Cyclability (z_{50})

Cyclability is measured as described in Section 2.5.4.3. It is the number of cycles required for ΔA_0 to reach half of its original value at the wavelength of maximum absorption of the sample.[4]

2.5.4.5 Fatigue

When a PC species is continuously irradiated with UV light its colourability decreases. This phenomenon is described as fatigue, and can be ascribed to chemical degradation (nearly always due to oxidation). In terms of the previous measurements, fatigue can be given as the time of irradiation required for ΔA_0 to reach half of its original value at the wavelength of maximum absorption of the sample.[1,4] The requirements for fatigue resistance are application dependent.

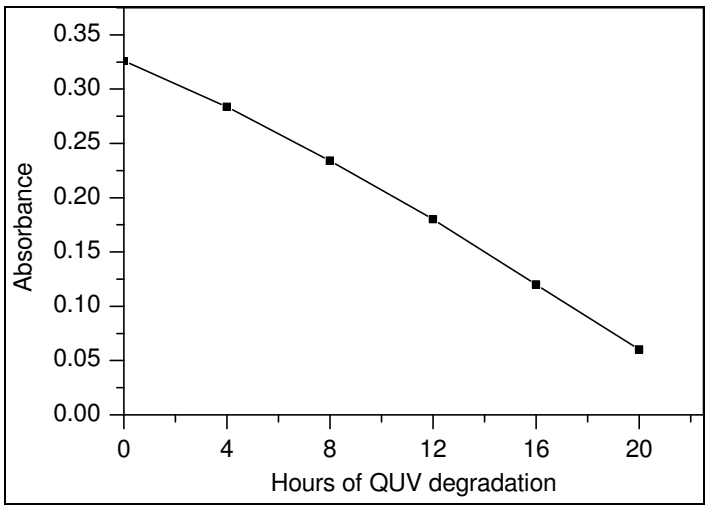

Figure 2.16. Fatigue measurement of a PC film at λ_{max} after every 4hr degradation.

Measurements can be made using artificial weathering chambers, typically incorporating a xenon arc lamp,[36] or by irradiation with a high-pressure mercury lamp.[69] In order to perform degradation studies after irradiation, samples need to be deactivated. Heat or visible light sources can be used for deactivation prior to storage in the dark.[36]

2.5.5 Spectroscopic data analysis

In order to interpret spectroscopic data and related PC parameters, general spectroscopic laws need to be considered. According to the Beer–Lambert law the absorbance of a sample is related to its concentration and the path length of the light travelling through it, according to the following equation:

$$I = I_0 e^{-\varepsilon c l} \qquad (5)$$

where ε is the molar absorptivity coefficient, c the concentration of the absorbing species and l the path length the light has to travel through the sample.[104]

Expressed in its logarithmic form, the Beer–Lambert law can be written as:

$$\log\left(\frac{I_0}{I}\right) = A = \varepsilon cl \qquad (6)$$

It is generally accepted that this relationship is linear for a passive dye in a dilute concentration. Failure to adhere to the Beer–Lambert law may occur at higher concentrations due to the formation of dimers or other complex aggregates.[104] Many researchers have applied the Beer–Lambert law to PC systems in solution and solid matrices.[36,102] The conditions of linearity need to be well understood for these active dye compounds. Mennig et al.[29] established that the photochromism of a SO compound in a organic–inorganic matrix adhered to the Beer–Lambert law up to a film thickness of 40μm, after which the response became non-linear.

2.6 Conclusions

This chapter sets the foundation for the main focus of the study, which is to improve the PC properties of SO compounds. Techniques such as polymeric dispersion, copolymerisation and sol-gel encapsulation have been widely reported to improve fatigue resistance of these compounds. However, to the best of the author's knowledge, the use of PC miniemulsions with protective additives such as UV absorbers has not been reported.

References

(1) Brown, G. H. *Photochromism*; John Wiley & Sons,Inc: Canada, 1971.
(2) Crano, J. C.; Guglielmetti, R., J. *Organic Photochromic and Thermochromic Compounds*; Marcel Dekker: New York, 1999.
(3) Durr, H. *Pure and Applied Chemistry* **1990**, *62*, 1477.
(4) Bouas-Laurent, H.; Durr, H. *Pure and Applied Chemistry* **2001**, *73*, 639.
(5) McArdle, C. B. *Applied Photochromic Polymer Systems*; Blackie & Son: London, 1992.
(6) Durr, H.; Bouas-Laurent, H. *Photochromism: Molecules and Systems*; Elsevier Science Publishers: New York, 1990.
(7) Klukowska, A.; Posset, U.; Schotiner, G.; Jankowska-Frydel, A.; Malatesta, V. *Material Science: Poland* **2004**, *22*, 187.
(8) Koppetsch, K. J. MSc thesis, Worcester Polytechnic Institute, USA, 2000.
(9) Such, G.; Evans, R. E.; Yee, L. H.; Davis, T. P. *Journal of Macromolecular Science* **2003**, *C43*, 547.
(10) Wang, M.-S.; Yeh, C.-L.; Hu, A. T. *Polymer International* **1995**, *38*, 101.
(11) Raboin, L.; Matheron, M.; Biteau, J.; Gacoin, T.; Boilot, J.-P. *Journal of Materials Chemistry* **2008**, *18*, 3242.
(12) Li, X.; Li, J.; Wang, Y.; Matsuura, T.; Meng, J. *Journal of Photochemistry and Photobiology A: Chemistry* **2004**, *161*, 201.
(13) Crano, J. C.; Flood, T.; Knowles, D.; Kumar, A.; Van Gemert, B. *Pure and Applied Chemistry* **1996**, *68*, 1395.

(14) Lin, J.-S. *European Polymer Journal* **2003**, *39*, 1693.
(15) Nakamura, S.; Uchida, K.; Murakami, A.; Irie, M. *Journal of Organic Chemistry* **1993**, *58*, 5543.
(16) Ortica, F.; Levi, D.; Brun, P.; Guglielmetti, R.; Mazzucato, U. et al. *Journal of Photochemistry and Photobiology A: Chemistry* **2001**, *138*, 123.
(17) Chibisov, A. K.; Gorner, H. *Journal of Physical Chemistry A* **1997**, *101*, 4305.
(18) Pozzo, J. L.; Samat, A.; Guglielmetti, R.; De Keukeleire, D. *Journal of the Chemical Society, Perkin Transactions 2* **1993**, 1327.
(19) Wilkinson, F.; Hobley, J.; Naftaly, M. *Journal of the Chemical Society, Faraday Transactions* **1992**, *88*, 1511.
(20) Voloshin, N.; Chernyshev, A.; Bezuglyi, S.; Metelitsa, A.; Voloshina, E. et al. *Russian Chemical Bulletin* **2008**, *57*, 151.
(21) Delbaere, S.; Micheau, J. C.; Berthet, J.; Vermeersch, G. *International Journal of Photoenergy* **2004**, *6*, 151.
(22) Tamai, N.; Masuhara, H. *Chemical Physics Letters* **1992**, *191*, 189.
(23) Berthet, J.; Delbaere, S.; Lokshin, V.; Bochu, C.; Samat, A. et al. *Photochemical and Photobiological Sciences* **2002**, *1*, 333.
(24) Hobley, J.; Malatesta, V.; Millini, R.; Montanari, L.; O Neil Parker, W. *Physical Chemistry Chemical Physics* **1999**, *1*, 3259.
(25) Patel, D. G.; Benedict, J. B.; Kopelman, R. A.; Frank, N. L. *Chemical Communications* **2005**, 2208.
(26) Malatesta, V.; Renzi, F.; Wis, M. L.; Montanari, L.; Milosa, M. et al. *Journal of Organic Chemistry* **1995**, *60*, 5446.
(27) Malatesta, V.; Millini, R.; Montanari, L. *Journal of the American Chemical Society* **1995**, *117*, 6258.
(28) Higgins, S. *Chemica Oggi* **2003**, *1*, 63.
(29) Mennig, M.; Fries, K.; Lindenstruth, M.; Schmidt, H. *Thin Solid Films* **1999**, *351*, 230.
(30) Sriprom, W.; Neel, M.; Gabbutt, C. D.; Heron, B. M.; Perrier, S. *Journal of Materials Chemistry* **2007**, *17*, 1885.
(31) Rauzy, E.; Berro, C.; Morel, S.; Herbette, G.; Lazzeri, V. et al. *Polymer International* **2004**, *53*, 455.
(32) Lyubimov, A. V.; Zaichenko, N. L.; Marevtsev, V. S. *Journal of Photochemistry and Photobiology A: Chemistry* **1999**, *120*, 55.
(33) Such, G. K.; Evans, R. A.; Davis, T. P. *Macromolecules* **2006**, *39*, 1391.
(34) F. Ribot, A. L., C. Eychenne-Baron, C. Sanchez, *Advanced Materials* **2002**, *14*, 1496.
(35) Pardo, R.; Zayat, M.; Levy, D. *Journal of Sol-Gel Science and Technology* **2006**, *40*, 365.
(36) Klukowska, A.; Posset, U.; Schottner, G.; Wis, M. L.; Salemi-Delvaux, C. et al. *Material Science* **2002**, *20*, 95.
(37) Mo, Y.-G.; Dillon, R. O.; Snyder, P. G.; Tiwald, T. E. *Thin Solid Films* **1999**, *355-356*, 1.
(38) Wang, M.-S.; Xu, G.; Zhang, Z.-J.; Guo, G.-C. *Chem. Commun.* **2009**, *46*, 361.
(39) Pardo, R.; Zayat, M.; Levy, D. *J. Mater. Chem* **2009**, *19*, 6756.
(40) Ke, X.; Yan, X.; Song, S.; Li, D.; Yang, J. J. et al. *Optical Materials* **2007**, *29*, 1375.
(41) Hou, L.; Schmidt, H.; Hoffmann, B.; Mennig, M. *Journal of Sol-Gel Science and Technology* **1997**, *8*, 927.
(42) Tianyong, Z.; Xuening, F.; Jian, S.; Chunlong, Z. *Dyes and Pigments* **1999**, *44*, 1.
(43) Lelu, S.; Novat, C.; Guyot, A.; Boureat-Lami, E. *Polymer International* **2003**, *52*, 542.
(44) Arunkumar, E., Forbes, C.C., Smith, B.D. *European Journal of Organic Chemistry* **2005**, *2005*, 4051.
(45) Ando, K.; Kawaguchi, H. *Journal of Colloid and Interface Science* **2005**, *285*, 619.
(46) Takasu, M.; Shiroya, T.; Takeshita, K.; Sakamoto, M.; Kawaguchi, H. *Colloid and Polymer Science* **2003**, *282*, 119.
(47) Han, M.; Lee, E.; Kim, E. *Optical Materials* **2002**, 579.
(48) Lee, E.; Choi, M.; Han, Y.; Cho, H.; Kim, S. et al. *Fibers and Polymers* **2008**, *9*, 134.
(49) Su, J.; Chen, J.; Zeng, F.; Chen, Q.; Wu, S. et al. *Polymer Bulletin* **2008**, *61*, 425.

(50) Zhu, M.-Q.; Zhu, L.; Han, J. J.; Wu, W.; Hurst, J. K. et al. *Journal of the American Chemical Society* **2006**, *128*, 4303.
(51) Jyongsik Jang; Joon Hak Oh; Li, X. L. *Journal of Materials Chemistry* **2004**, *14*, 2872
(52) H. Mohd. Ghazaly, E. S. D., V. L. Dimonie, A. Klein, M. S. El-Aasser, *Journal of Applied Polymer Science* **2001**, *81*, 1721.
(53) Antonietti, M.; Landfester, K. *Progress in Polymer Science* **2002**, *27*, 689.
(54) Landfester, K.; Schork, F. J.; Kusuma, V. A. *Comptes Rendus Chimie* **2003**, *6*, 1337.
(55) Steiert, N.; Landfester, K. *Macromolecular Materials and Engineering* **2007**, *292*, 1111.
(56) Chu, N. Y. C. US 4440672, 1984.
(57) Fries, K.; Lisong, H.; Pietsch, M.; Mennig, M.; Schmidt, H. US 6 639 039, 2003.
(58) Kamada, M.; Suefuku, S. US 5 208 132, 1993.
(59) Robert, A.; Tardieu, P.; Maisonnier, S.; Cano, J.-P. US 6770710, 2004.
(60) Tardieu, P.; Maisonnier, S.; Robert, A.; Cano, J.-P. US 6740699, 2004.
(61) Parry, H.; Corns, N.; Towns, A. New uses for photochromics; James Robinson; 20 September 2004; http://www.james-robinson.ltd.uk.
(62) Nakazumi, H.; Makita, K.; Nagashiro, R. *Journal of Sol-Gel Science and Technology* **1997**, *8*, 901.
(63) Singh, K. B.; Deoghare, G.; Tirumkudulu, M. S. *Langmuir* **2009**, *25*, 751.
(64) Leyland, V.,Guidelines for applying photochromic dyes in coatings or inks; James Robinson, *personal communication,* 2007.
(65) Leyland, V.,Reversacol solubility data; James Robinson, *personal communication,* 2007.
(66) P. A. Chiarelli, M. S. J., J. L. Casson, J. B. Roberts, J. M. Robinson, H.-L. Wang, *Advanced Materials* **2001**, *13*, 1167.
(67) Yi, Y.-R.; Lee, I.-J. *Journal of Photochemistry and Photobiology A: Chemistry* **2002**, *151*, 89.
(68) Alvarez-Herrero, A.; Pardo, R.; Zayat, M.; Levy, D. *Journal of the Optical Society of America B* **2007**, *24*, 2097.
(69) Tan, T.-F.; Han, J.; Pang, M.-L.; Fu, Y.-F.; Ma, H. et al. *Tetrahedron* **2006**, *62*, 4900.
(70) Lukyanov, B. S.; Metelitsa, A. V.; Voloshin, N. A.; Alexeenko, Y. S.; Lukyanova, M. B. et al. *International Journal of Photoenergy* **2005**, *07*, 17.
(71) Macuil, R. D.; Gayou, V. L. *Journal of Physics: Conference Series* **2006**, *28*, 139.
(72) Pang, Y.; Fengy, W.; Chen, J.; Liu, Y.; Cai, W. *Journal of Materials Science and Technology* **2007**, *23*, 477.
(73) Angiolini, L.; Giorgini, L.; Bozio, R.; Pedron, D. *Synthetic Metals* **2003**, *138*, 375.
(74) Lee, B.; Kim, J.; Cho, M. J.; Lee, S. H.; Choi, D. H. *Dyes and Pigments* **2004**, *61*, 235.
(75) Choi, D.-H.; Ban, S. Y.; Kim, J. H. *Bulletin of the Korean Chemical Society* **2003**, *24*, 441.
(76) Li, D.; Hutchinson, R. A. *Macromolecular Symposia* **2006**, *243*, 24.
(77) Haro, M.; Giner, B.; Gascon, I.; Royo, F. M.; Lopez, M. C. *Macromolecules* **2007**, *40*, 2058.
(78) Walsh, C. B.; Franses, E. I. *Thin Solid Films* **1999**, *347*, 167.
(79) Harrick Scientific Products, Applications Note No.90112, UV-VIS Diffuse Reflection Spectroscopy of Thermochromic Materials.
(80) Wenlandt, W. W.; Hect, H. G. *Reflectance Spectroscopy*; John Wiley & Sons: New York, 1966.
(81) Casades, I.; Álvaro, M.; García, H.; Pillai, M. N. European Journal of Organic Chemistry 2002, 2002, 2074.
(82) Nakao, R.; Horii, T.; Kushino, Y.; Shimaoka, K.; Abe, Y. *Dyes and Pigments* **2002**, *52*, 95.
(83) Zhang, T. R.; Feng, W.; Lu, R.; Bao, C. Y.; Li, T. J. et al. *Materials Chemistry and Physics* **2003**, *78*, 380.
(84) Kim, C. W.; Oh, S. W.; Kim, Y. H.; Cha, H. G.; Kang, Y. S. *Journal of Physical Chemistry C* **2008**.
(85) Khairutdinov, R. F.; Giertz, K.; Hurst, J. K.; Voloshina, E. N.; Voloshin, N. A. et al. *Journal of the American Chemical Society* **1998**, *120*, 12707.
(86) Favaro, G.; Malatesta, V.; Mazzucato, U.; Ottavi, G.; Romani, A. *Journal of Photochemistry and Photobiology A: Chemistry* **1995**, *87*, 235.

(87) Hobley, J.; Malatesta, V.; Hatanaka, K.; Kajimoto, S.; Williams, S. L. et al. *Physical Chemistry Chemical Physics* **2002**, *2*, 180.
(88) Tamai, N.; Miyasaka, H. *Chemical Revisions* **2000**, *100*, 1875.
(89) Wohl, C. J. MSc thesis, Virginia Polytechnic Institute and State University, USA, 2002.
(90) Bosman, G. MSc thesis, University of Stellenbosch, RSA, 2008.
(91) Rini, M.; Holm, A.-K.; Nibbering, E. T. J.; Fidder, H. *Journal of the American Chemical Society* **2003**, *125*, 3028.
(92) Maurel, F.; Aubard, J.; Millie, P.; Dognon, J. P.; Rajzmann, M. et al. *Journal of Physical Chemistry A* **2006**, *110*, 4759.
(93) Wilkinson, F.; Worral, D. R.; Hobley, J.; Jansen, L.; Williams, S. L. et al. *Journal of the Chemical Society, Faraday Transactions* **1996**, *92*, 1331.
(94) Hur, Y.; Ock, K.; Kim, K.; Jin, S.; Gal, Y. et al. *Thin Solid Films* **2002**, *419*, 207.
(95) Knowles, A.; Burgess, C. *Techniques in Visible and Ultraviolet Spectrometry, Volume 3: Practical Absorption Spectrometry*; Chapman and Hall: London, 1984.
(96) Brady, S.; Bracegirdle, B. *Introduction to light microscopy*; BIOS Scientific Publishers: Oxford, 1998.
(97) Meyer-Arendt, J. R. *Introduction to classical and modern optics*; Prentice-Hall, Inc.: New Jersey, 1995.
(98) Hecht, J. *Understanding Lasers: An Entry-level Guide*; 2nd ed.; IEEE Press: Piscataway, 1993.
(99) Carl Zeiss;Microscope light sources; 21 August 2009; http://zeiss-campus.magnet.fsu.edu.
(100) Crano, J. C.; Guglielmetti, R., J. *Organic Photochromic and Thermochromic Compounds*; Marcel Dekker: New York, 1999.
(101) Trung, V. Q. PhD thesis, Technischen Universität Dresden, Germany, 2002.
(102) Pimienta, V.; Froute, C.; Deniel, M. H.; Lavabre, D.; Guglielmetti, R. et al. *Journal of Photochemistry and Photobiology A: Chemistry* **1999**, *122*, 199.
(103) Andersson, N.; Alberius, P.; Ortegren, J.; Lindgren, M.; Bergstrom, L. *Journal of Materials Chemistry* **2005**, *15*, 3507.
(104) Gauglits, G.; Vo-Dinh, T. *Handbook of Spectroscopy*; Wiley-VCH: Germany, 2003.

3 Experimental set-ups required to characterise photochromic materials

3.1 Introduction

Before preparing PC miniemulsion samples, attention had to be given to the modification of equipment with which to measure their PC properties. The correct method of analysis to determine the various PC properties such as fading kinetics and fatigue resistance had first to be established. The focus of this chapter is therefore the determination of a suitable method of sample preparation, and the set up of analytical instrumentation, including the light source requirements, for the measurement of PC properties.

3.1.1 Methodology

In this study two PC dyes, a SNO dye, Reversacol Palatinate Purple (PP), and a chromene dye, Photosol 7-106 (PT), were used. See Figure 3.1.

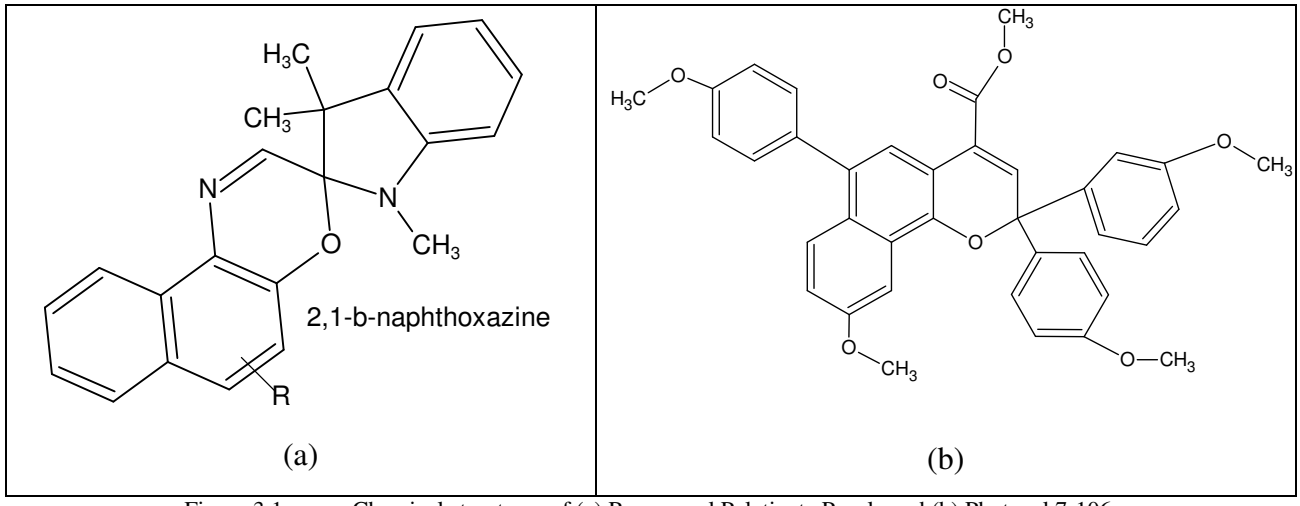

Figure 3.1. Chemical structures of (a) Reversacol Palatinate Purple and (b) Photosol 7-106.

Evaluations of the PC dyes in solution were carried out by dissolving the dyes in a suitable solvent described in Section 3.2. For evaluation of the PC miniemulsions three reference samples were prepared (Exp 3, 17 and 19). Details of the preparation of the miniemulsions are described in Section 4.2.2 and the experimental formulations in Appendix C. Exp 3 had a total solids content (TSC) of 30% BMA, a sodium dodecyl sulphate (SDS) concentration

of 1% and AIBN concentration of 0.36% on the total formulation. Exp 17 and Exp 19 were based on Exp 3. Exp 17 included 1.3% PT and Exp 19 1.0% PP entrapped in the miniemulsion particles. Exp 3 and Exp 17 were used to evaluate the use of spin coating, solvent casting and film applicators required to obtain homogeneous coatings. A handheld UV lamp, a mercury lamp, a UV-LED, and a deuterium lamp were tested as activation sources for films of Exp 17. A He-Ne laser, visible light LED, and a tungsten lamp were tested as deactivation light sources. Reproducibility of colourability, fading kinetics, cyclisation, and fatigue resistance achieved with a UV LED as activation source was investigated using films of Exp 17 and Exp 19. The adherence of PC data to the Beer–Lambert law was also investigated.

3.2 Photochromic dyes in solution

A solution of PP was prepared in high purity tetrahydrofuran (THF, Aldrich, 99.9%), due to the high solubility of the dye in this solvent (see Table 3.1). The Aldrich Chromasolve THF has an absorbance of below 0.004 at 315nm.[1] The MC species of interest absorbs above this wavelength, at approximately 595nm, depending on the solvent or matrix it is dissolved in. A solution of PT in THF was also prepared (see Table 3.2).

Table 3.1. PP solubility data (in g/l)[2]

	Acetone	**Methanol**	**Toluene**	**Ethyl acetate**	**THF**	**N-Methyl-pyrrolidone**
Palatinate Purple	12	<2	78	21	290	210

Table 3.2. PC dye solutions in THF

Sample	**Concentration (g/ml)**
PP	5.1×10^{-4}
PT	6.54×10^{-4}

Absorbance measurements were recorded for solutions in 1cm pathlength cuvettes. Pure THF was used in the reference compartment. Scans were performed from 1100 to 190nm, using a UV 1700 spectrophotometer (Shimadzu). The instrument has a double beam configuration with a 1.0nm fixed slit width and an optical resolution of 1nm over the wavelength range 800–190nm.

In order to determine whether the activation of the closed PC species form (A) to the open MC form (B) occurs, the solutions were analysed via UV-Vis before and after irradiation. The cuvette containing the sample solution was cooled by placing it in an ice bath with salt. The sample was agitated during irradiation to obtain homogeneous activation of the solution. Reducing the temperature minimises the effect of the thermal backwards reaction.[3] Irradiation at 365nm was accomplished using a handheld UV lamp (Spectroline model ENF 260C/FE), approximately 5cm away from the sample outside the instrument, for about 5min. The cuvette was dried and placed in the instrument immediately after irradiation. A wavelength scan from 1100 to 190nm was carried out. There was roughly a 15s time delay between switching off the irradiation and starting the wavelength scans. Results are displayed in Figure 3.2.

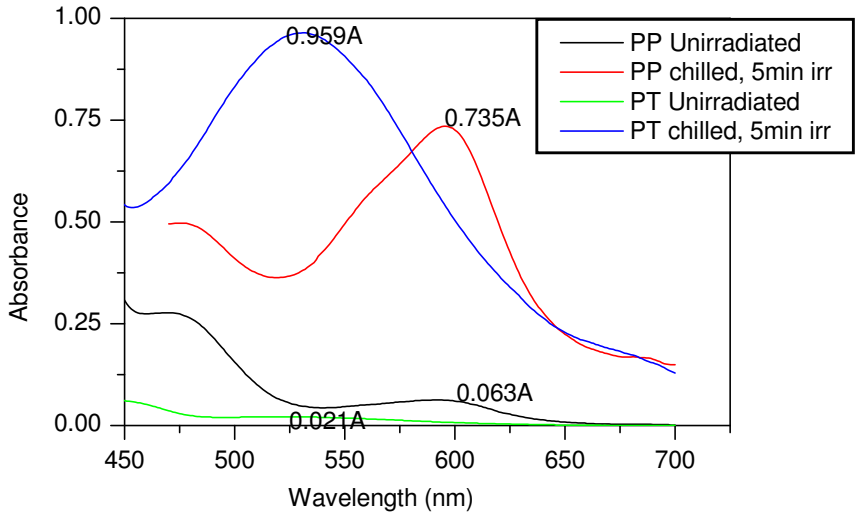

Figure 3.2. Irradiation (irr) of PP and PT at 365nm after cooling.

Activation to the coloured form was observed at 595nm for the PP solution (purple) and at 534nm for the PT solution (pink). The deactivation occurred too fast to interpret data quantitatively (see discolouration in Figure 3.3). The baselines of the chilled solutions shifted, possibly due to the presence of moisture vapour forming on the cuvette as a result of the cooling.

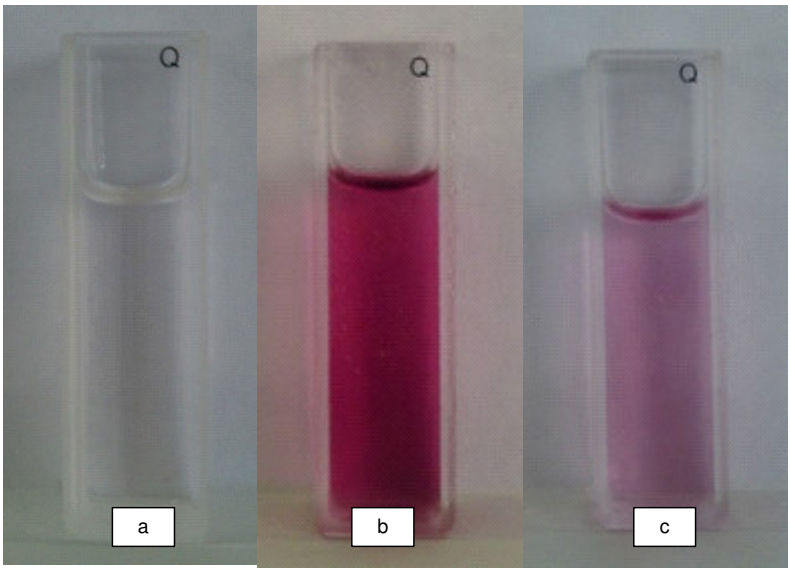

Figure 3.3. PT (a) before irradiation (b) ~5s after irradiation (c) ~20s after irradiation.

In order to acquire quantitative data from a UV-Vis instrument the set-up would require an accurate temperature controlled sample chamber, such as could be obtained with a cryostat, in order to maintain temperatures low enough to suppress deactivation. Alternatively, a flash photolysis instrument would be required for very fast analysis.[4-5]

3.3 Photochromic dyes in polymeric thin films

The entrapment of PC dye in polymer matrices restricts the movement of the molecules, and suppresses the deactivation process.[3,6] The suppressed kinetics in polymer matrices simplifies measuring the PC properties. Factors related to the preparation of samples of miniemulsions for spectroscopic testing have been mentioned in Section 2.5.1. Spin coating and solvent casting procedures, and different film applicators, were evaluated in an effort to produce films of uniform thickness. The film consistency was evaluated using AFM and a film thickness gauge.

3.3.1 Spin coating

A spin coater (Laurell Technologies, model WS-400A-6NPP/Lite/10k) was used to apply the films onto microscope slides. The glass slides were cut in half to approximately 38mm in length. The slides were then cleaned with acetone, placed in a 20% NaOH solution in an oven at 50°C, washed with deionised water, sonicated for 5min, washed with deionised

water, dabbed dry with laboratory paper, and any dust from the paper blown off with compressed air. A similar process was used by Klukowska et al.[7] to minimise any contamination that could cause film defects.

Filter paper (Microscience 589-1) was used to filter a selected miniemulsion sample (Exp 3). Crystalline particulates or other contaminants were removed in order to obtain optically clear films from the miniemulsion. A 1.5ml sample was dropped onto a glass slide within 20s during the acceleration period, and the sample was spun for a total of 2min. The filtered Exp 3 sample was diluted to obtain 30%, 18% and 3% TSC dilutions. Samples of each dilution were prepared using spin rates of 6000, 4000 and 2000rpm, keeping all other conditions (e.g. sample volume and drop rate) constant. The uniformity of the films was evaluated with a Nanosurf Easy scan 2 AFM using a silicon tip in contact mode. The cantilever spring constant was approximately 5N/m. A cut was made in the length of each slide. Care had to be taken not to scratch the glass slide while cutting through the polymer film. Three step-height measurements were taken at the top, middle and bottom of each sample, respectively. A cross-section was made perpendicular to the step of each image to measure the height, which is indicative of the film thickness (see Figure 3.4).

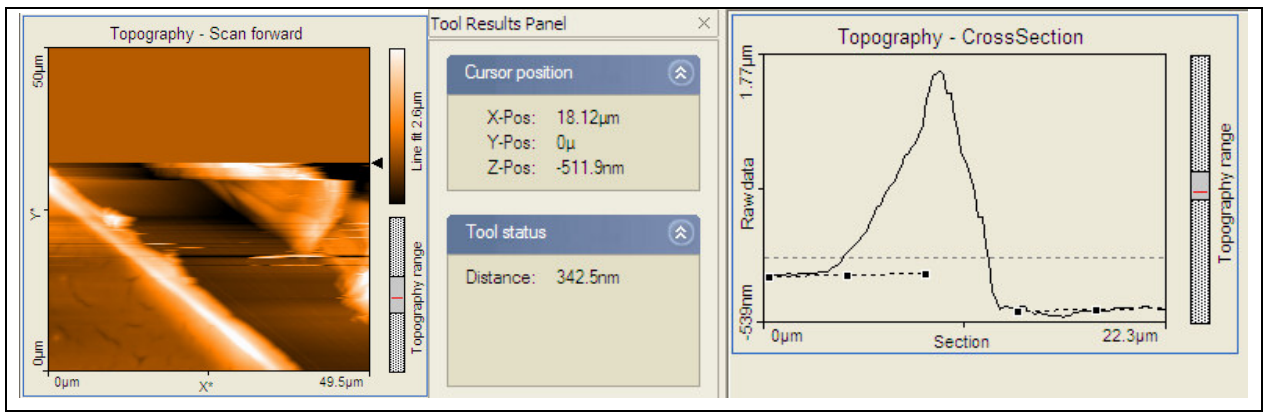

Figure 3.4. An AFM step-height image at the top of a slide (18% TSC sample, 2000rpm) and a cross-section measurement made from it.

The edge of the cut in the polymer films was not always well defined in the topography scans. Undefined edges made height measurements from the topography cross-section difficult. Clear identification of the top of the polymer film in comparison to the bottom of the cut was difficult. This caused a large error in film thickness measurements.

Conclusions regarding film uniformity and spin coating conditions could however not be made (see Table A.1 in Appendix A). A general trend regarding film uniformity indicated that the middle section of the films was much thicker than the outer sections. This is a problem commonly found in spin coating; solutions do not spread out evenly after being dropped in the middle of a coated substrate.[5]

3.3.2 Solvent casting

In order to cast a film in a dish, the sample should level well, and therefore it needs to have a low viscosity. A sample of Exp 17 was diluted to 10%, 15% and 20% TSC. Samples with a minimum volume of 4ml were required to cover the base of a circular aluminium dish of roughly 5cm diameter. Volumes of 4, 5 and 8ml of the respective dilutions were poured into the aluminium dishes and placed on a hotplate at approximately 40°C overnight. Four millilitres of each dilution was also placed in a circular silicone dish (diameter approximately 3cm) and left on a hotplate overnight. After about 15hr the samples in the aluminium dishes were dry, and very non-uniform films with mottled patterns were obtained. Their average film thicknesses ranged from 200 to 800µm. The film thickness was measured using a Sheen SE1250 FNP film thickness gauge with a probe on a non-ferrous metal plate as the zero reference point. The samples dried in the silicone dishes contained air bubbles. The air could be caused by boiling of the free monomer in the solutions.

3.3.3 Film applicators

Several films of Exp 17 at 30% TSC were prepared with film applicators of different gap sizes to evaluate their film thickness and uniformity. The films were drawn on glass panels cleaned with distilled water in an ultrasonic bath and dried in a 60°C oven for 30min. After applying the samples, the glass plates were again placed in the 60°C oven and dried overnight, to provide some flexibility to the films. The samples were then removed from the oven and cut to fit the film holder of the UV-Vis instrument. The film thicknesses were measured across the sample area using a Sheen SE1250 FNP film thickness gauge. Ten film thickness measurements were recorded for each film prepared (see Figure 3.5 and Table A.2 in Appendix A).

The sample prepared with the 20µm film applicator did not deliver a continuous film. The film of the sample prepared with the 40µm film applicator was too thin to remove from the glass panel without it disintegrating. Films of the samples prepared using the 60, 75, 100 and 125µm film applicators could be removed, cut to size, and analysed for uniformity. The films prepared using the 60–100µm applicators were optically clear and defect free. The films prepared using the 125µm applicator had large non-uniform areas with cracks. Only a few defect-free samples of the correct size (larger than 10x30mm) could be obtained.

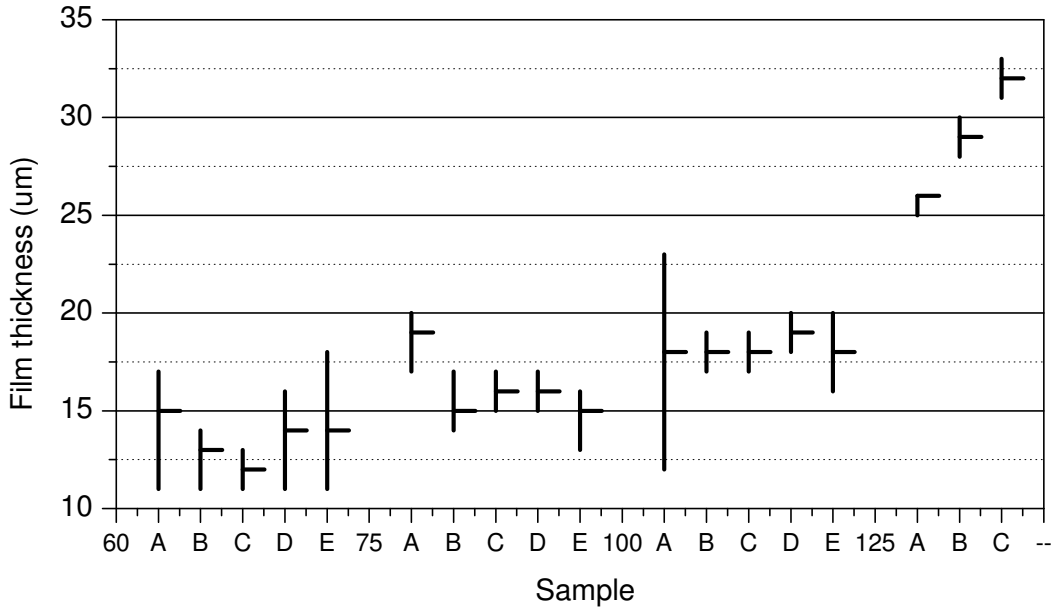

Figure 3.5. Film thickness and uniformity measurements of sample Exp 17 prepared with film applicators.

The graph indicates minima, maxima and the mean film thickness of ten measurements per sample.

The 75µm cube film applicator delivered more uniform films than the longer rectangular film applicators with 20, 40, 60 and 100µm gap sizes. The few defect-free samples obtained from the films drawn with the 125µm rectangular applicator were more uniform than the ones produced with the 75µm cube applicator. The majority of the films produced with the 125µm film applicator were not defect-free, and this applicator is not ideal for producing optically clear films for UV measurements.

3.4 Experimental set-up for UV-Vis measurements of photochromic films

Exp 17 was used to evaluate different experimental configurations. Thin films of the test sample were prepared on glass plates using a film applicator with a 75µm gap size as previously described in Section 3.3.3. The films produced were approximately 16µm thick.

The Institute of Laser Research at the University of Stellenbosch was approached to assist with testing light sources and instrument modifications. The intensity obtained through the different light sources and system set-ups was measured using a power meter (Coherent Fieldmaster, model LM-3,). Films from Exp 17 were placed in a film holder accessory for a UV-Vis instrument, for all the analysis.

The following light sources were tested to evaluate their effectiveness in activating or deactivating the test sample:

Activation light sources:

- Handheld UV lamp, mercury lamp, UV LED and deuterium lamp.

Deactivation light sources:

- He-Ne laser, visible light LED (Vis LED) and tungsten lamp.

Experimental configurations incorporating these light sources were described in Section 2.5.2. Both options A and B described in the literature review will be evaluated here.

Option C described in the literature review involves building a custom-made instrument specifically designed to monitor the absorbance during the activation or deactivation process.[8] Separate optical benches are required to align the activation and deactivation beams at a certain angle to the optical bench, with the monitoring beam to record a signal in either a transmission or reflectance mode.[8] The signal detected by the photodiode is an analogue signal of power versus current. The analogue signal needs to be converted to digital via an analogue to digital (A/D) converter. Digital signals obtained should then be interpreted via software to a computer. A custom built instrument as described fell beyond the scope of this investigation.[9]

3.4.1 Instrumental set-up

A UV-1650PC instrument (Shimadzu) was used in the experimental configurations of Option A and Option B to monitor the absorbance profiles of the films. The UV-1650PC instrument is a double-beam configuration instrument (see Figure 3.6) with a 2.0nm fixed slit width and a 2nm resolution over the wavelength range 190–1100nm. The cross-section of the light beam on the cell is approximately 1mm wide and 10mm high. The wavelength at which the light sources are switched can be selected from 295 to 364nm. The halogen lamp is a 50W long-life type 2000H and the deuterium lamp is a socket type. A silicon photodiode detector was used.

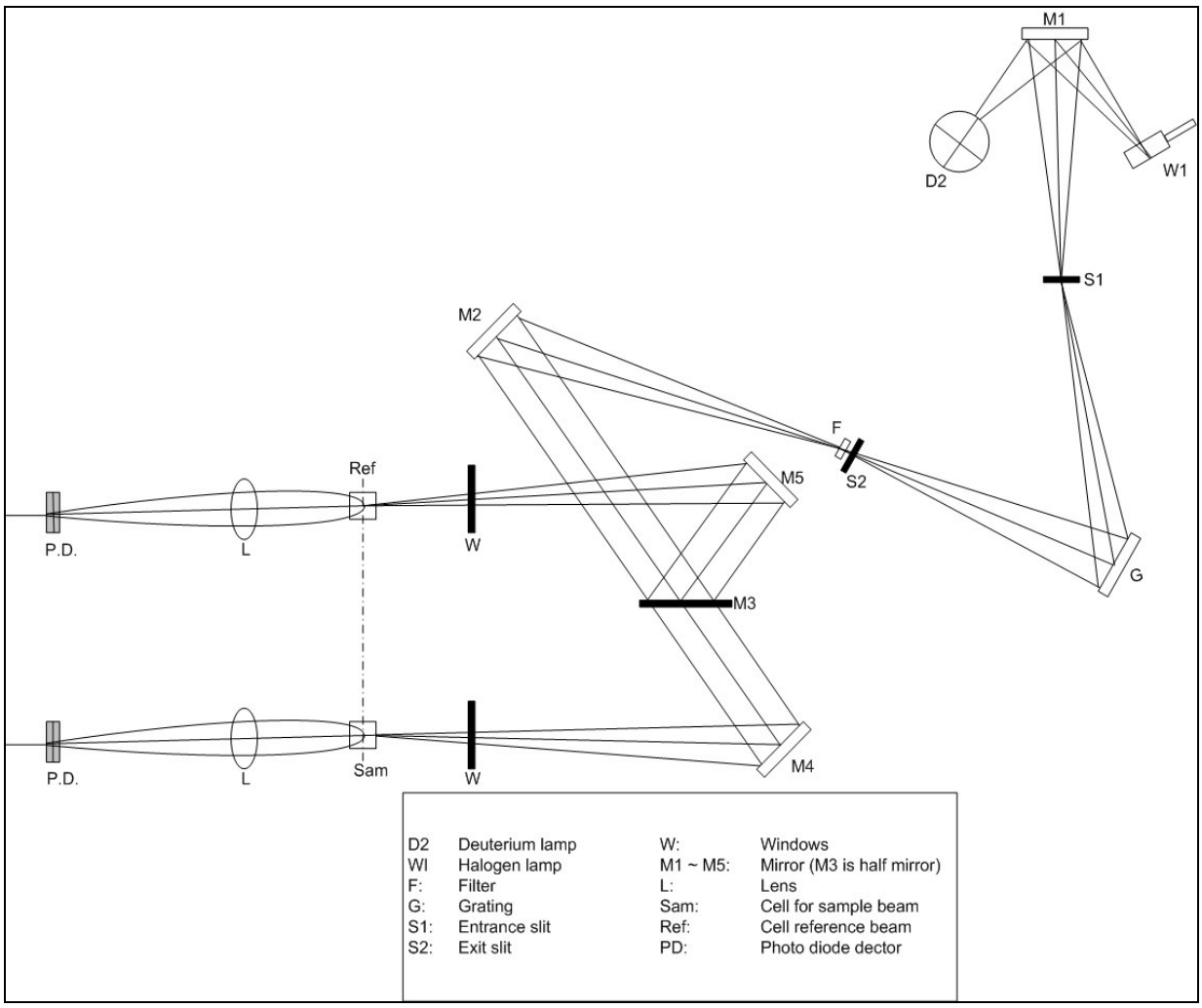

Figure 3.6. The optical schematics of the UV-1650PC instrument.[10]

3.4.1.1 Incorporating fibre optics

The use of fibre optics to modify a UV-Vis instrument (Option B) for measurement of PC parameters has been previously described by Lee et al.[11] Fibre optic cables were used to focus both the excitation and deactivation light sources and align them in the instrument so as to fall onto the sample at a 45º angle to the monitoring beam. The use of a fibre optic cable allows non-uniform irradiation from light sources such as arc lamps to be mixed inside the fibre channel to produce more coherent irradiation.[12] The capability of a fibre optic cable (1mm diameter) to let light through at 365nm (using the deuterium lamp) and at 633nm (using the tungsten lamp) was tested on an open-bench spectrophotometer (Figure 3.7). Signals for both wavelengths could be obtained with a H30DS spectrophotometer (Zeiss).

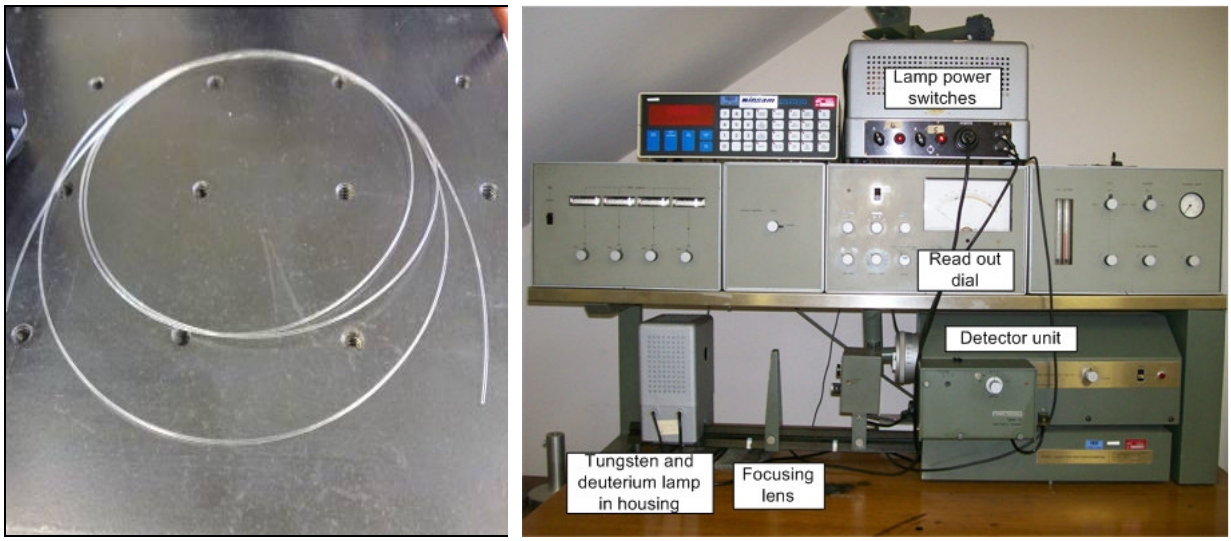

(a) (b)

Figure 3.7. Photographs of: (a) a fibre optic cable, and (b) the Zeiss H30DS spectrophotometer.

The use of a fibre optic cable allows activation or deactivation inside the instrument with the lid completely closed, while simultaneously measuring absorbance as irradiation is emitted. In order to disperse the light entering the instrument from a fibre optic cable, a lens is needed to cover the 1x10mm section of the monitoring beam with irradiation. The fibre optic cable must irradiate the sample at a 45º angle to the monitoring beam. In the UV-1650PC instrument the fibre optic system could not be incorporated in the space available because the fibre optic can not bend in a radius of less than 5cm, and only 4cm was available to fit the cable and lens into the instrument. The option of using a fibre optic system inside the UV-Vis instrument set-up was not available and therefore Option B had

to be implemented, making use of lenses and mirrors to reflect the light from the source into the instrument and onto the sample.

3.4.2 Activation light sources

3.4.2.1 Handheld UV lamp

Model:

A long wavelength (365nm) UV radiation lamp (Spectroline model ENF 260C/FE).

Set-up requirements:

A handheld UV lamp can be used to irradiate the sample outside the UV-Vis instrument (Option A).

Experimental:

The test film (Exp 17), mounted in the film holder accessory, was placed in a dark cupboard. The UV lamp was placed approximately 5cm away from the sample and an intensity of 1mW/cm^2 was measured after a warm up time of 30min. The test film of Exp 17 was used to determine whether this irradiation would be sufficient for activation. Upon irradiation, immediate activation from the closed colourless to the open pink form was observed (Figure 3.8).

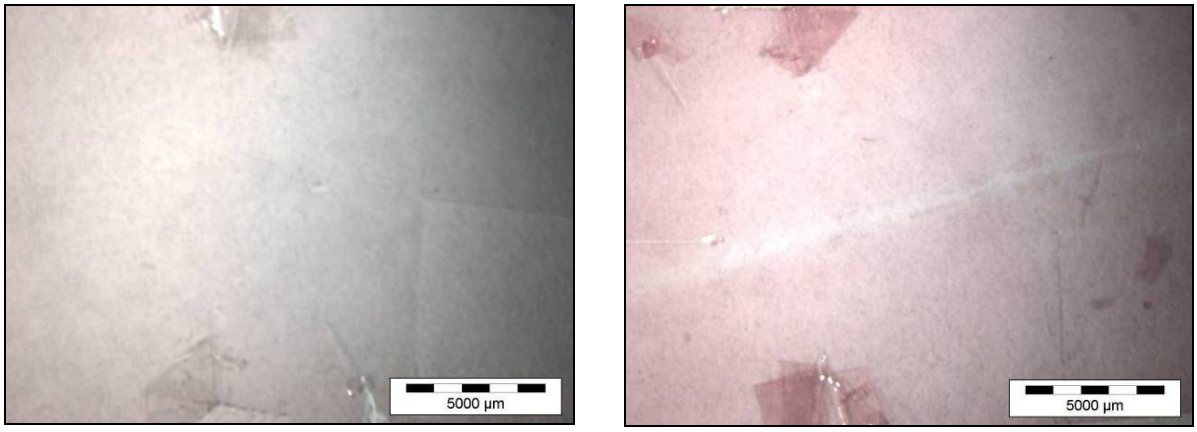

(a) (b)

Figure 3.8. Exp 17 film (a) before irradiation and (b) after 5min irradiation with a handheld UV lamp at 365nm.

The film was irradiated for 1, 5 and 10min respectively and the absorbance recorded before and after 0, 5, 10 and 30min for each irradiation period. Results are shown in Table 3.3 and Figure 3.9.

Table 3.3. Exp 17: Handheld UV lamp absorbance

UV TLC	1min irradiation	5min irradiation	10min irradiation
Before irradiation	0.006	0.008	0.009
After irradiation	0.116	0.157	0.173
5min after irradiation	0.029	0.044	0.056
10min after irradiation	0.015	0.029	0.042
30min after irradiation	0.009	0.023	0.036

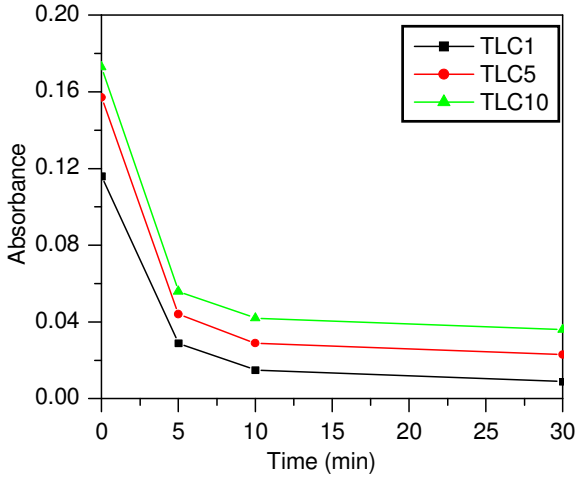

Figure 3.9. Exp 17: Handheld UV lamp absorbance decay over time

Results indicate that the longer the irradiation time the higher the absorbance of the film. During the first 5min of deactivation the sample that was irradiated for 10min showed the fastest rate of deactivation. From 10 to 30 minutes the rate of deactivation was similar for the different samples although the actual absorbance was higher for the sample with the longest irradiation time.

3.4.2.2 Mercury lamp

Model:

An Osram Hg 100 lamp was used in the experiment, which has several spectral lines, including a line at 365nm which emits 10.7% of the total irradiation intensity of the lamp. See Figure 3.1.

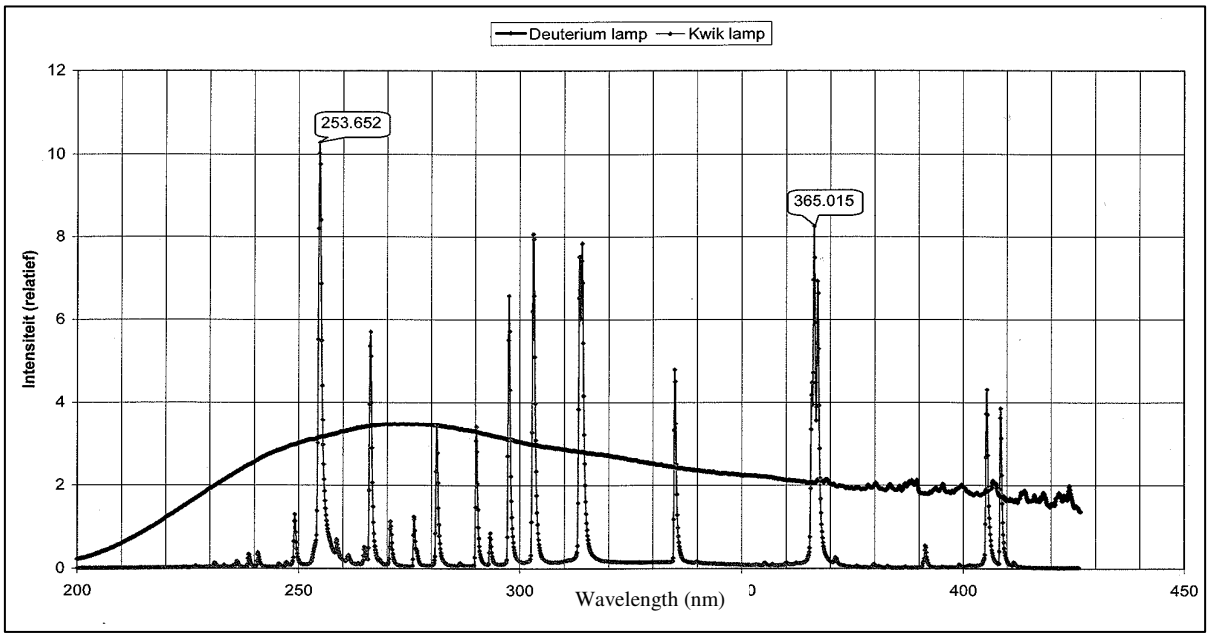

Figure 3.10. Spectral lines of the Osram Hg 100 (Kwik) and deuterium lamps measured with the Zeiss H30DS spectrophotometer.

Set-up requirements

A mercury lamp can be used to irradiate the sample outside the UV instrument (Option A) or it can be mounted on an optical bench with a lens to focus the light onto the sample (Option B, see Figure 3.11).

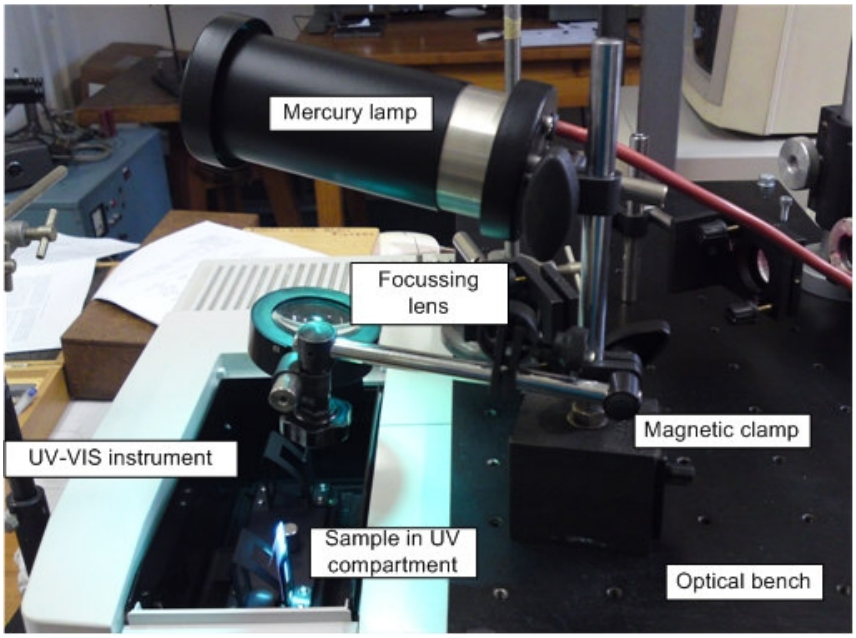

Figure 3.11. The Hg 100 lamp mounted on an optical bench.

Experimental:

After a warm-up time of 30min a light intensity of 23mW/cm^2 was obtained when the light source is used alone outside the instrument at a distance of approximately 5cm. When used in conjunction with a lens to focus the light source inside the UV-Vis instrument, an intensity of 35mW/cm^2 was obtained. Immediate activation of the test film of Exp 17 to a deep purple occurred when using this light source. As in the case of the handheld UV light source, samples were irradiated for 1, 5 and 10min respectively, and the absorbance recorded before and after 0, 5, 10 and 30min of irradiation (Table 3.4 and Figure 3.12).

Table 3.4. Exp 17: UV Hg100 lamp absorbance

Hg 100	1min irradiation	5min irradiation	10min irradiation
Before irradiation	0.002	0.013	0.039
After irradiation	0.196	0.255	0.263
5min after irradiation	0.044	0.08	0.102
10min after irradiation	0.021	0.052	0.075
30min after irradiation	0.013	0.039	0.061

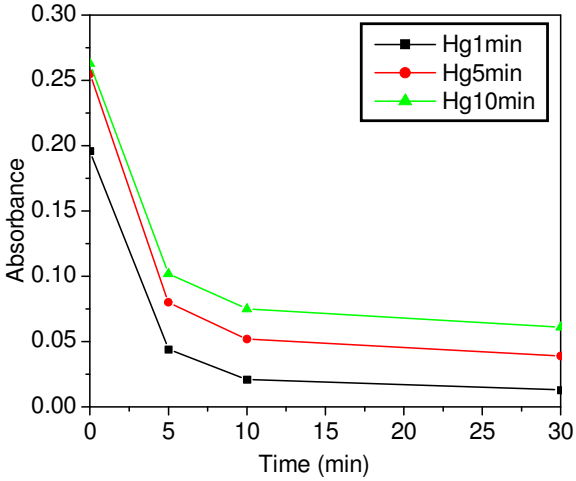

Figure 3.12. Exp 17: UV Hg100 lamp absorbance decay over time.

The intensity obtained using the Hg 100 lamp was much higher than with the handheld UV lamp. As reported in literature, higher intensity irradiation results in higher absorption measurements, and increase as the irradiation time increases.[13] Similar to observations made when using the handheld UV lamp, the deactivation rate after the first 10min becomes constant between the different irradiation periods and the actual absorbance is higher for the sample with the longest irradiation time.

3.4.2.3 UV LED

Model:

A high output chip-type UV LED (Nichia, model NCCU033G) with a wavelength of 360–370nm (Figure 3.13) was used in this evaluation.

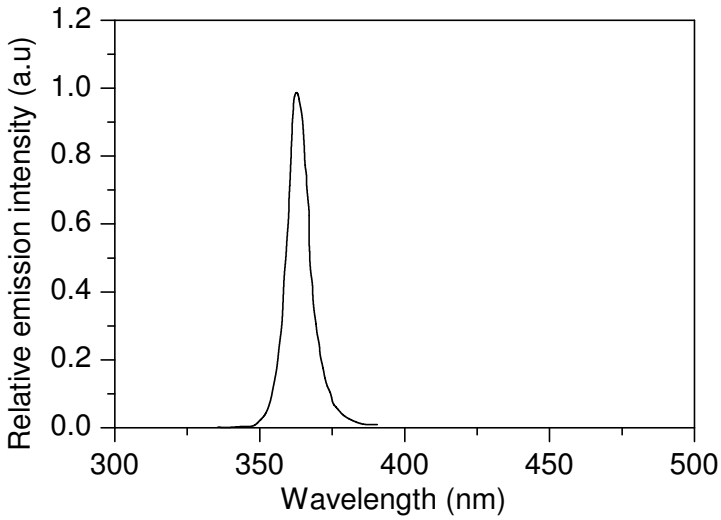

Figure 3.13. Nichia high output chip-type UV LED spectrum.[14]

Set-up requirements:

The UV LED (Figure 3.14) can be used to irradiate the sample outside the UV instrument (Option A). Alternatively, the front panel of the LED can be removed from its housing in order to mount the LED directly into the instrument (Option B, Figure 3.15). Using the LED inside the UV-Vis instrument requires a mirror to be mounted inside the instrument to reflect the light onto the sample. In order to protect the instrument's detectors from stray light, a manual shutter was used to close the detector path when switching the light source on and off. A hole was made in the front panel of the UV-Vis sample compartment through which the wires of the light source could be channelled, allowing complete closure of the compartment to block all stray light. The intensity of the UV light from the LED was controlled using a power supply (Manson 561902).

Figure 3.14. Nichia high output chip-type UV LED.

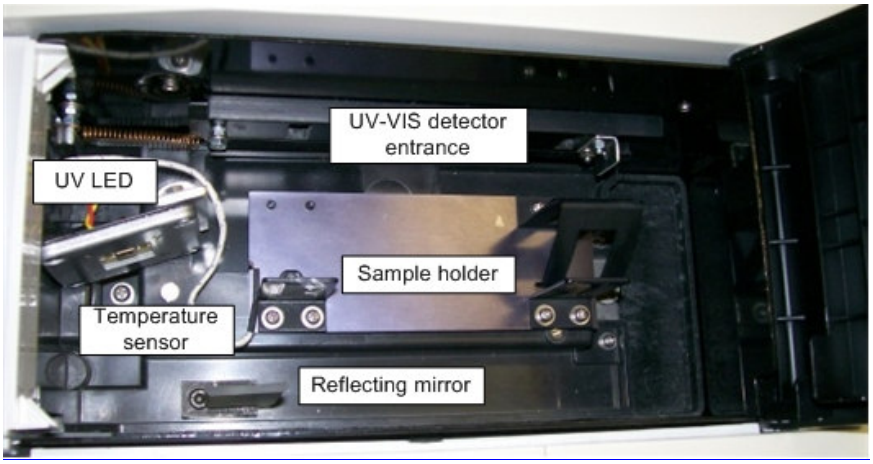

Figure 3.15. UV1650PC with chip-type UV LED.

Experimental set-up:

When using the LED outside the UV instrument, an intensity of 65mW/cm^2 was obtained at a distance of approximately 5cm. When mounting the UV LED in the instrument and using a mirror to reflect the light onto the sample, an intensity of only 1–1.5mW/cm^2 was measured on the sample area. The large reduction in intensity is most likely caused by the coating on the reflecting mirror.[9] Upon irradiation of the Exp 17 film, a pink/purple colour developed. Absorbance data at different irradiation intervals and thermal deactivation periods are given in Table 3.5 and displayed in Figure 3.16.

Table 3.5. Exp 17: UV LED absorbance

UV LED	1min irradiation	5min irradiation	10min irradiation
Before irradiation	0.009	0.010	0.008
After irradiation	0.076	0.124	0.137
5min after irradiation	0.018	0.035	0.041
10min after irradiation	0.011	0.022	0.028
30min after irradiation	0.010	0.017	0.023

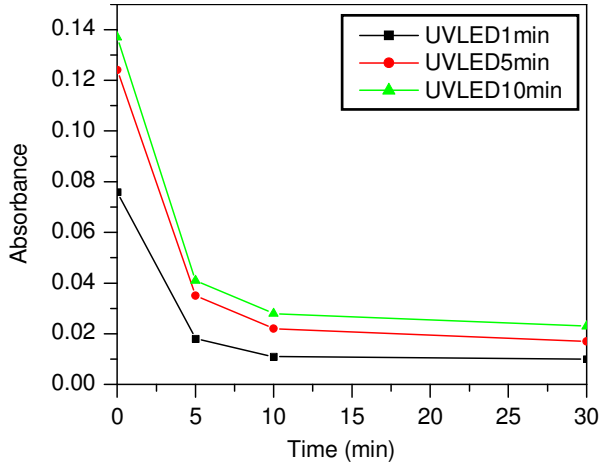

Figure 3.16. Exp 17: UV LED absorbance decay over time.

The UV LED chip in set-up Option B provided a slightly lower intensity than that obtained when using the handheld UV lamp. The intensity was much lower than obtained with the Hg 100 lamp, as is evident from the absorbance measurements. The deactivation rate was the highest for the sample with the longest irradiation time of 10min.

3.4.2.4 Deuterium lamp

Model:

A deuterium lamp from a Zeiss H30DS spectrophotometer lamp stand was used. It provides a line-free continuum from 180 to 400nm. See Figure 3.10 (Section 3.4.2.2) for the spectral output lines.

Set-up requirements:

The deuterium lamp from a Zeiss H30DS spectrophotometer lamp stand can be used to irradiate the sample outside the UV instrument (Option A).

Experimental:

The test film (Exp 17) in the film holder was placed approximately 8cm away from the deuterium lamp source. After a warm-up time of 30min, an intensity of 10mW/cm^2 was measured. Upon irradiation of the film of Exp 17 only slight activation from the closed and colourless form to the open and pink form was observed, even at long irradiation intervals (Table 3.6 and Figure 3.17).

Table 3.6. Exp 17: Deuterium lamp absorbance

UV DEUT	1min irradiation	5min irradiation	10min irradiation
Before irradiation	0.007	0.009	0.011
After irradiation	0.021	0.031	0.037
5min after irradiation	0.009	0.011	0.018
10min after irradiation	-	-	0.016
30min after irradiation	-	-	0.016

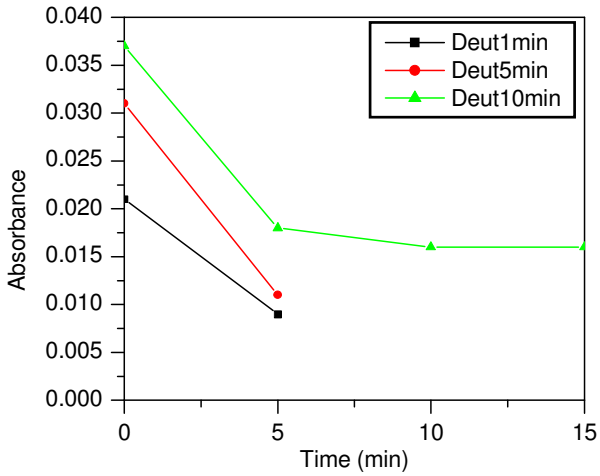

Figure 3.17. Exp 17: Deuterium lamp absorbance decay over time.

Thermal fading measurements for the samples irradiated for 1min and 5min were only recorded after 5min because samples were almost completely deactivated after this time period. The deuterium lamp had a higher intensity than the handheld UV lamp and the UV LED, but it had a much broader spectral output. A broad spectral output could minimise the effect of the irradiation intensity at 365nm for activation, because deactivation irradiation is also present. The deuterium set-up showed very low absorbance values compared to values of the other light sources.

3.4.2.5 Activation light source comparison

Results of the evaluation of the activation light sources for the PC dyes, in terms of the following properties, can be summarised as in Table 3.7.

Table 3.7. Summary of the evaluation of properties of various light sources used for the activation of PC films

Properties	**UV lamp**	**Mercury lamp**	**UV LED**	**Deuterium lamp**
Immediate activation of sample	x	x	x	x
High intensity		x		
Narrow spectral output	x		x	
No warm-up period			x	
Stable irradiation source			x	
Low heat dissipation			x	
Long lifetime (10 000hr)			x	
Multiple/fast switching on/off possible			x	
Instrumental set-up limited to Option A, i.e. time delay	x	x		x
Instrumental set-up Option B is feasible			x	

From the activation data of the different light sources over time (Figure 3.18) it was evident that the mercury lamp set-up provided the highest absorbance (colouration).

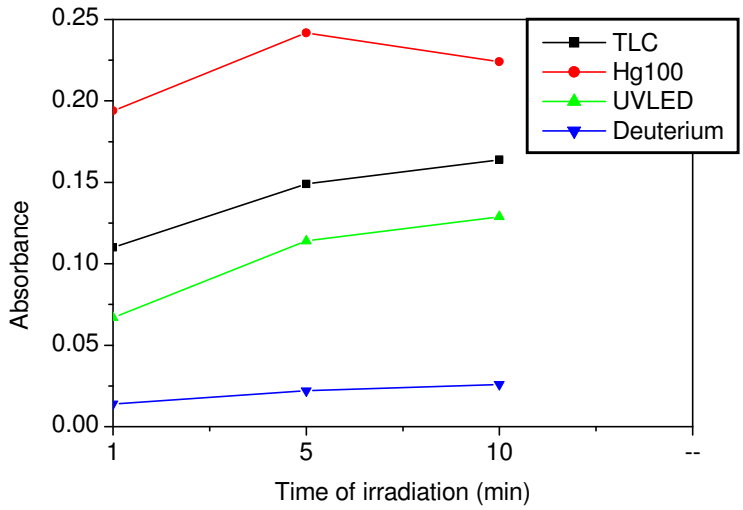

Figure 3.18. Absorbance comparisons of activation light sources: (a) TLC lamp, (b) mercury lamp, (c) UV LED, and (d) deuterium lamp

Taking warm-up time, irradiation stability, light source lifetime, operating temperature and the instrumental configurations into consideration, it emerged that the UV LED provided more accurate quantitative data while monitoring activation and deactivation in-situ; hence it was used for subsequent evaluations with the different deactivation sources.

3.4.3 Deactivation light sources

The UV LED was used as the most constant light source to evaluate the deactivation light sources, Initially, the time taken for a thin film to reach the photostationary state with the UV LED was determined (Figure 3.19). The film was placed in the sample compartment and the activation was measured while the sample was irradiated. When the photostationary state was reached the UV LED was switched off and the deactivation was measured.

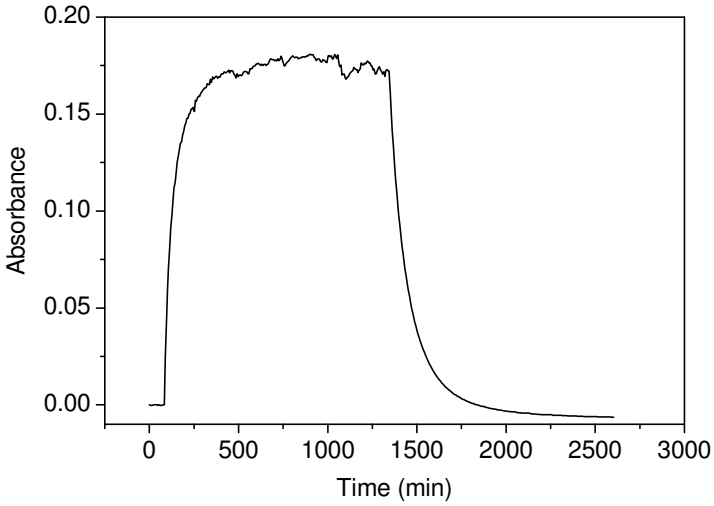

Figure 3.19. Activation kinetics of Exp 17 irradiated with UV LED.

From the activation kinetics it was determined that the thin film requires at least 15min of UV LED irradiation to reach the photostationary state This irradiation period was subsequently used in further analysis with the different deactivation light sources.

Firstly, the deactivation kinetics of the test film (Exp 17) was determined without the use of a deactivation light source, prior to evaluating different deactivation light sources. Measurements were taken in the dark (i.e. while the sample was in the instrument) at 23°C to evaluate the thermal deactivation over time (Table 3.8 and Figure 3.20).

Table 3.8. Exp 17: Thermal deactivation

Time	Absorbance
Initial	0.006
After 15min UV LED irr.	0.131
5min in dark	0.039
10min in dark	0.030
15min in dark	0.028
20min in dark	0.026
25min in dark	0.025
30min in dark	0.024
35min in dark	0.024
40min in dark	0.024
50min in dark	0.023
55min in dark	0.023
60min in dark	0.023

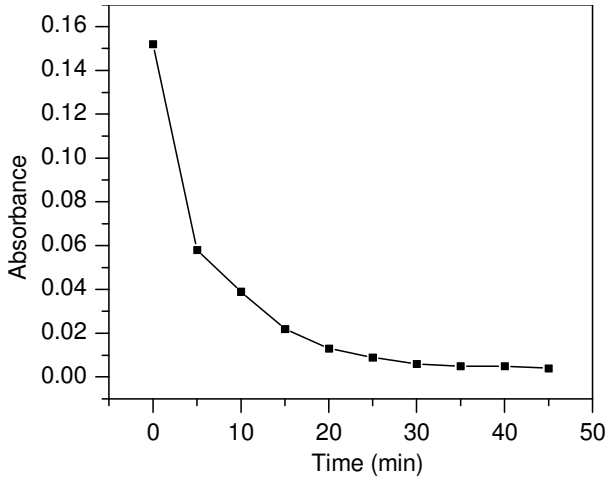

Figure 3.20. Exp 17: Thermal deactivation.

3.4.3.1 A He-Ne laser

Model:

The He-Ne laser used was a Siemens LGK 7653 with a maximum power of 25mW/cm^2 and a wavelength of 633nm.

Set-up requirements:

The He-Ne laser can be used to irradiate the sample outside the UV instrument (Option A) or it can be mounted on an optical bench to focus the light onto the sample (Option B; Figure 3.21). The light from the He-Ne laser was expanded using a concave lens and then focussed with a convex lens onto a reflecting mirror to channel the light into the instrument (Figure 3.22). The light from the He-Ne laser covered the 1mm wide and 10mm high area of the monitoring beam of the instrument.

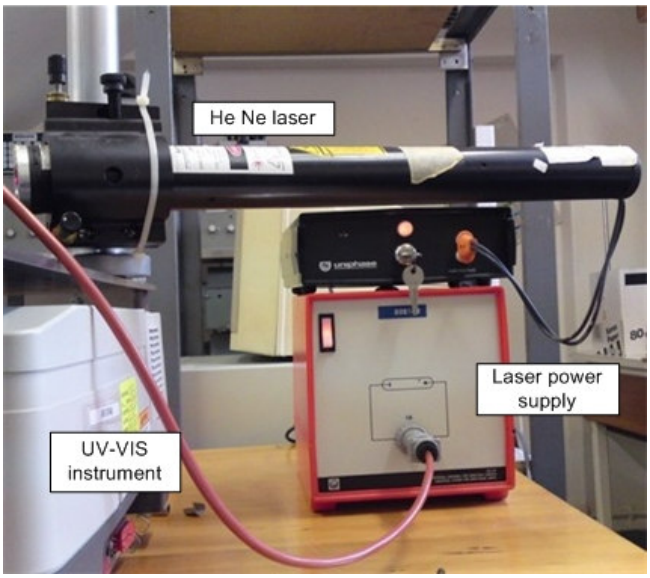

Figure 3.21. The He-Ne laser.

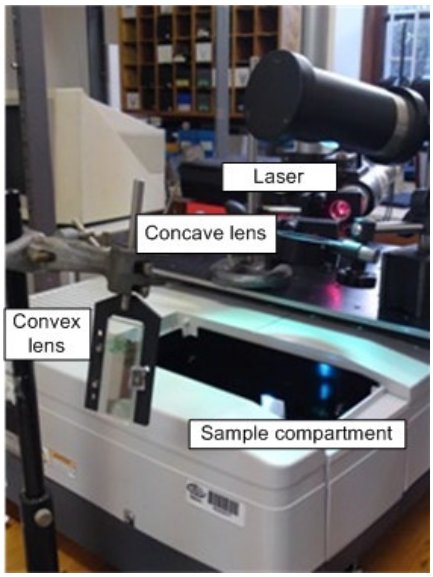

Figure 3.22. The He-Ne laser light path.

Experimental:

A light intensity of 0.5mW/cm^2 can be obtained when the light source is used outside the instrument at a distance of approximately 10cm from the sample. When used in combination with the lenses and the mirror to focus the light source inside the UV-Vis instrument, an intensity of 0.4mW/cm^2 was obtained.

The absorbance of the test film (Exp 17) was recorded before and after a 15min irradiation period with the UV LED. During the first 10min after irradiation thermal activation occurs fast. The sample was left in the instrument and the absorbance after 5min and 10min was recorded. To force further deactivation, the sample was subjected to irradiation from the He-Ne laser. The absorbance was recorded as the time of irradiation increased (Table 3.9 and Figure 3.23).

Table 3.9. Exp 17: He-Ne laser deactivation

Time	Absorbance
Initial	0.004
After 15min UV LED irr.	0.144
5min in dark	0.048
10min in dark	0.034
5min HeNe irr.	0.018
10min HeNe irr.	0.015
15min HeNe irr.	0.013
20min HeNe irr.	0.011
25min HeNe irr.	0.010
30min HeNe irr.	0.006
35min HeNe irr.	0.006
40min HeNe irr.	0.006
50min HeNe irr.	0.006

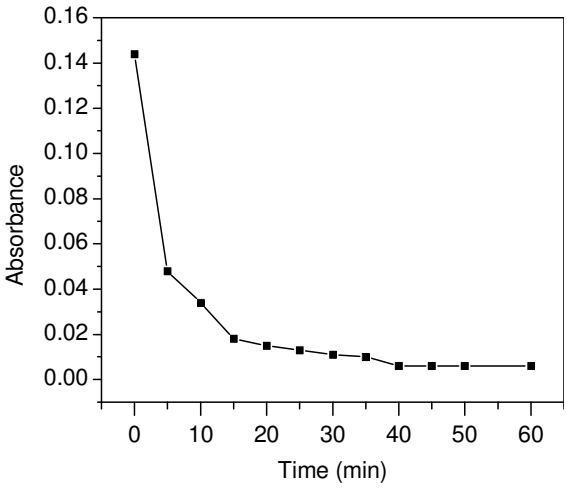

Figure 3.23. Exp 17 He-Ne laser deactivation.

3.4.3.2 Visible light LEDs

Model:

A clear Ultra Red LED104 (Microtec) with a peak wavelength of 630nm (Figure 3.24) was used.

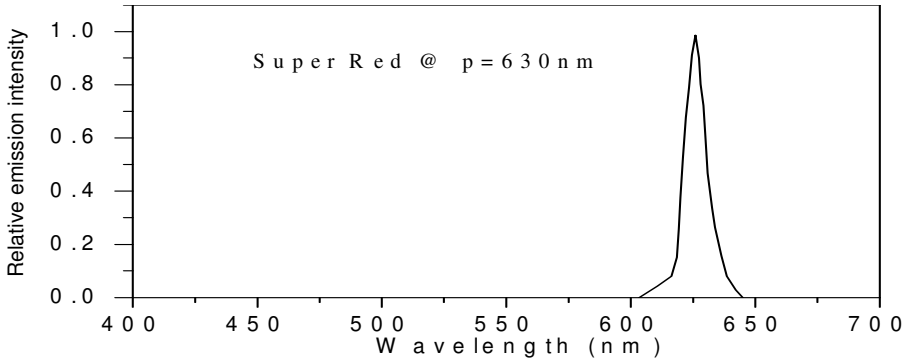

Figure 3.24. Spectral lines of the Microtec Ultra LED 104.[15]

Set-up requirements:

The Vis LED can be used to irradiate the sample outside the UV-Vis instrument (Option A; Figure 3.25) or it can be built into the instrument (Option B). To test the ability of the Vis LED to deactivate the test film (Exp 17) the LED was coupled to a power supply (Manson 561902).

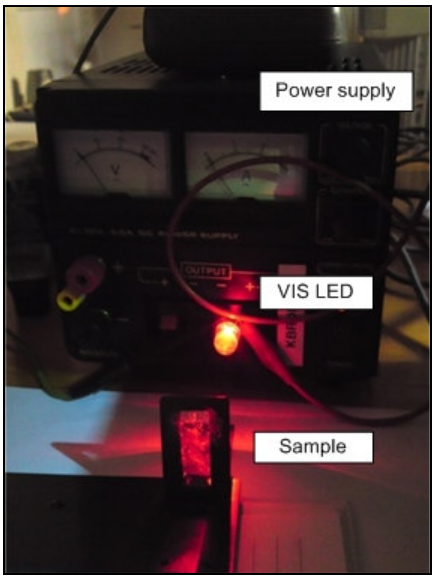

Figure 3.25. The Clear Ultra Red LED104.

Experimental:

The test film (Exp 17) was placed 1cm from the light source. An intensity of 5mW/cm^2 was recorded. Absorbance was recorded before and after 15min of irradiation with the UV LED, and 5min and 10min after thermal deactivation, and with forced deactivation with the Vis LED at different time intervals (Table 3.10 and Figure 3.26).

Table 3.10. Exp 17: Vis LED deactivation

Time	Absorbance
Initial	0.007
After 15min UV LED irr.	0.120
5min in dark	0.042
10min in dark	0.029
5min Vis LED irr.	0.035
105min Vis LED irr.	0.032
15min Vis LED irr.	0.028
20min Vis LED irr.	0.028
25min Vis LED irr.	0.027
30min Vis LED irr.	0.024

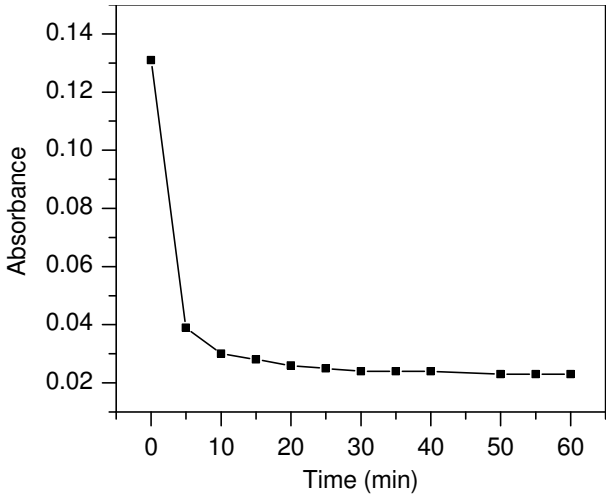

Figure 3.26. Exp 17: Vis LED deactivation.

3.4.3.3 Tungsten lamp

Model:

A tungsten lamp from a Zeiss H30DS spectrophotometer lamp stand was used. It provides a line-free continuum from 300 to 1000nm (Figure 3.27).

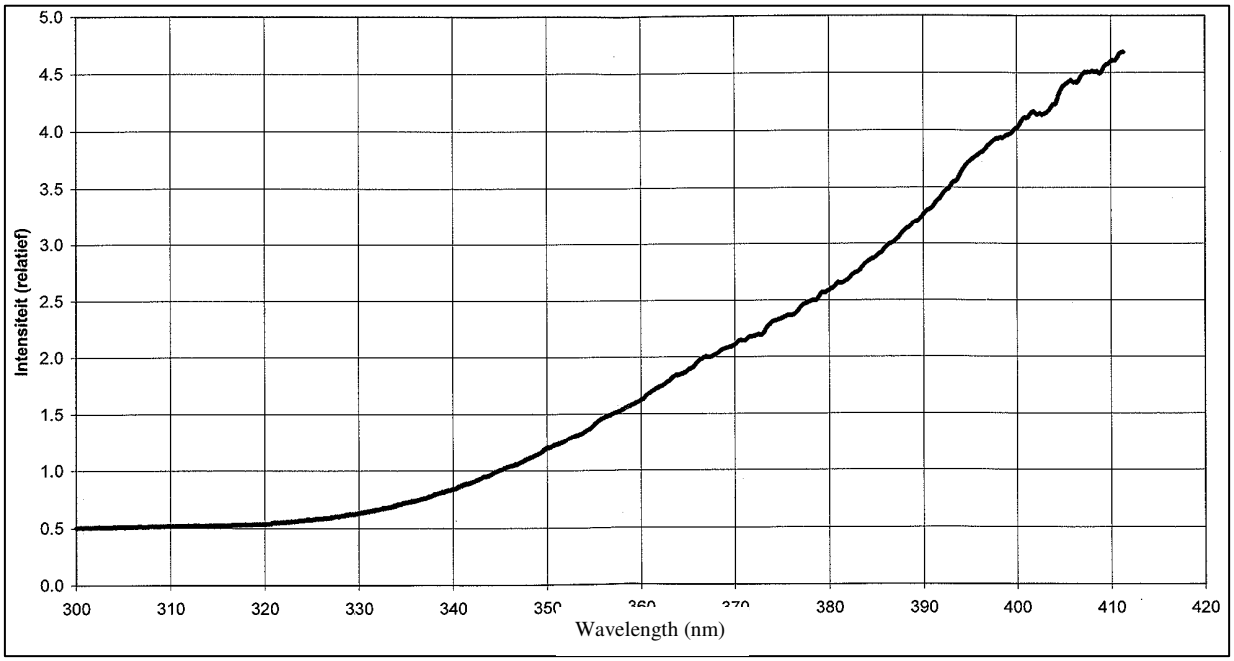

Figure 3.27. Spectral lines of the Zeiss H30DS tungsten lamp.

Set-up requirements

A tungsten light source was used in the experimental set-up Option A. The tungsten lamp has a spectral output in the region 300 – 400nm, which is capable of activation of the MC species. To eliminate activation of the dye, a colour filter (Schott OG 570, Figure 3.28) was used to cut off irradiation below 570nm (Figure 3.29).

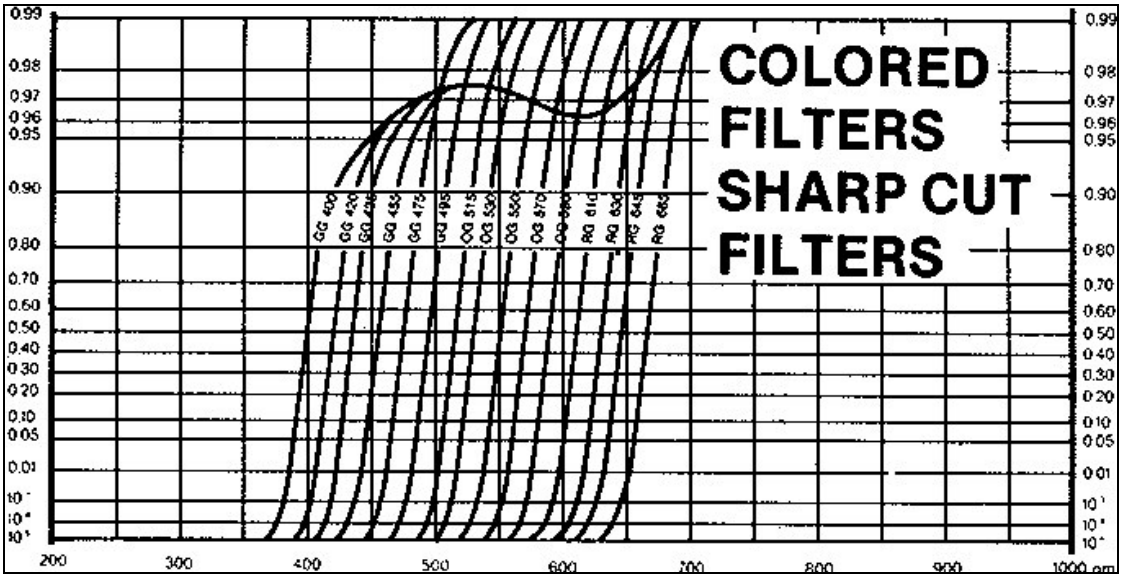

Figure 3.28. Spectral lines of the Schott OG570 filter.[14]

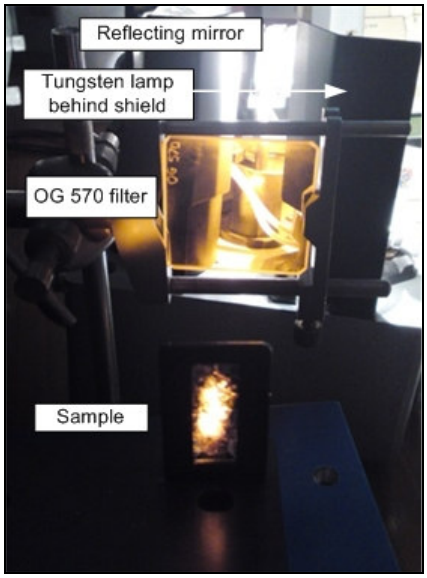

Figure 3.29. Tungsten lamp with Schott OG 570 filter.

Experimental:

The tungsten light source was 5cm from a reflecting mirror, which was 7cm from the cut-off filter. The test film (Exp 17) in the film holder was placed on a lab jack approximately

5cm away from the tungsten lamp source. After a warm-up time of 30min, an intensity of 65mW/cm^2 was measured. The absorbance of the test film before and after irradiation with the UV LED, after thermal deactivation and after forced deactivation with the tungsten filter set-up, was recorded over time (Table 3.11 and Figure 3.30).

Table 3.11. Exp 17: Tungsten lamp deactivation

Time	Absorbance
Initial	0.012
After 15min UV LED irr	0.152
5min in dark	0.058
10min in dark	0.039
5min Tungst. irr.	0.022
10min Tungst. irr.	0.013
15min Tungst. irr.	0.009
20min Tungst. irr.	0.006
25min Tungst. irr.	0.005
30min Tungst. irr.	0.005
35min Tungst. irr.	0.004

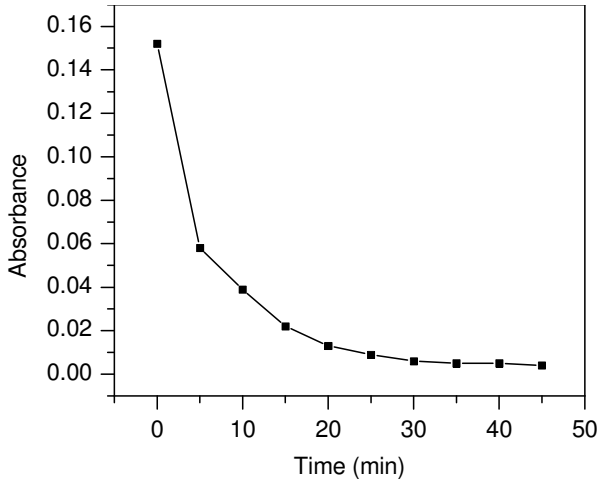

Figure 3.30. Exp 17: Tungsten lamp deactivation.

3.4.3.4 Deactivation light source comparison

After an evaluation of the deactivation light sources for the PC dyes the following properties are ascribed to the different light sources (Table 3.12).

Table 3.12. Summary of the evaluation of properties of various light sources used for the deactivation of PC films

Properties	**He-Ne laser**	**Vis LED**	**Tungsten lamp**
High intensity			x
Narrow spectral output	x	x	x*
No warm-up period		x	
Stable irradiation source		x	x
Low heat dissipation		x	
Long lifetime (10 000hr)		x	
Instrumental set-up limited to Option A, i.e. time delay	x		x
Instrumental set-up Option B is feasible		x	

*Note: The tungsten lamp required cut-off filters to narrow the spectral output.

To compare the percentage deactivation attainable with each light source, data were normalised against the absorbance after the 15min UV LED irradiation (Table 3.13 and Figure 3.31). Data for the 5min and 10min intervals were obtained via deactivation in the dark. After a total period of 15min the respective light sources were switched on to induce further deactivation.

Table 3.13. Deactivation light source comparisons

Time (min)	Dark	HeNe irr.	Vis LED irr.	Tungst irr.
0	100	100	100	100
5	29.77	33.33	35.00	38.16
10	22.90	23.61	24.17	25.66
15	21.37	12.50	29.17	14.47
20	19.85	10.42	26.67	8.55
25	19.08	9.03	23.33	5.92
30	18.32	7.64	23.33	3.95
35	18.32	6.94	22.50	3.29
40	18.32	4.17	20.00	3.29

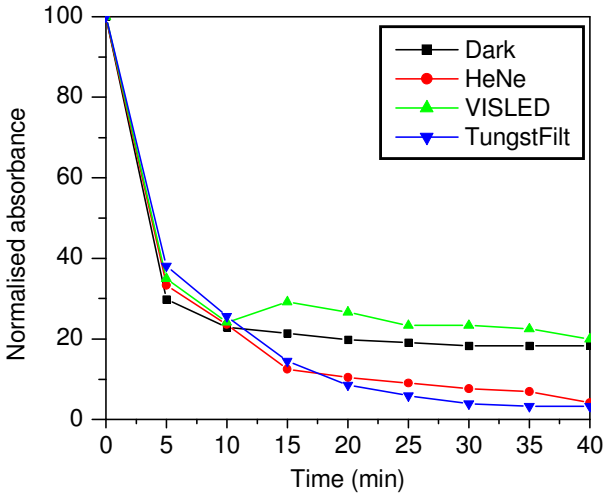

Figure 3.31. Deactivation light source comparisons.

From the experimental data (Table 3.13) it is evident that the tungsten lamp with filter is most effective in accomplishing complete deactivation of the open form of the dye back to the closed form in the latex film. If complete deactivation is required, the tungsten lamp with filter can be used to minimise the absorbance. This deactivation can however not be monitored with the sample inside the instrument.

3.4.4 Optimal set-up

In order to obtain reproducible and quantitative PC kinetic data, the intensity, warm-up time, irradiation stability, operating temperature, lifespan and the possibility of fast on/off switching of the irradiation sources were considered in order to identify the optimal set-up. The UV LED did not result in the highest colourability of the PC film due to the lower intensity from the reflective mirror. However, this light source outperformed the other sources in all of the other evaluation criteria. Light loss after reflection was mainly due to: (i) scattering of dust particles from the surface and (ii) absorption of light by the alumina surface layer on the mirror, and which was more pronounced in the UV region.[16] Due to

the lower irradiation it was possible to perform in-situ measurements of the activation and deactivation of the test film of Exp 17 under irradiation at 365nm and thermal bleaching. The lower intensity of the UV LED was favourable and it did not cause accelerated degradation that is possible at higher optical power. In literature references an optical power of 5mW is often used for activation measurements for this specific reason.[17]

The in-situ measurements of PC data with the UV LED should be evaluated for repeatability of kinetic data. In kinetic measurements the temperature plays a critical role and therefore the temperature inside the sample compartment should be monitored to ensure that samples are measured at the same temperature. In-situ deactivation can only be measured for the thermal decay process. By obtaining measurements at the same temperature a comparison of half-lives for the different experimental formulations can be made. Cyclisation measurements can be made via UV LED activation and thermal decay cycles. For fatigue resistance, where complete deactivation is required before measuring the colourability of the film, the tungsten lamp with a OG570 filter can be incorporated. The repeatability of all the kinetic data, using the aforementioned analysis, should however first be determined.

The UV-Vis absorption measurements can be used to measure properties of transparent films, such as PC miniemulsions. Paint films produced from the miniemulsions can however not be analysed via absorption UV-Vis since they will be opaque, and will therefore require reflectance UV measurements. Colourimetric measurements can be performed to obtain some quantitative data of opaque paint films.

3.4.5 Evaluation of photochromic kinetic data reproducibility

Films of Exp 17 and Exp 19, prepared with film applicators of different gap sizes, were used to test the reproducibility of the UV LED set-up. From the different films produced, the most uniform films (with similar mean thickness values) were selected with which to perform the repeatability experiments. Five samples of Exp 17 and Exp 19, 16-21µm thick, prepared with the 75µm cube film applicator, were selected for this evaluation.

A single activation/deactivation cycle was performed on each of the films and measured at λ_{max} values of 529nm and 595nm, respectively. To ensure optimal reproducibility the films were placed into the film holder of the UV-Vis instrument and the open area demarcated

(10x30mm). When deactivation was forced with the tungsten lamp the area exposed to the light was marked to ensure that the same 8x18mm area was deactivated each time. The films were positioned in such a manner that the light beam of the UV-Vis instrument (1x10mm) fell within the deactivated area. See Figure 3.32.

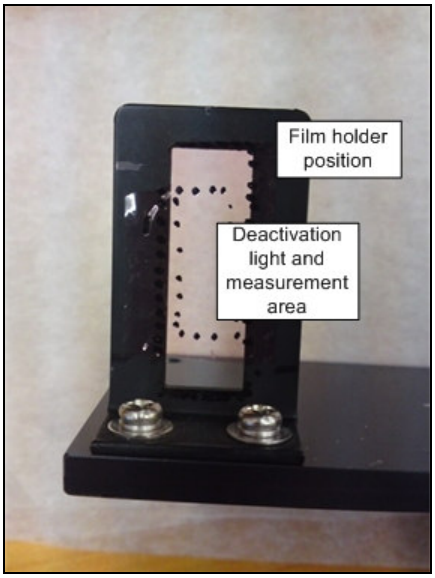

Figure 3.32. PC miniemulsion film demarcated for testing in the UV-Vis sample holder.

When the UV LED light source was switched on and then off again a fluctuation in the data was observed due to the difference in stray light entering the photodiode detector. The data series of each film had to be manually corrected for these fluctuations. From the corrected data the colourability, thermal decay constant and half-life could be determined for each sample. Figure 3.33 shows the raw activation/deactivation data for five samples of Exp 17, labelled (A–E).

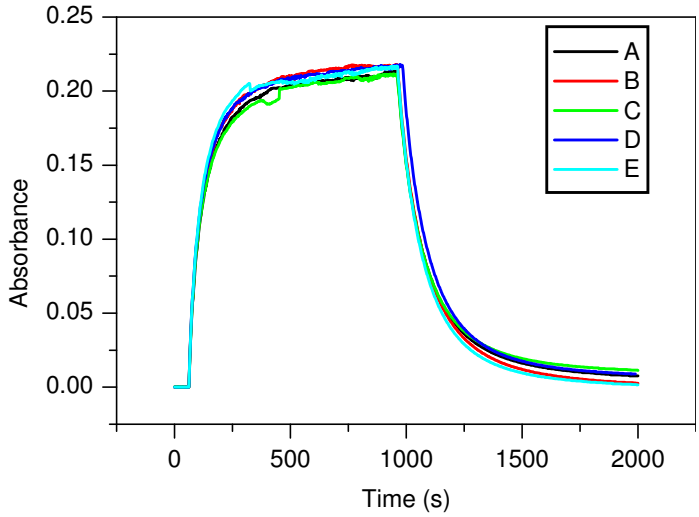

Figure 3.33. Exp 17: Repeatability of activation/deactivation scans at 529nm.

Mono-exponential fits were applied to the thermal decay curves, as indicated in Figure 3.34, to determine the thermal decay constant (k*f*) and the half-life ($t_{1/2}$). Using t1 from the first-order exponential decay fit k*f* was given as 1/t1.

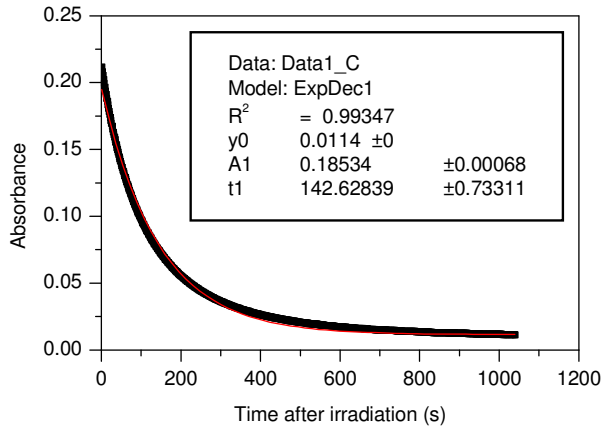

Figure 3.34. Thermal decay curve with mono-exponential fit (red line) for Exp 17 (75µm, Film C).

Results of all the PC kinetic data obtained for films of Exp 17 and Exp 19 are summarised in Table 3.19.

Table 3.14. Exp 17 and Exp 19: PC kinetic data

	Film thickness (µm)				**Colourability**		**Deactivation rate**		**Half-life $t_{½} = (\ln 2)/k$**	
	Mean	**Min**	**Max**	**Max – Min**	**ΔA_0**	**Percentage from mean**	**Decay constant (k_f)**	**Percentage from mean**	**Seconds**	**Percentage from mean**
Photosol 7-106, Exp 17										
A	18	17	18	1	0.2134	1.00	5.58E-03	11.46	124.26	11.90
B	20	19	21	2	0.2179	1.09	6.34E-03	0.60	109.40	1.48
C	18	18	19	1	0.2118	1.74	7.01E-03	11.23	98.86	10.97
D	19	18	20	2	0.2178	1.04	5.65E-03	10.35	122.64	10.44
E	20	19	23	4	0.2169	0.62	6.93E-03	9.97	100.06	9.89
AVERAGE					0.2156		6.30E-03		111.04	
Reversacol Palatinate Purple, Exp 19										
A	17	14	20	6	0.5232	7.36	2.31E-02	5.71	30.03	5.94
B	21	19	23	4	0.5253	7.79	2.47E-02	0.82	28.05	1.04
C	16	14	18	4	0.4647	4.64	2.52E-02	2.86	27.51	2.95
D	19	16	21	5	0.4451	8.66	2.56E-02	4.49	27.09	4.43
E	18	15	20	5	0.4783	1.85	2.39E-02	2.45	29.05	2.48
AVERAGE					0.3391		2.45E-02		28.346	

Each measurement taken for the average film thickness of every sample had an error of ±1µm. The mean thickness of 10 measurements is reported as well as the minimum and maximum values measured. The thickness range (indicated by the minimum value subtracted from the maximum, Max–Min) gives an idea of the homogeneity of the film. The UV-Vis instrument does not perform a point measurement since the beam covers a 1x10mm area and one should therefore consider the film homogeneity using multiple point measurements. In order to determine the reproducibility of the method, samples with a very narrow thickness range (i.e. very homogeneous samples) should be used. Films of Exp 17 were more homogeneous and colourability values were within a 2% range of each other. Films of Exp 19 were not very homogeneous and deviations of more than 8% were obtained in colourability measurements. Because of the non-homogeneity of the films, normalisation of data to the same film thickness would not be a true representation of the data. Where possible, films with a maximum thickness range of 4µm, and a difference of 2µm mean film thickness, should be used to keep the percentage deviation in colourability below 5%.

The fading kinetics for Exp 19 were very reproducible, with a 3s variation between the half-lives of the five measurements (6% maximum deviation from the mean). The films of Exp 17 showed much slower fading kinetics, which deviated significantly (12% deviation from mean) compared to the films of Exp 19.

Cyclability was evaluated using a Volt Line 24hr daily timer, with 15min intervals, allowing automatic on and off switching of the UV LED. Switching the UV irradiation on and off was performed to measure the decay of the colourability upon repeated activation and deactivation. For practical reasons a maximum of 50 cycles were performed.

Cyclisation data for Exp 17 (Figure 3.35) could not be corrected for the fluctuation from the stray light, and was therefore viewed as raw data. For Exp 19 (with faster deactivation time, Figure 3.36), data points were constructed for absorbance before and after each activation/deactivation cycle.

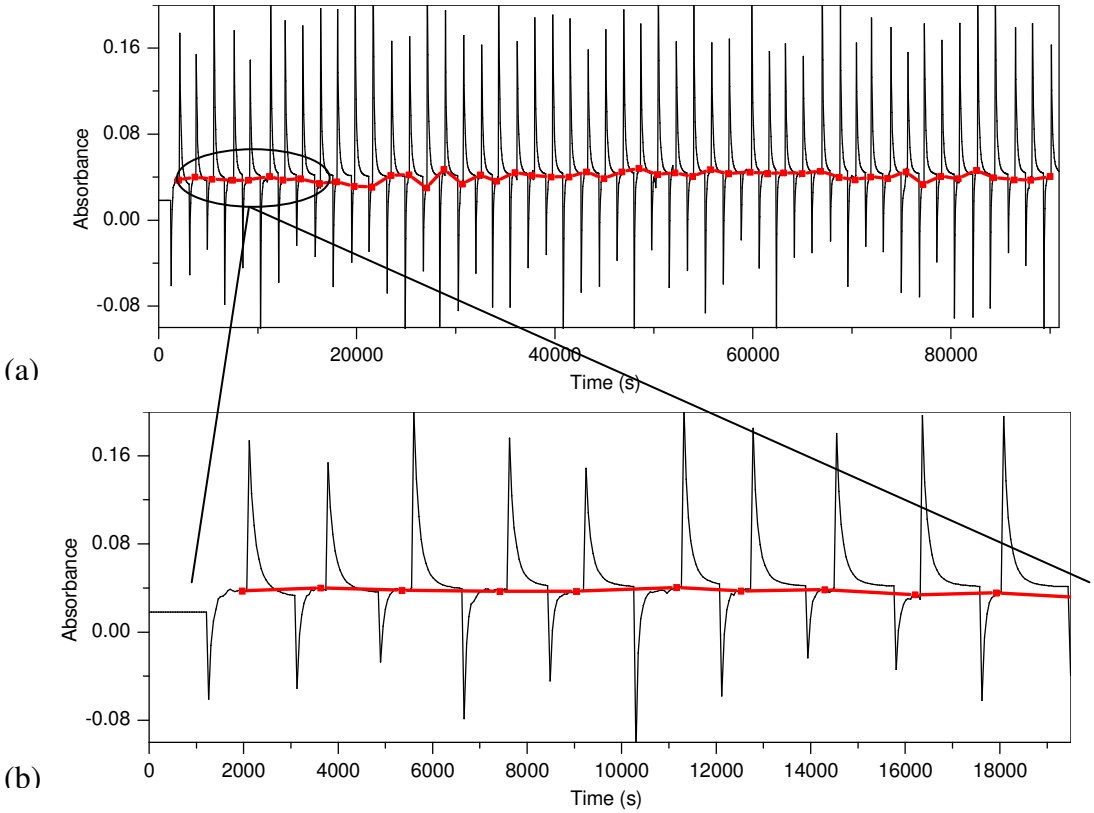

Figure 3.35. Cyclability measurement for Exp 17: (a) 50 cycles, (b) expansion of first 10 cycles (■ indicates colourability after each cycle).

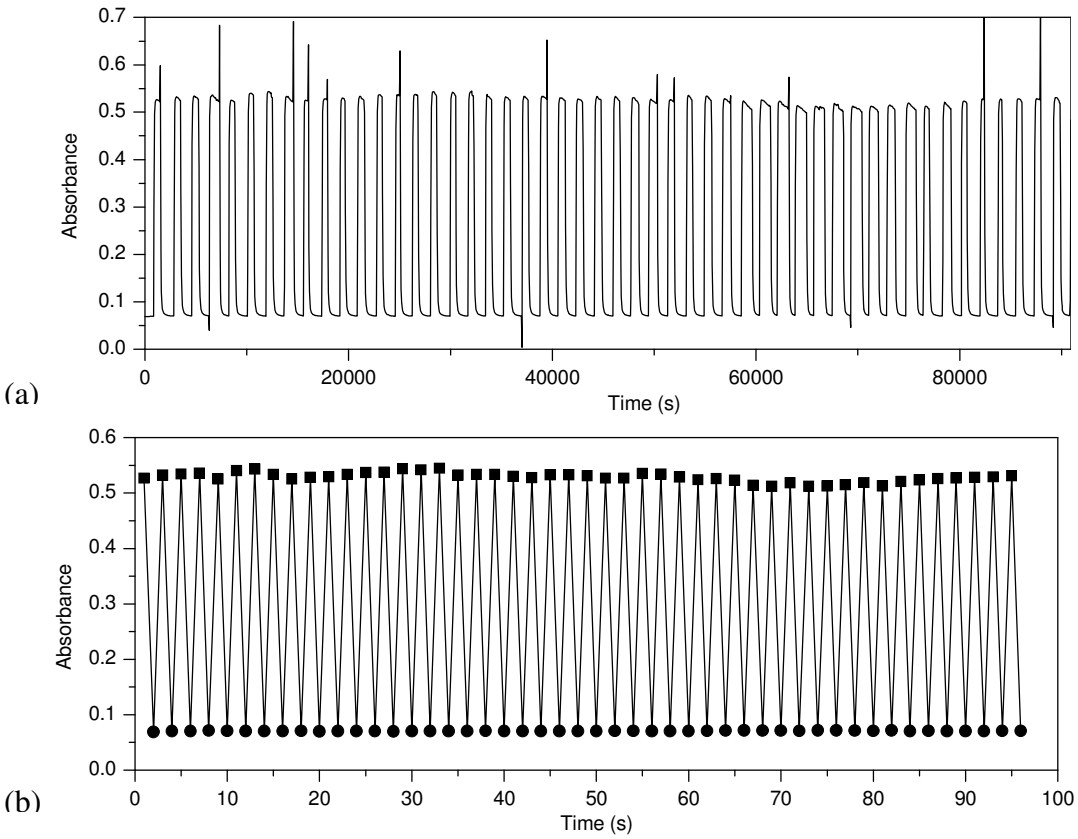

Figure 3.36. Cyclability measurement for Exp 19: (a) raw data from UV-Vis, (b) reworked data (■ indicates colourability after each cycle, • indicates absorbance after each decay).

During cyclisation measurements, data for Exp 17 showed much more deviation from the initial measurement (29%) than data for Exp 19, which showed a maximum deviation of 3% from the original value. Large deviations in between some cycles could be caused by incomplete deactivation of the Exp 17 sample. After fifty cycles of irradiation, samples from neither Exp 17 nor Exp 19 showed a significant decrease in colourability. Colourability after fifty cycles varied 8% and 0.77% from the original values for samples of Exp 17 and Exp 19, respectively. This was within the experimental error for the measurements.

Fatigue resistance was determined by placing films in an accelerated degradation (QUV) instrument and recording the colourability after every four hours of exposure until ΔA_0 reached half of its original value. Three films were used for each sample and the absorbance over time was recorded (see Table 3.15). Data were then normalised to the absorbance value at time zero for that specific film (Table 3.16) and colourability versus hours exposed to QUV plotted (Figure 3.37).

Table 3.15. Exp 17 and Exp 19: Absorbance values of fatigue resistance

Sample no.	**Fatigue kinetics (Absorbance at …hr QUV exposure)**								
	0	**4**	**8**	**12**	**16**	**20**	**24**	**28**	**32**
Photosol 7-106 Exp 17									
A	0.2168	0.1890	0.1810	0.1735	0.1752	0.1541	0.1328	0.1125	0.0847
B	0.2028	0.1855	0.1740	0.1698	0.1660	0.1365	0.1216	0.1086	0.0873
C	0.2225	0.1951	0.2015	0.1880	0.1666	0.1506	0.1281	0.1128	0.0921
Reversacol Palatinate Purple Exp 19									
A	0.5232	0.4633	0.4577	0.3875	0.3264	0.2638	0.1420	-	-
B	0.4451	0.4246	0.3758	0.3375	0.2612	0.2380	0.1151	-	-
C	0.4783	0.4562	0.4361	0.3977	0.2952	0.2021	0.0885	-	-

Table 3.16. Exp 17 and Exp 19: Normalised fatigue resistance data

Sample no.	**Fatigue kinetics (Absorbance normalised against time 0hr QUV exposure)**								
	0	**4**	**8**	**12**	**16**	**20**	**24**	**28**	**32**
Photosol 7-106 Exp 17									
A	100	87.1771	83.4871	80.0277	80.8118	71.0793	61.2546	51.8911	39.0683
B	100	89.0970	83.5735	81.5562	79.7310	65.5620	58.4054	52.1614	41.9308
C	100	87.6854	90.5618	84.4944	74.8764	67.6854	57.5730	50.6966	41.3933
Reversacol Palatinate Purple Exp 19									
A	100	88.5512	87.4809	74.0635	62.3853	50.4205	27.1407	-	-
B	100	95.3943	84.4305	75.8257	58.6834	53.4711	25.8594	-	-
C	100	95.3795	91.1771	83.1487	61.7186	42.2538	18.5030	-	-

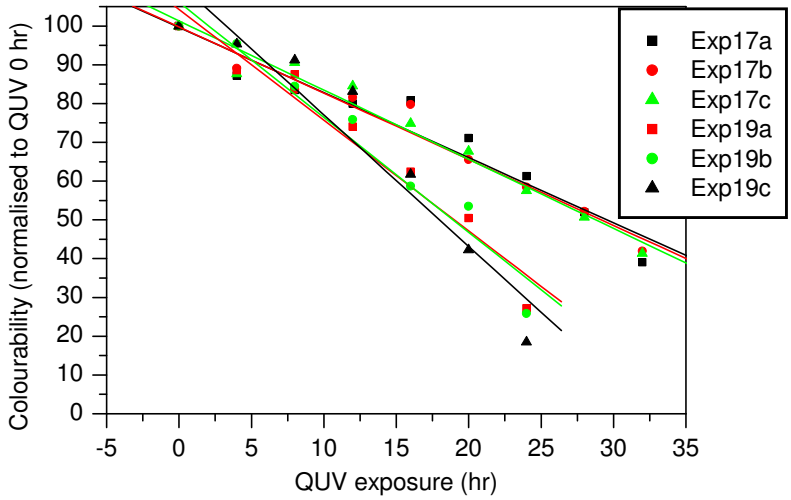

Figure 3.37. Exp 17 and Exp 19: Fatigue resistance.

After each four-hour cycle of QUV exposure care was taken to place samples in the sample holder in the same position to minimise variation of absorbance data. Results of triplicate analyses of the fatigue resistance for both Exp 17 and Exp 19 were in good correlation with each other. In order to make quantifiable conclusions a linear fit was plotted against each data set. Fatigue resistance was not completely linear but a straight line provided a good guide to distinguish between two samples. A correlation coefficient (R) of 1 indicates a completely straight line. A good fit to a straight line was obtained for each data set with standard deviations (SD) within the error of the measurement. Using the value of the slope from the straight line (M), equations can give a numerical assessment for the rate of fatigue. A steeper slope indicates faster fatigue kinetics, which was evident for samples of Exp 19 compared to those of Exp 17. See Table 3.17.

Table 3.17. Exp 17 and Exp 19: Linear fit to fatigue resistance data

Sample no	R	SD	M
Photosol 7-106 Exp 17			
A	-0.9681	5.0940	-1.6792
B	-0.9843	3.5832	-1.7059
C	-0.9848	3.6896	-1.7841
Reversacol Palatinate Purple Exp 19			
A	-0.9751	6.1457	-2.8566
B	-0.9758	6.2906	-2.9644
C	-0.9555	9.9255	-3.3947

3.4.6 Evaluation of photochromic kinetic data adherence to the Beer–Lambert law

Films of Exp 17 and Exp 19 prepared with 60, 75, 100 and 125µm film applicators, ranging from 10 to 35µm, were analysed to determine the effect of film thickness on PC kinetic data (Table 3.18).

Table 3.18. Exp 17 and Exp 19: Colourability vs. film thickness

Sample no.	Film uniformity properties (µm)				Colourability
	Mean	Min	Max	Max–Min	(ΔA_0)
Photosol 7-106 Exp 17					
A	10	10	11	1	0.1208
B	12	11	13	2	0.1400
C	13	11	14	3	0.1412
D	15	13	16	3	0.1825
E	18	17	18	1	0.2134
F	18	17	19	2	0.2082
G	18	17	19	2	0.2168
H	18	18	19	1	0.2118
I	19	18	20	2	0.2178
J	20	19	21	2	0.2179
K	20	19	23	4	0.2169
L	26	25	26	1	0.2548
M	29	28	30	2	0.2719
Reversacol Palatinate Purple Exp 19					
A	11	10	12	2	0.3344
B	12	11	14	3	0.3461
C	16	14	18	4	0.4264
D	17	14	20	6	0.5232
E	18	15	20	5	0.4783
F	19	16	21	5	0.4451
G	21	19	23	4	0.5253
H	27	26	29	3	0.5388
I	29	27	30	3	0.546
J	35	33	36	3	0.5764

Plotting the absorbance versus film thickness should give a straight line if the films adhere to the Beer–Lambert law. Data for Exp 17 and 19 were plotted in Figure 3.38 and linear fits imposed on the data. Table 3.19 gives the R value, SD and slope (M) of these linear fits.

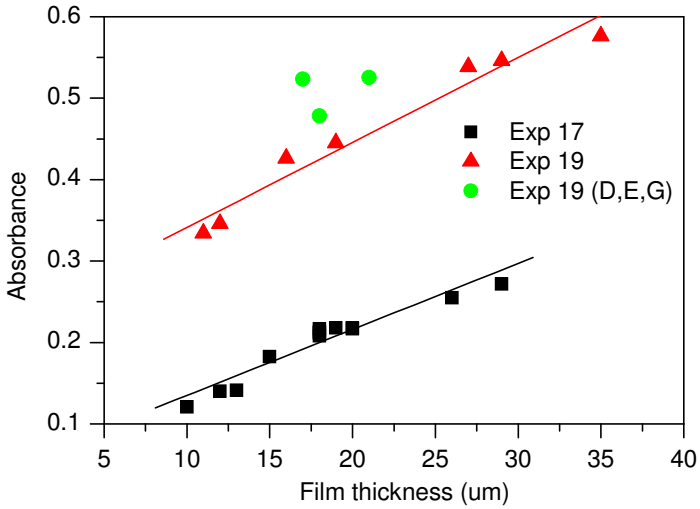

Figure 3.38. Exp 17 and Exp 19: Colourability vs. film thickness.

From the linear fits, colourability data of Exp 19 again show larger errors compared to the data of Exp 17, and some data points had to be disregarded. Points for Exp 19 D, E and G (circles in Figure 3.38) were eliminated from the linear fit because of the irregularities. The homogeneity of the films plays an important role. The variance in film thickness for the three films eliminated from the data was above 4µm.

Table 3.19. Exp 17 and Exp 19: Linear fit to colourability vs. film thickness data

Sample no	R	SD	M
Exp 17	0.9590	0.0131	0.0081
Exp 19	0.9800	0.0213	0.0104

Both sets of data conform to the Beer–Lambert law in the film thickness range 10–35µm and a PC dye concentration of approximately 1% on total formulation.

3.5 Discussion and conclusions

Conversion of the colourless, closed form of the PC species A to the coloured, open form of the species B in solution form was measured for a SNO (PP) and a chromene (PT) dye after activation with a handheld UV lamp. Quantitative evaluations were however not possible since the thermal backwards reaction occurs too fast. This reaction is severely hampered in the solid state. To obtain quantitative data of PC miniemulsions in the solid form (i.e. dried films) the following were reviewed: suitable samples had to be prepared, the best instrumental set-up with which to determine quantitative PC kinetic data had to be

evaluated and the most effective activating and deactivating light sources had to be identified.

The use of spin coating, solvent casting and film applicators were considered in order to obtain uniform coatings. The uniformity of the samples prepared using spin coating was evaluated by measuring the film thickness at the top, middle and bottom section of each slide. The coatings in the middle section of the slides were found to be thicker than at the edges. Films obtained with the solvent casting method exhibited a mottled effect and were not uniform. Applying samples with film applicators onto glass plates gave the most uniform coatings. The 75µm cubic film applicator gave the best results, with a maximum variation in thickness of 4µm across the sample area.

For the instrumental set-up, an in-situ method where activation and deactivation could be measured was preferable. The use of fibre optics for this was not feasible with the UV 1650 instrument due to space constraints inside the instrument. From the activation light sources that were evaluated only, the UV LED could be mounted inside the UV-Vis instrument to allow in-situ measurements. The handheld UV lamp, mercury lamp and deuterium lamp had to be used outside the UV-Vis instrument, which prevented monitoring of activation and delayed monitoring of deactivation. The mercury lamp showed the highest activation owing to its high intensity, but the UV LED source was preferred for the following reasons: suitability for in-situ measuring, no warm-up requirement, stable irradiation, low heat dissipation, and long lifetime. The He-Ne laser, Vis LED and tungsten source were used outside the UV-Vis instrument to impart deactivation of the coloured PC films. For complete deactivation of the films a tungsten light source, with a filter cutting off radiation with activation capability, was the most efficient, due to its high intensity.

Using the UV LED mounted inside the UV-Vis instrument for activation and the tungsten source with filter for deactivation, the reproducibility of kinetic data was evaluated. The film uniformity of each sample and the difference of the average film thicknesses between samples play an important role in evaluating reproducibility of the PC kinetics. For the more homogeneous chromene dye films the colourability measurements were more reproducible, however the fading kinetics, which are much slower than kinetics of the SNO dye, were less reproducible. For optimal reproducibility of kinetic measurements, films

with a maximum variation of 4µm between the minimum and maximum thickness should be used. The average film thickness of the replicate samples should preferably not vary by more than 2µm in order to minimise deviation to below 5%. A maximum of 50 cycles of activation and deactivation could be performed with the instrumental set-up used. During this period no decrease in colourability was observed for films either Exp 17 or Exp 19. The reproducibility of fatigue resistance between triplicate samples was very good. Linear fits plotted against the data gave a quantitative indication of the rate of fatigue; with a standard deviation below 10%. Applying the Beer–Lambert law to the colourability data of the two PC dyes incorporated in a concentration of 1% indicates adherence, as long as the films are homogeneous (less than 4µm difference in thickness).

In Chapter 4 the experimental set-up and kinetic measurements established in Chapter 3 will be applied to both miniemulsion and solution polymers incorporating PC dyes and a HALS stabiliser to improve fatigue resistance.

References

(1) Sigma-Aldrich Tetrahydrofuran specifications comparison; Sigma-Aldrich; 17 September 2009; http://www.sigmaaldrich.com/solvents.

(2) Leyland, V.,Reversacol Solubility data; James Robinson, *personal communication,* 2007.

(3) Durr, H.; Bouas-Laurent, H. *Photochromism: Molecules and Systems*; Elsevier Science Publishers: New York, 1990.

(4) Wilkinson, F.; Worral, D. R.; Hobley, J.; Jansen, L.; Williams, S. L. et al. *Journal of the Chemical Society, Faraday Transactions* **1996**, *92*, 1331.

(5) Koppetsch, K. J. MSc thesis, Worcester Polytechnic Institute, USA, 2000.

(6) Raboin, L.; Matheron, M.; Biteau, J.; Gacoin, T.; Boilot, J.-P. *Journal of Materials Chemistry* **2008**, *18*, 3242.

(7) Klukowska, A.; Posset, U.; Schotiner, G.; Jankowska-Frydel, A.; Malatesta, V. *Material Science: Poland* **2004**, *22*, 187.

(8) Crano, J. C.; Guglielmetti, R., J. *Organic Photochromic and Thermochromic Compounds*; Marcel Dekker: New York, 1999.

(9) Deutschlander, U.,UV instrumentation set-up; The Institute of Laser Research, US, *personal communication,* 2009.

(10) Instruction manual user's system guide UV-1650PC spectrophotometer; Shimadzu Corporation.

(11) Lee, B.; Kim, J.; Cho, M. J.; Lee, S. H.; Choi, D. H. *Dyes and Pigments* **2004**, *61*, 235.

(12) Carl Zeiss;Microscope light sources; 21 August 2009; http://zeiss-campus.magnet.fsu.edu.

(13) McArdle, C. B. *Applied Photochromic Polymer Systems*; Blackie & Son: London, 1992.

(14) Nichia Corporation brochure, Specifications for Nichia chip type UV LED.

(15) Microtec Ltd. brochure, Specifications for LED 10mm Clear Ultra Red (LED104).

(16) Knowles, A.; Burgess, C. *Techniques in Visible and Ultraviolet Spectrometry, Volume 3: Practical Absorption Spectrometry*; Chapman and Hall: London, 1984.

(17) Alvarez-Herrero, A.; Pardo, R.; Zayat, M.; Levy, D. *Journal of the Optical Society of America B* **2007**, *24*, 2097.

4 Experimental design of a miniemulsion system

4.1 Introduction

In Chapter 4 the experimental details for preparing miniemulsion and solution polymers of BMA and the subsequent analysis performed on these polymers are reported. First a design of experiments (DOE) was applied to obtain a stable BMA miniemulsion formulation. The optimised formulation was used to entrap a PC dye and a HALS stabiliser in the miniemulsion particles. These samples were compared to samples prepared in the conventional way of mixing dye and additives into a solution polymer. The colourability, fading kinetics and fatigue resistance of the samples were evaluated.

4.2 Experimental

4.2.1 Chemicals

AIBN (Fluka) was recrystallised from methanol (Merck, 99.9%), vacuum dried and stored at -12°C prior to use. n-BMA (Degussa, 99.5%) was washed with a 0.3M potassium hydroxide (Merck, 85%) solution to remove the inhibitor. The monomer was stored at 7°C on anhydrous magnesium sulphate (Merck, 62–70%) to prevent polymerisation before use and to remove any moisture. Hexadecane (Aldrich, 99%), THF (Aldrich, 99.9%), SDS (BDH Ltd., 99.5%), Photosol 7-106 (PPG), Reversacol Palatinate Purple (James Robinson, 99%) and Tinuvin 292 (Ciba) were used as received.

4.2.2 Miniemulsion preparation and polymerisation

The oil-soluble components were mixed in the monomer and the water-soluble components were separately mixed in deionised water. The respective solutions were mixed for 10min to obtain homogeneous solutions, after which the oil phase was added to the water phase. The combined solution was mixed at 600rpm for 1hr to obtain a pre-emulsion. The pre-emulsion was sonicated using a Vibracell Autotune series high intensity ultrasonic processor 750 VCX (Sonics & Materials Inc.) for 15min at 50% amplitude. Sample volumes of 100–150ml were sonicated before polymerisation. The sonicated pre-emulsions were transferred to a 250ml three-neck flask fitted with a condenser and nitrogen purge. Solutions were degassed with nitrogen (ca. 7ml/min) for 10min before

lowering them into a thermostatted oil bath at 60°C. Samples with PC dye present were shielded from direct light by covering the vessel in aluminium foil.

4.2.3 Solution polymerisation of butyl methacrylate

All the components of the formulation (bulk BMA solution polymer, Table B.4, Appendix B) were mixed and transferred to a three-neck flask with a condenser and nitrogen purge. The solution was degassed for 10min before lowering it into a thermostatted oil bath at 70°C to run the reaction under reflux. The PC dye (PP) and HALS stabiliser (Tinuvin 292) were mixed into the BMA solution polymer (as per Exp 27–Exp 30, Table B.4, Appendix B) using a Vortex Genie-2 mixer (Scientific Industries Inc.)

4.2.4 Analysis of photochromic miniemulsions and solution polymers

4.2.4.1 Percentage conversion

Conversion of the monomer to polymer (%TSC) was determined gravimetrically. Aliquots of approximately 1.5ml of the liquid latex were sampled through a rubber septum, using a needle and plastic syringe, at specified time intervals during the reaction. The aliquots were first air dried before placing them in an oven at 60°C for 2hr to achieve complete drying.

4.2.4.2 Particle size

Particles size analysis of the diluted samples was performed using a Malvern Zetasizer 1000HSa or Malvern NANO Z590. Analyses were based on the light scattering principle.

4.2.4.3 Morphology analysis using transmission electron microscopy

The morphology of the nanoparticles was studied via transmission electron microscopy (TEM). Samples were diluted (20 times) and stained with a uranyl acetate solution (2% in water). The stained samples were coated onto 200 mesh carbon-coated copper grids and left to dry. Images were acquired with a LEO 912 TEM operated at 120kW, and equipped with a 2kx2k pixel Proscan CCD camera.

4.2.4.4 Molecular weight

Molecular weight (MW) and molecular weight distributions (MWD) were determined using size-exclusion chromatography (SEC). Dried polymer samples were dissolved in THF (5mg/ml) and filtered through a 0.45µm filter. The SEC instrument comprised of a Waters 717 autosampler, Waters 1515 isocratic pump, Waters 2487 dual wavelength detector and Waters 2414 refractive index detector, run by Breeze software (Waters). THF prestabilised with 1mg/L butylated hydroxytoluene (BHT) was used as solvent at a flow rate of 1ml/min. Two PLgel 5um MIXED-C 300x7.5mm columns and a precolumn (PLgel 5um Guard 50x7.5mm) were used. The column oven was kept at 30°C and an injection volume of 100µl was used. The system was calibrated with narrow PSt standards ranging from 580 to 3,053,000g/mol. MW results are reported equivalent to linear PSt standards.

4.2.4.5 Photochromic kinetics

The miniemulsion and solution polymer samples were drawn down onto glass plates and the colourability, fading kinetics and fatigue resistance analysed as described in Chapter 3, Section 3.4.5.

4.2.4.6 Photochromic degradation

A Chemtra QUV instrument equipped with a UV-B lamp was used to study the fatigue resistance of PC films. The intensity of the UV-B lamps peaks at 313nm, with an irradiance of approximately 0.95 $W/m^2/nm$. Absorbance measurements were made after every 4 hours of exposure to UV light.

4.3 Experimental design of the butyl methacrylate miniemulsion

An experimental design was performed to evaluate three parameters that play an important role in the stability and rate of polymerisation of miniemulsions. A starting point formulation, based on work by Han et al.[1], where PC dye was encapsulated in a Sty matrix, was used (Table 4.1). The oil soluble initiator (AIBN) was chosen as the initiator system because this delivered the smallest size spherical nanoparticles.[2] The Sty monomer used was replaced in this study with a lower T_g monomer (n-BMA) to allow easier transition of the pi-orbitals of the PC species from the closed to the open form to increase colourability and allow faster deactivation than in more rigid matrices.[2] In miniemulsion polymerisation

a hydrophobe acts as a costabiliser to prevent diffusional degradation of the monomer droplets (Ostwald ripening).[1] The PC dye acts as a hydrophobe in the miniemulsion formulation; however, during the initial optimisation of the BMA miniemulsion formulation the PC dye was not included. A standard long-chain alkane (hexadecane) was used to provide stabilisation to the monomer droplets. SDS was used as a surfactant in the system. The total monomer concentration to aqueous phase (i.e. TSC) as well as the surfactant concentration was varied in the first phase of the experimental design to obtain the most stable miniemulsion at the highest TSC. In the second phase the initiator concentration was optimised to decrease the inhibition of the reaction and maintain a high reaction rate. After the BMA miniemulsion formulation was optimised the PC dye and UV stabiliser were incorporated, and the PC properties of the films prepared from the miniemulsions were investigated.

Table 4.1. Starting point formulation of BMA miniemulsion

Oil phase:	**% w/w**
AIBN	0.36
n-BMA	15.95
Hexadecane	0.42
Water phase:	
SDS	1.00
Water	82.27
TOTAL	**100.00**

4.4 Variation of the solids content and surfactant level

In miniemulsion polymerisation the maximum attainable TSC is limited by the viscosity of the reaction mixture. With an increase in TSC the PS and PSD increase.[3] When the TSC decreases and collision rates are slower a decrease in PS is observed. Ostwald ripening and insufficient mechanical stirring is not a major concern in miniemulsion polymerisation.[4] Applying ultrasonication at a saturation limit ensures that a steady state miniemulsion is obtained. It is rather the colloidal stability that sets the limit in obtaining higher TSC miniemulsions.[4] The type and amount of surfactant incorporated is therefore very important. Most literature references use the anionic surfactant SDS as a model system.[4] Ionic surfactant systems produce smaller PS miniemulsions more efficiently than non-ionic

surfactants.[5] SDS is typically incorporated at levels of 0.25–25% relative to the monomer phase.[4]

In this study the TSC was varied from 15 to 40% by weight of the monomer phase. The surfactant type was not varied, but the level ranged from 0.25 to 2% weight on total formulation. Formulations for Exp 1–Exp 12 are tabulated in Table B.1 and Table B.2, Appendix B. The variations in the formulations and their PS and PSD results are summarised in Table 4.2 and Figure 4.1.

Table 4.2. Exp 1–Exp 12: Formulation variations, PS and PSD of miniemulsions

	Formulation			**Experimental**	
Variant	**Sample no.**	**TSC (%)**	**SDS (%)**	**PS (nm)**	**PSD**
TSC	Exp 1	40	1	99.6±2.00	0.019±0.01
	Exp 2	35	1	93.0±3.50	0.011±0.02
	Exp 3	30	1	89.1±3.00	0.009±0.01
	Exp 4	15	1	73.7±0.90	0.044±0.01
SDS	Exp 5	30	0.25	112.0±3.40	0.022±0.02
	Exp 6	30	0.5	100.8±1.90	0.039±0.01
	Exp 3	30	1	89.1±3.00	0.009±0.01
	Exp 7	30	1.5	83.7±0.03	1.300±0.01
	Exp 8	30	2	76.8±0.04	1.500±0.01
TSC and SDS	Exp 9	15	0.25	87.4±1.10	0.038±0.01
	Exp 10	15	2	60.1±0.40	0.053±0.01
	Exp 11	40	0.25	128.7±3.10	0.023±0.01
	Exp 12	40	2	80.7±1.60	0.038±0.01

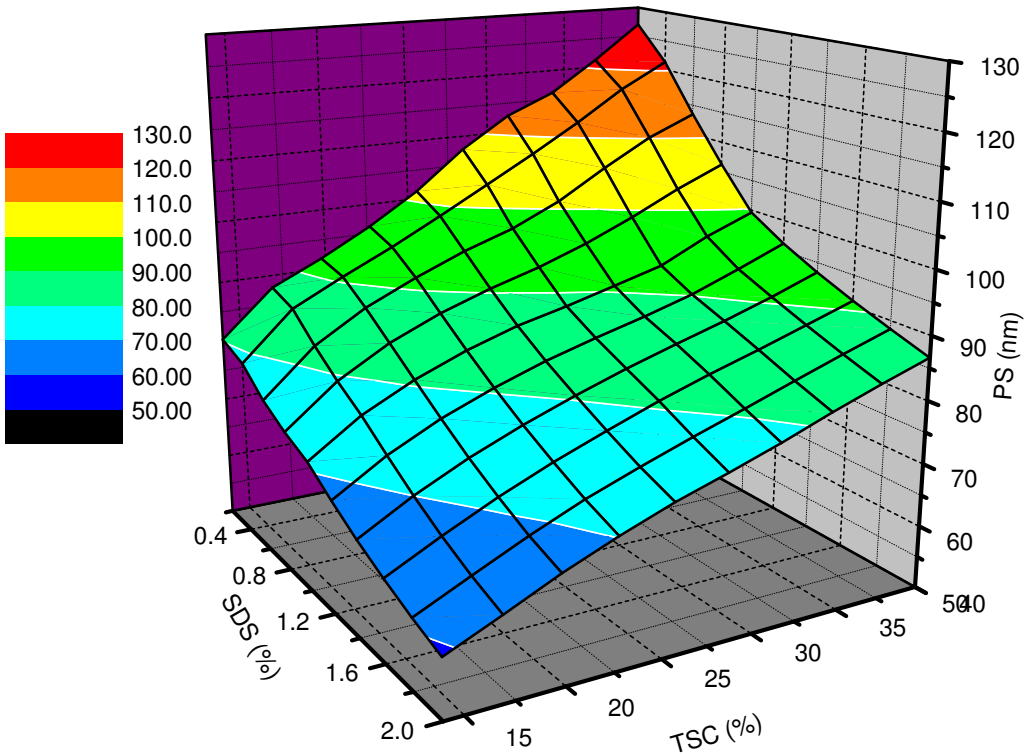

Figure 4.1. Three-dimensional plot showing the effect of the variation of TSC and SDS on the PS of the BMA miniemulsion system.

Results confirm literature reports of an increase in PS as the TSC increases and a decrease in PS as the surfactant concentration increases (Figure 4.1). A higher concentration of surfactant is required as the TSC increases to maintain a similar average PS. After 20min into the polymerisation of these samples the 40% TSC sample could not be stirred with the magnetic stirrer set-up. Samples with TSC below 35% gave reaction mixtures with more manageable viscosities. The sample with 30% TSC and 1% SDS had the narrowest PSD.

Figures 4.2–4.4 show the increase in TSC as monomer conversion takes place over time. All reactions reached full conversion within 60min of the polymerisation. With a higher TSC and higher SDS content the conversion was faster. All reactions experienced a minimum inhibition period of 10min.

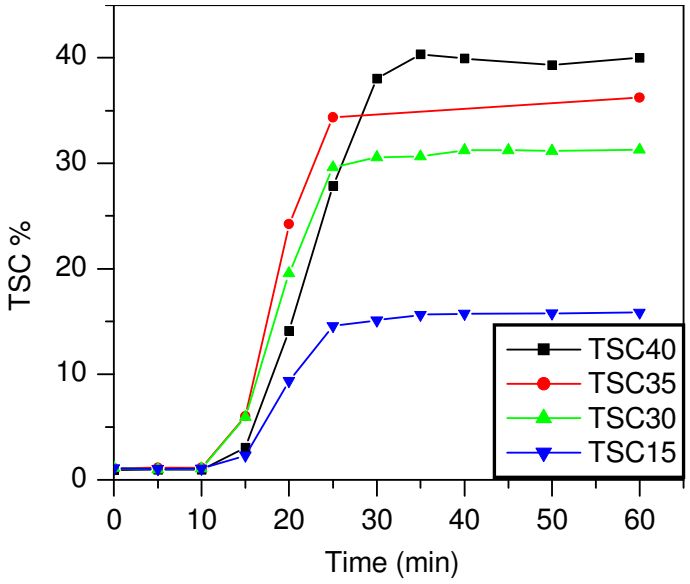

Figure 4.2. Conversions of formulations with different TSC.

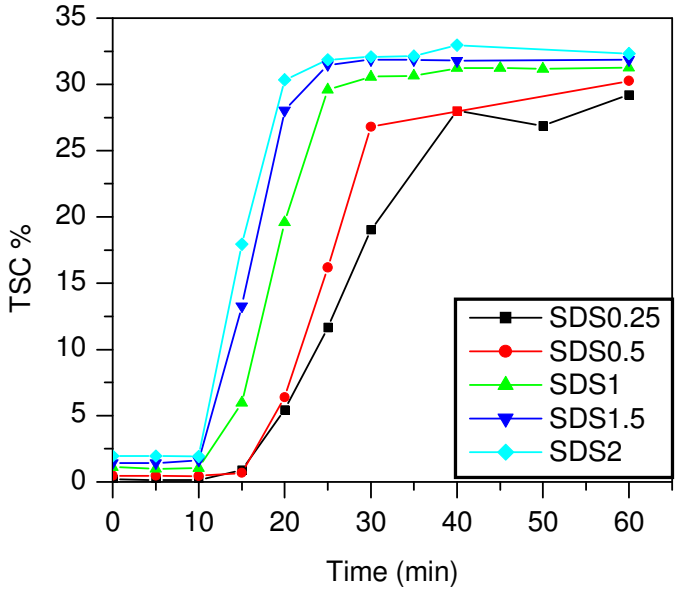

Figure 4.3. Conversions of formulations with different SDS content.

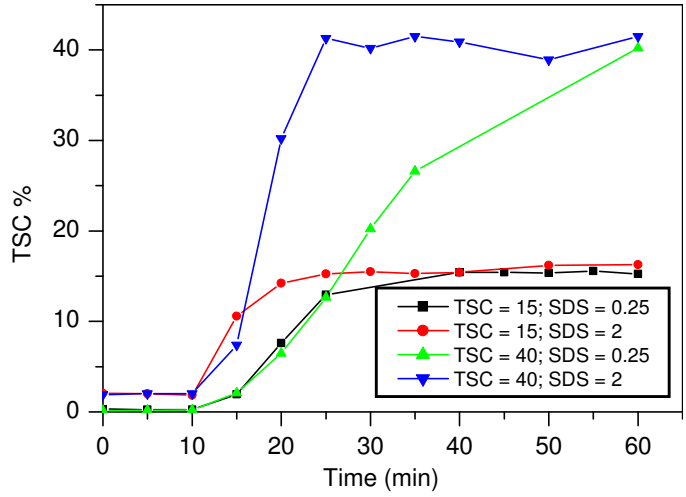

Figure 4.4. Conversions obtained when varying the TSC and SDS contents of the formulations.

4.5 Variation of the initiator level

In miniemulsion polymerisation, either water soluble or oil soluble initiators can be used. The choice of initiator affects the morphology of the particles produced.[6] Oil soluble initiators have some advantages over water soluble initiators. They offer better control of the polymerisation, providing a narrow PSD, and can limit diffusional degradation of monomer droplets during polymerisation.[4,6] When oil soluble initiators are dissolved in the monomer phase they are restricted to a small volume, and radicals formed in this space can easily terminate. Therefore, for an equivalent concentration of initiator, kinetics of emulsion polymerisation with oil soluble initiators are slower than with water soluble initiators.[6]

The concentration of initiator influences the rate and total conversion of the polymerisation reaction: the higher the initiator concentration the faster the reaction takes place and the higher the conversions obtained.[7] Chern and Liou reported that the concentration of AIBN can have different effects on PS, depending on the costabiliser used in the system. For a Sty miniemulsion with dodecyl methacrylate as costabiliser the PS increased as the initiator level decreased, while with stearyl methacrylate the PS was unaffected.[7]

In Table 4.3 results of varying the AIBN concentration in the BMA miniemulsion from 0.08 to 0.65% weight on polymer solids is reported. The TSC of the formulation was kept at 30% and the SDS content at 1% on polymer solids.

Table 4.3. Exp 13–Exp 16, Exp 3 and Exp 3b: Formulation variations, PS and PSD of miniemulsions

Sample no.	**Formulation**	**Experimental**	
	AIBN (%)	**PS (nm)**	**PSD**
Exp 13	0.65	86.2±1.20	0.046±0.01
Exp 14	0.50	85.6±2.00	0.064±0.02
Exp 3*	0.36	89.1±3.00	0.009±0.01
Exp 3b*	0.36	86.5±2.00	0.042±0.02
Exp 15	0.22	88.3±1.50	0.081±0.01
Exp 16	0.08	95.6±0.07	1.700±0.01

*Note: Exp 3 was previously carried out where the sample had an AIBN concentration of 0.36%. Exp 3b was performed to verify the results obtained.

Below a concentration of 0.36% AIBN on total formulation the rate of conversion decreased drastically (Figure 4.5). PS and PSD increased below this level and full conversion could not be achieved.

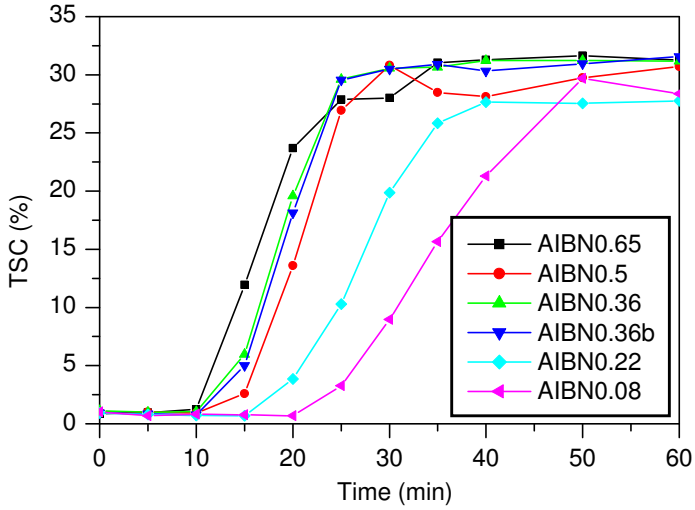

Figure 4.5. Conversions obtained when varying the AIBN contents of the formulations.

A formulation containing a TSC of 30%, SDS content of 1% and AIBN concentration of 0.36% afforded a sample with manageable viscosity, small PS, a narrow PSD, and fast and complete conversion of polymerisation. This formulation (Exp 3) was used in subsequent experiments (Exp 17–Exp 26) to entrap the PC dye and a UV stabiliser.

4.6 Entrapment of the photochromic dye in the miniemulsion particles

Entrapment of compounds in emulsion systems allows protection from various environmental elements, such as UV light.[8] Entrapment also provides better storage stability, colour stability and durability.[8] For compounds to be entrapped in the monomer phase they should have a hydrophobic nature.[5] The two dyes used in this study are not water soluble and can therefore be dispersed and embedded in the monomer phase. Using miniemulsion polymerisation, the film formation of the embedded particles was adjusted, allowing their incorporation into water-based systems.[8]

The quantity of SNO dye (PP) available was limited, and therefore it had to be used sparingly. The PC chromene (PT) was used as a test sample to study the process of dye entrapped in a BMA miniemulsion. During the entrapment of the PC dye (PT, Exp 17) the pre-emulsion was yellow before polymerisation. During polymerisation of the sample a slight pink colour developed. The colour suggested that a fraction of the PC dye was in the open form. The pink colour of the miniemulsion (Figure 4.6) and the film prepared from it was much less intense than the colour obtained after UV irradiation (Figure 4.14), meaning that only a small fraction of the PC dye was in its open form. The pink colour disappeared during storage in the dark, in the oven. This confirmed that the dye exhibited reversible photochromism, where the open form is forced back to the closed form via thermal bleaching.

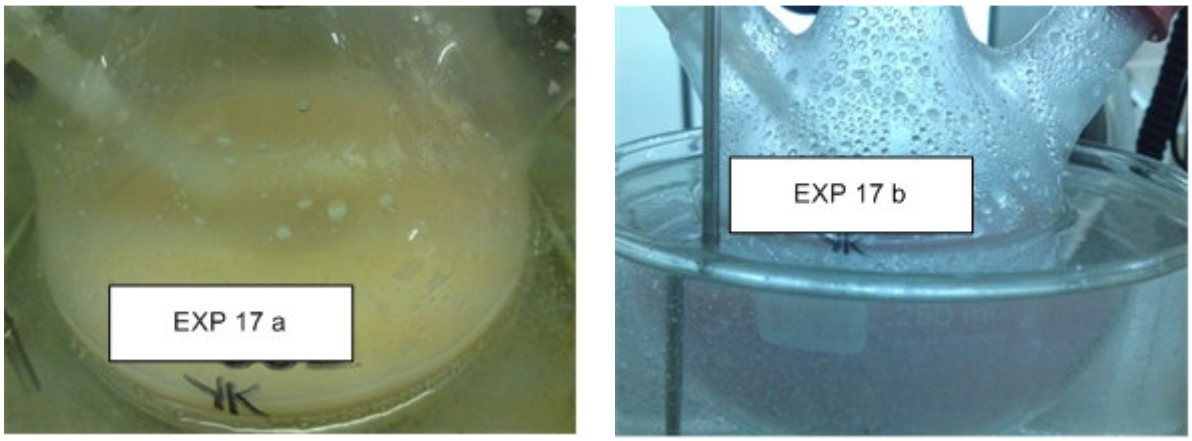

Figure 4.6. Exp 17 colour: (a) before polymerisation and (b) during polymerisation.

Various concentrations of SNO dye were used: 0.5, 1 and 2% weight on polymer solids. A brown colour was observed, when mixing the SNO dye with the oil phase. When the oil

phase was added to the water phase the pre-emulsion had a green colour, which darkened during the polymerisation stage (Figure 4.7). During the film preparation stage at 60°C in the oven the slight green colour persisted. After drying a film of the sample and upon activation with UV light, a very dark purple colour was observed (Figure 4.14). The slight green colour of the film before activation indicated that a small fraction of dye was permanently in the open form. The closed, yellow form of the dye, and the small fraction in the open form, can result in the green colour observed.

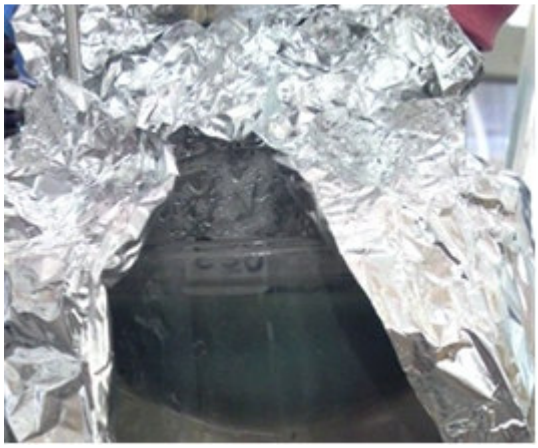

Figure 4.7. The dark green colour observed during polymerisation of Exp 19.

Experimental results of the miniemulsions produced using the two different PC dyes, in different concentrations, are given in Table 4.4.

Table 4.4. Exp 17–Exp 20: Formulation variations, PS and PSD of miniemulsions

Sample no.	**Formulation**	**Experimental***	
	PC on polymer (% w/w)	**PS (nm)**	**PSD**
Photosol 7-106			
Exp 17	1.27	98.787	0.057
Reversacol Palatinate Purple			
Exp 18	0.52	93.077	0.092
Exp 19	1.01	92.607	0.087
Exp 20	2.21	90.257	0.079

Note: The Malvern Zetasizer 1000HSa was no longer operational and the Malvern NANO Z590 was used for these and future experiments. This instrument does not give an ± error indication after the results.

Entrapment of the PC dye resulted in a slight increase in PS: approximately 90nm before entrapment and above 90nm after entrapment (Table 4.4). When the dye concentration was increased the PS decreased again. This can not be explained in terms of the hydrophobic nature of the dye because the inclusion of a hydrophobe in a miniemulsion reaction should not affect the PS, it only assists in obtaining equal pressure in the different particles to prevent Ostwald ripening.[4]

No significant effect was observed in the reaction kinetics after inclusion of the PC dyes. See Figure 4.8.

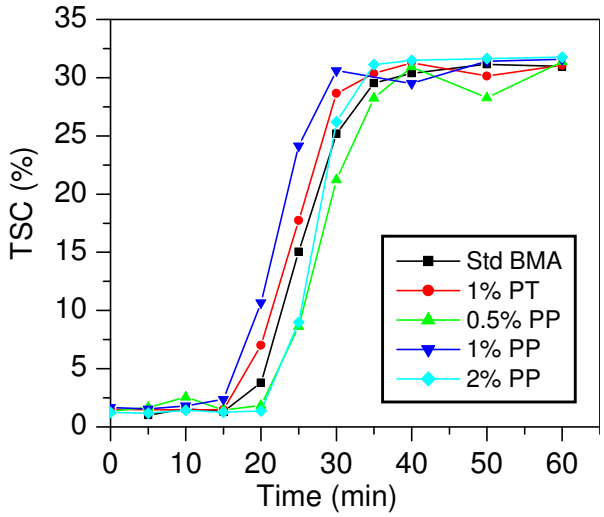

Figure 4.8. Conversions obtained when varying the PC dye contents of the formulations.

The particle morphology of the samples was investigated using TEM. A stain was applied to cover the polymer particles, to provide contrast. Negative stained images were obtained from which the morphology could be studied. The TEM images (Figures 4.9–4.11) showed no deformation in the particle morphology upon entrapment of the PC dyes in the miniemulsion. No difference between the BMA and dye matrix could be observed.

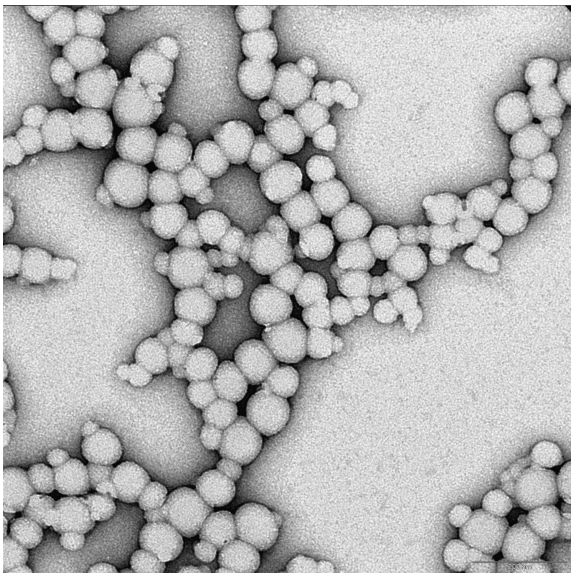

Figure 4.9. Negative stained TEM image of Exp 3 (no PC dye).

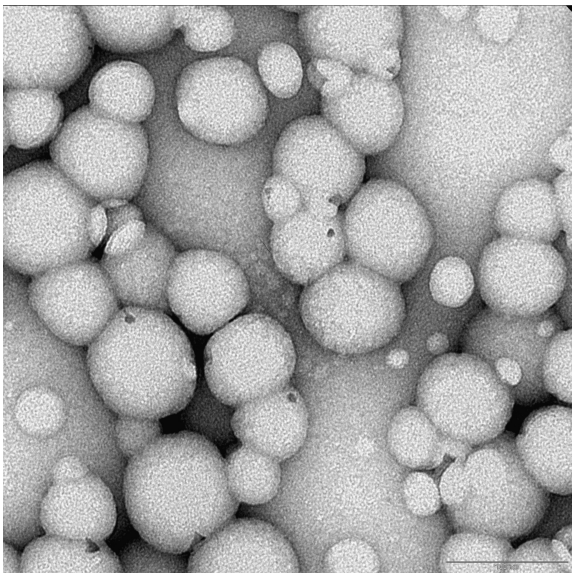

Figure 4.10. Negative stained TEM image of Exp 17 (1% PT).

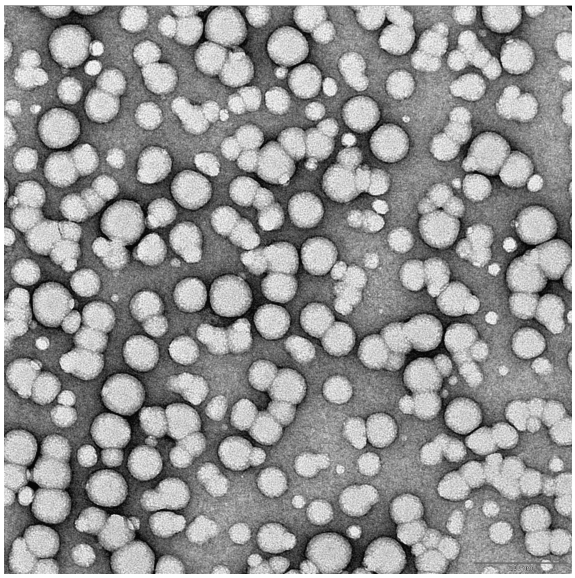

Figure 4.11. Negative stained TEM image of Exp 20 (1% PP).

Colourability and half-life measurements of Exp 17–Exp 20 are reported in Table 4.5 and depicted in Figure 4.12 and 4.13.

Table 4.5. Exp 17–Exp 20: Film properties and PC kinetics

Sample no.	**Film thickness measurements (µm)**				**PC kinetics**		
	Mean	**Min**	**Max**	**Max–Min**	**Colourability (Abs.)**	**Decay constant (k*f*)**	**Half-life ($t_{1/2}$; s)**
Photosol 7-106							
Exp 17 (1%)							
A	18	17	18	1	0.2134	5.58E-03	124.26
B	20	19	21	2	0.2179	6.34E-03	109.40
C	18	18	19	1	0.2118	7.01E-03	98.86
D	19	18	20	2	0.2178	5.65E-03	122.64
E	20	19	23	4	0.2169	6.93E-03	100.06
Reversacol Palatinate Purple							
Exp 18 (0.5%)							
A	18	16	19	3	0.3260	2.64E-02	26.25
B	17	16	19	3	0.3013	2.58E-02	26.82
C	16	15	18	3	0.3018	2.55E-02	27.20
D	16	14	18	4	0.3094	2.56E-02	27.09
E	18	16	20	4	0.3318	2.54E-02	27.33
Exp 19 (1%)							
A	17	14	20	6	0.5232	2.31E-02	30.03
B	21	19	23	4	0.5253	2.47E-02	28.05
C	16	14	18	4	0.4647	2.52E-02	27.51
D	19	16	21	5	0.4451	2.56E-02	27.09
E	18	15	20	5	0.4783	2.39E-02	29.05
Exp 20 (2%)							
A	16	15	18	3	0.5993	2.66E-02	26.09
B	18	15	20	5	0.5873	2.64E-02	26.21
C	19	17	20	3	0.6396	2.66E-02	26.04
D	17	14	19	5	0.6375	2.65E-02	26.11
E	18	16	20	4	0.6566	2.63E-02	26.31

The chromene dye showed the lowest colourability value even at a higher dye concentration than the SNO dye (Table 4.5 and Figure 4.12). The activation and deactivation of the chromene dye was slower in the BMA matrix than the SNO dye: the half-life was about 100s for the chromene dye and 30s for the SNO dye, respectively.

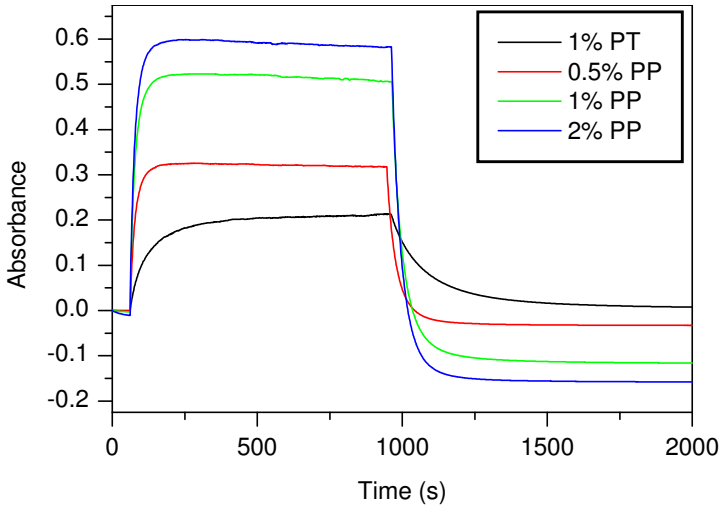

Figure 4.12. Exp 17–Exp 20: Film colourability and fading curves.

An increase in the level of SNO dye resulted in a steady increase in the colourability (Figure 4.14). The increase in absorbance was not linear with an increase in dye concentration.

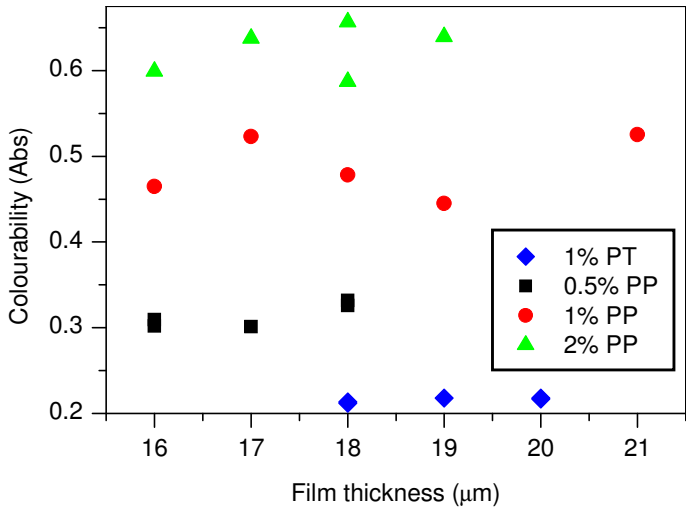

Figure 4.13. Exp 17–Exp 20: Film colourability at different thicknesses and dye concentrations.

During QUV irradiation a dark pink and purple colour was observed for Exp 17 and Exp 20 (Figure 4.15).

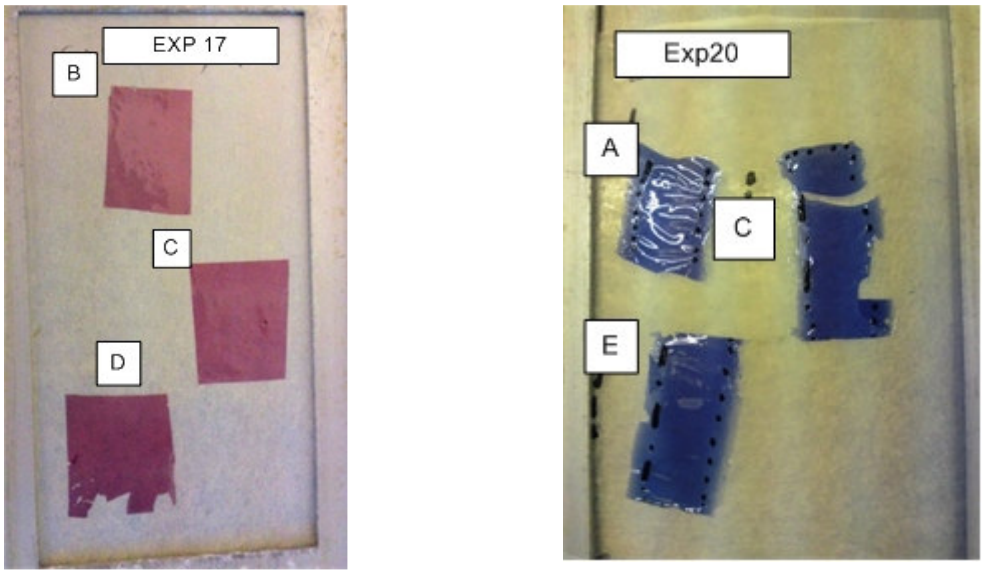

(a) (b)

Figure 4.14. (a) Exp 17 (1% PT) and (b) Exp 20 (2% PP) after QUV irradiation.

Raw data of the absorbance values of each point measurement conducted after 4hr QUV irradiation are included in Appendix D. Figure 4.15 indicates the fatigue resistance of the chromene dye and Figure 4.16 the fatigue resistance of the SNO dye.

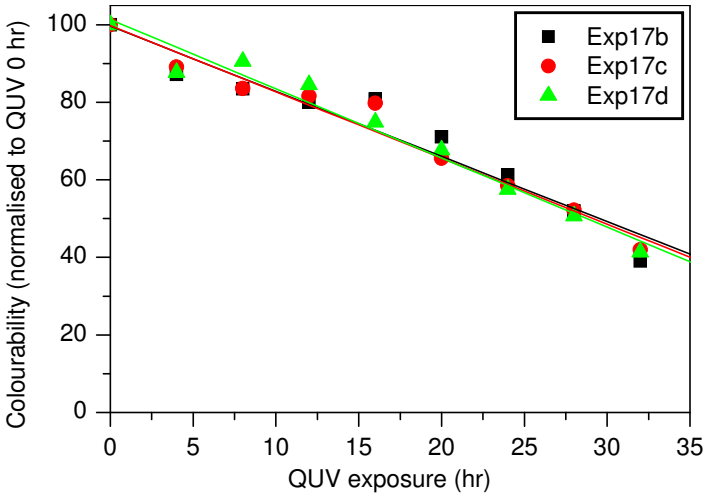

Figure 4.15. Fatigue resistance of Exp 17 (1% PT).

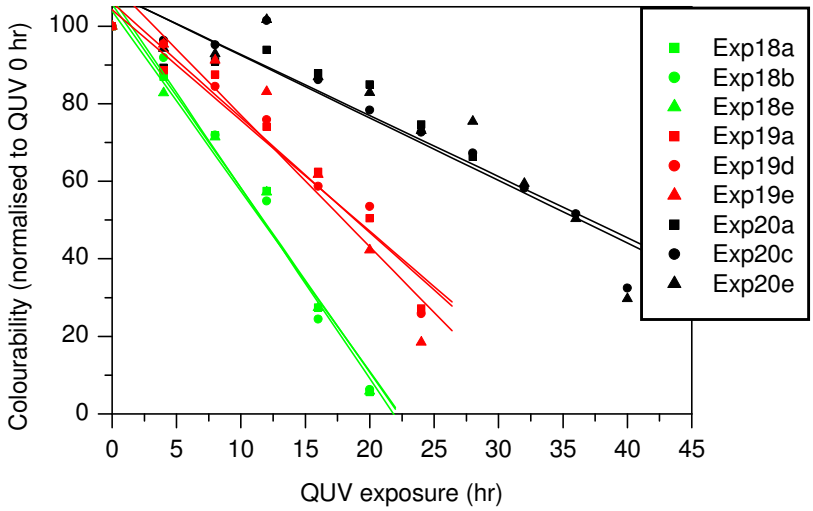

Figure 4.16. Fatigue resistance of Exp 18 (0.5% PP), Exp 19 (1% PP) and Exp20 (2% PP).

Fatigue resistance experiments revealed that the chromene dye (1.27% w/w) could last for the same amount of QUV exposure as the SNO dye at higher concentrations (2% w/w). As the concentration of the SNO dye increased the resistance against UV degradation increased. This was confirmed by analysing the data of the linear regression fits in Table 4.6.

Table 4.6. Exp 17–Exp 20: Linear fit to fatigue resistance data

Sample no	R	SD	M
Photosol 7-106			
Exp 17 (1% PT)			
B	-0.9681	5.0940	-1.6792
C	-0.9843	3.5832	-1.7059
D	-0.9848	3.6896	-1.7841
Reversacol Palatinate Purple			
Exp 18 (0.5% PP)			
A	-0.9878	6.2728	-4.7496
B	-0.9886	6.2413	-4.9140
E	-0.9873	6.2640	-4.6506
Exp 19 (1% PP)			
A	-0.9751	6.1457	-2.8566
D	-0.9758	6.2906	-2.9644
E	-0.9555	9.9255	-3.3947
Exp 20 (2% PP)			
A	A linear regression could not be fitted because the data set was incomplete		
C	-0.9559	6.9270	-1.6124
E	-0.9269	8.9252	-1.5760

4.7 Incorporation of a light stabiliser with the photochromic dye

To prevent one of the main routes of degradation of PC dyes, i.e. via radical attack, a HALS (Tinuvin 292) was incorporated. Its chemical composition (Figure 4.17) comprises a mixture of bis(1,2,2,6,6-pentamethyl-4-piperidyl) sebacate (MW 509) and methyl 1,2,2,6,6-pentamethyl-4-piperidyl sebacate (MW 370).

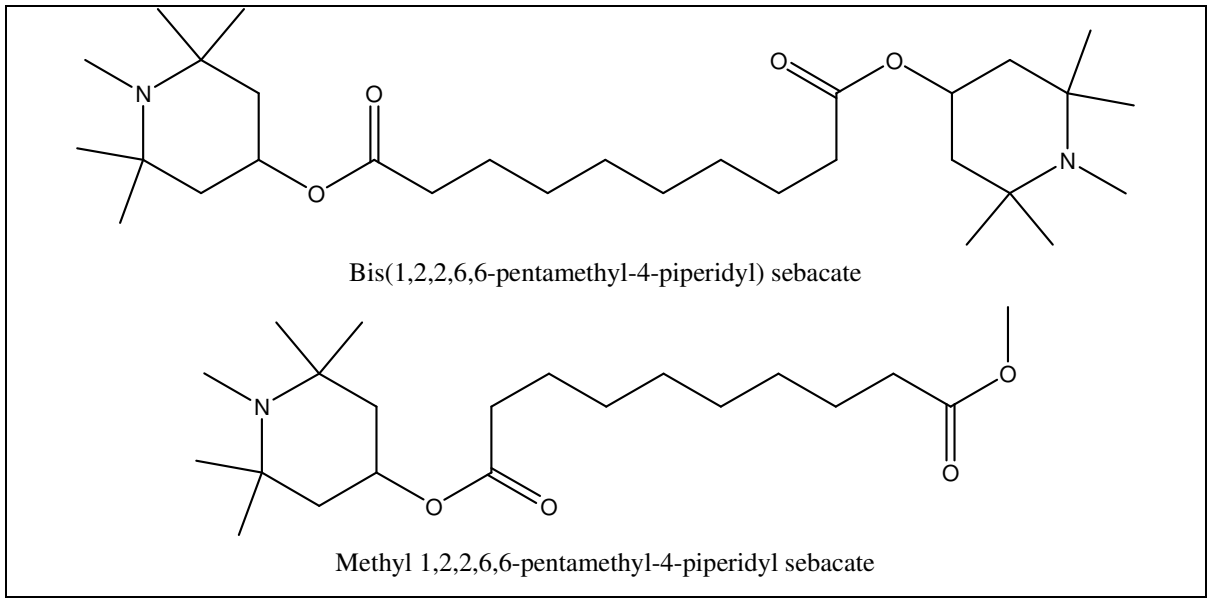

Figure 4.17. The two chemical components in Tinuvin 292.

Monomer was replaced by volume with Tinuvin 292 to keep the volume of the oil phase constant. The Tinuvin concentration was varied from 0.5 to 2% volume of polymer volume. A series of miniemulsions without any PC dye and a series of miniemulsions with 1% weight PC dye on polymer weight were prepared (Table 4.7).

Table 4.7. Exp 17–Exp20: Formulation variations, PS and PSD of miniemulsions

Sample no.	**Formulation**	**Experimental**	
	Tinuvin 292 on polymer (%v/v)	**PS (nm)**	**PSD**
Tinuvin 292 with no PC dye			
Exp 21	0.5	96.817	0.074
Exp 22	1	95.02	0.0907
Exp 23	2	92.34	0.0967
Tinuvin 292 with 1% Reversacol Palatinate Purple			
Exp 24	0.5	92.11	0.0707
Exp 25	1	93.703	0.075
Exp 26	2	90.427	0.0903

The PS of the BMA miniemulsion increased with the inclusion of Tinuvin 292 and the PC dye. As the concentration of both these additives increased the PS decreased and the PSD increased (Table 4.7).

No significant effect on the reaction kinetics was observed with the inclusion of Tinuvin 292 and the PC dyes in the miniemulsion system. See Figure 4.19. This indicates that the HALS stabiliser was not consumed during the reaction and it should still be active to protect the PC dyes from UV degradation upon irradiation.

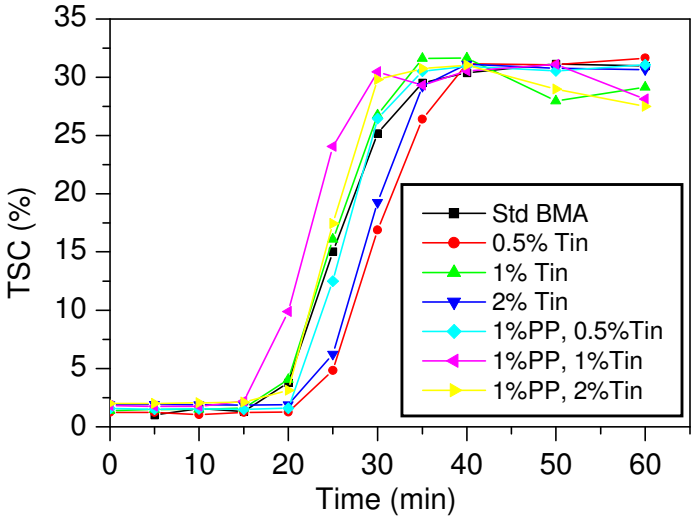

Figure 4.18. Conversions obtained when varying the HALS and PC dye contents of the formulations.

The incorporation of Tinuvin 292 did not change the morphology of the particles (Figure 4.19). No contrast between the Tinuvin 292, PC dye and BMA matrix was observed.

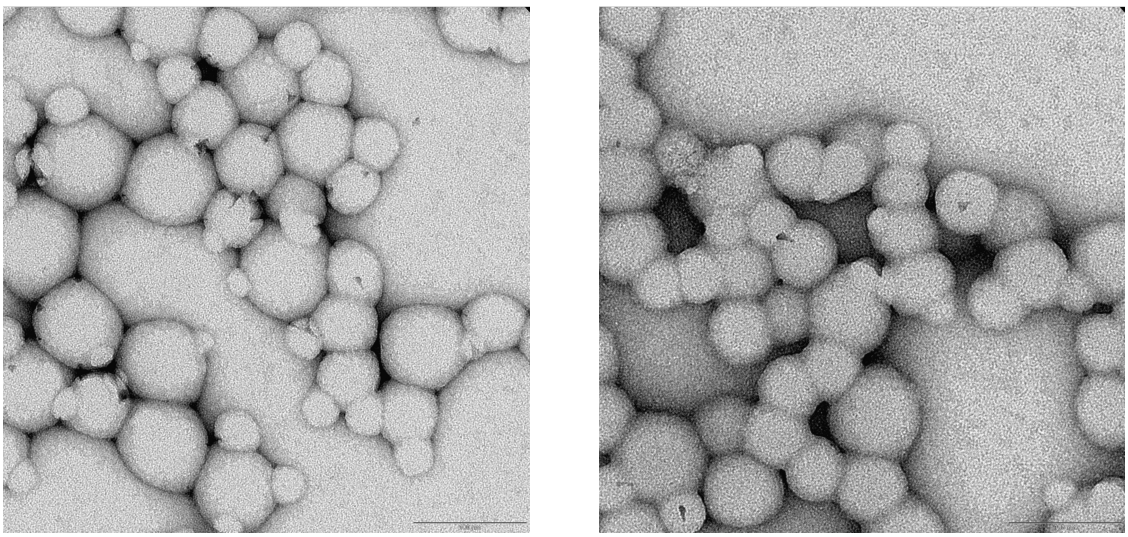

(a) (b)

Figure 4.19. Negative stained TEM images of (a) Exp 23 (2% Tinuvin 292) and (b) Exp 26 (1% PP and 2% Tinuvin 292).

Colourability and half-life measurements recorded for Exp 24–Exp 26 are tabulated in Table 4.8.

Table 4.8. Exp 24–Exp 26: Film properties and PC kinetics

Sample no.	Film thickness measurements (µm)				PC kinetics		
	Mean	Min	Max	Max–Min	Colourability (Abs.)	Decay constant (k*f*)	Half-life ($t_{1/2}$; s)
Exp 24 (0.5% Tinuvin 292)							
A	19	18	21	3	0.4324	1.97E-02	35.11
B	19	18	20	2	0.4744	2.38E-02	29.09
C	18	17	19	2	0.4102	2.90E-02	23.87
D	16	16	17	1	0.3993	2.68E-02	25.83
E	17	16	19	3	0.3536	2.76E-02	25.10
Exp 25 (1% Tinuvin 292)							
A	19	17	21	4	0.4716	2.98E-02	23.24
B	17	16	18	2	0.4736	2.99E-02	23.18
C	20	18	21	3	0.5032	2.95E-02	23.50
D	18	17	19	2	0.4858	2.95E-02	23.46
E	17	16	17	1	0.4456	3.02E-02	22.93
Exp 26 (2% Tinuvin 292)							
A	17	16	18	2	0.3556	3.40E-02	20.39
B	18	16	19	3	0.3797	3.44E-02	20.13
C	16	16	17	1	0.3291	3.37E-02	20.57
D	21	20	22	2	0.4212	3.44E-02	20.16
E	20	19	21	2	0.4968	3.41E-02	20.31

The colourability of the samples with different Tinuvin 292 concentrations was similar to that of Exp 19 (1% w/w PC dye). The half-life decreased from Exp 19 to Exp 24 (0.5% v/v Tinuvin 292). As the concentration of the Tinuvin increased the half-lives decreased further.

Raw data of the fatigue resistance of Exp 24– Exp 26 are reported in Appendix C. The fatigue resistance as indicated in Figure 4.20 a–c and in Table 4.9 showed slightly better resistance for Exp 24–Exp 26 than was previously shown for Exp 19, without Tinuvin 292. The improvement was however not significant, and did not increase much with an increase in Tinuvin 292 at the levels of 0.5–2%. At a level of 2% Tinuvin 292 (Exp 26) the initial fatigue took longer to commence, but after 24hr reached half of its original value, as it did in Exp 24 and Exp 25. Much higher levels of Tinuvin 292 addition are probably required to achieve a more significant effect.

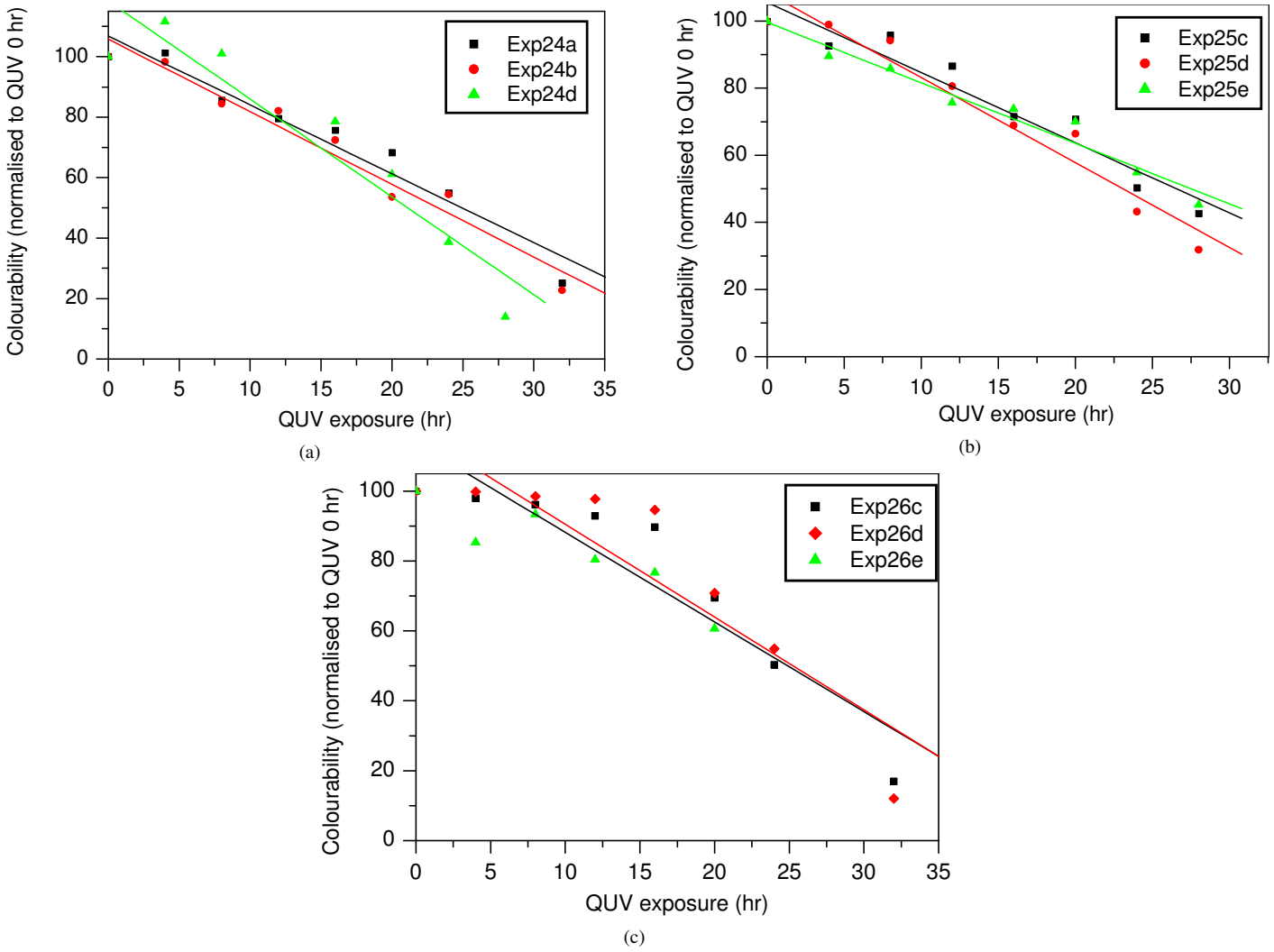

Figure 4.20. Fatigue resistance of (a) Exp 24 (0.5% Tinuvin), (b) Exp 25 (1% Tinuvin), and (c) Exp 26 (2% Tinuvin).

Table 4.9. Exp 24–Exp 26: Linear fit to fatigue resistance data

Sample no	R	SD	M
Exp 24 (0.5% Tinuvin 292)			
A	0.9733	6.1930	-2.2773
B	-0.9801	5.6201	-2.4033
D	-0.9448	12.9787	-3.2377
Exp 25 (1% Tinuvin 292)			
C	-0.9631	6.1916	-2.0923
D	-0.9731	6.3365	-2.5312
E	-0.9818	3.6959	-1.8033
Exp 26 (2% Tinuvin 292)			
C*	-0.9249	12.1458	-2.5628
D*	-0.8980	15.0062	-2.6556
E	A linear regression could not be fitted because the data set was incomplete.		

*Note: A linear regression line is not completely appropriate for this data set (Figure 4.20 c), but still indicates that fatigue resistance of Exp 26 is similar to that of Exp 24 and Exp 25.

4.8 Butyl methacrylate solution polymer samples

The newly synthesised PC miniemulsions were compared to conventional dispersions of the PC dye into a solution polymer. The same monomer used in the miniemulsion synthesis (BMA) was used in the solution polymer for comparison. In the solution polymer both the PC dye and the UV stabiliser could be added after polymerisation and does therefore not have a thermal history such as in the miniemulsion samples were it was added before polymerisation. Due to the small quantity of PC dye available only four variations of solution polymer samples were prepared. All samples included the use of PP at 1% weight on polymer solids. The concentration of Tinuvin 292 was increased from 0 to 2% volume on polymer volume. See Table 4.10.

Table 4.10. Exp 27–Exp 30: Film properties and PC kinetics

Sample no.	**Film thickness measurements (µm)**				**PC kinetics**		
	Mean	**Min**	**Max**	**Max–Min**	**Colourability (Abs.)**	**Decay constant (k*f*)**	**Half-life ($t_{1/2}$; s)**
Exp 27 (no Tinuvin 292)							
A	11	11	13	2	0.4178	2.75E-02	25.19
B	13	12	14	2	0.4160	2.72E-02	25.52
C	12	11	13	2	0.3761	3.34E-02	20.75
D	13	12	14	2	0.4033	2.93E-02	23.64
E	13	12	14	2	0.3849	2.97E-02	23.37
Exp 28 (0.5% Tinuvin 292)							
A	13	12	14	2	0.4453	3.28E-02	21.13
B	13	12	14	2	0.4042	3.22E-02	21.54
C	13	12	13	1	0.4104	3.41E-02	20.31
D	11	11	12	1	0.3753	3.31E-02	20.94
E	12	11	12	1	0.4002	3.38E-02	20.48
Exp 29 (1% Tinuvin 292)							
A	12	11	13	2	0.3694	3.60E-02	19.27
B	12	11	12	1	0.3780	3.41E-02	20.31
C	12	10	12	2	0.4277	3.24E-02	21.42
D	13	11	14	3	0.4156	3.25E-02	21.30
E	12	11	12	1	0.4017	3.16E-02	21.90
Exp 30 (2% Tinuvin 292)							
A	11	11	12	1	0.3924	3.75E-02	18.47
B	12	11	13	2	0.4101	3.69E-02	18.77
C	12	11	12	1	0.3727	3.75E-02	18.46
D	11	11	12	1	0.3837	3.86E-02	17.97
E	13	12	13	1	0.4397	3.76E-02	18.44

Films of the solution polymer samples were thinner after drying (11–13µm) than the miniemulsion films previously prepared (16–21µm). The colourability of Exp 27–Exp 30 is similar to that of their miniemulsion counterparts (Exp 17–Exp 20), even for slightly thinner films thicknesses. The half-lives of the solution polymers are shorter than for the miniemulsion samples. The half-life for Exp 27 is approximately 5 sec shorter than its equivalent miniemulsion Exp 19. PC kinetic data of Exp 26 confirm that a difference in film thickness influences colourability, but not half-life, and hence the decreased half-lives of the solution polymers can be ascribed to the nature of the polymer.

In solution polymerisation solvents can act as chain transfer agents, and high MW polymers are difficult to obtain due to the difference in termination and propagation kinetics.[9] Figure 4.21 shows that the MW of the solution polymer (Exp 27) was much lower and had a narrower MWD compared to the miniemulsion polymer (Exp 3).

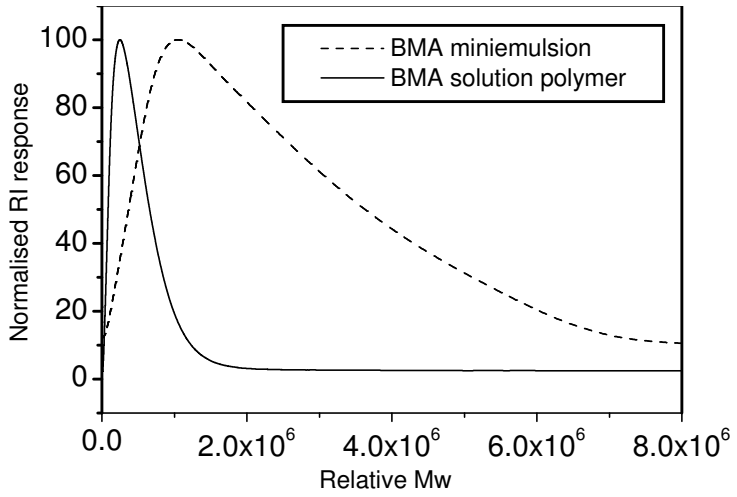

Figure 4.21. MW distribution of the BMA miniemulsion (Exp 3) and the BMA solution polymer (Exp 27).

Higher chain mobility in the solution polymer with lower MW allows faster deactivation of the PC dye. As per Exp 24–Exp 26 the half-lives of Exp 31–Exp 33 decreased as the concentration of Tinuvin 292 increased.

Raw data of the fatigue resistance of Exp 27–Exp 30 are found in Appendix C. An evident improvement in fatigue resistance was observed with the incorporation of Tinuvin 292 in the solution polymer (Figure 4.22.a). As the concentration of Tinuvin 292 increased the improvement of fatigue resistance was more noticeable than in the miniemulsion samples where it had a thermal history. At the level of 2% Tinuvin 292 on polymer volume the

fatigue resistance of Exp 30 was still weaker than for miniemulsion Exp 27. Exp 30 reached half of its original colourability within 24hr while Exp 27 lasted up to 28hr, and had a slower start in showing fatigue. Exp 20 with a PC dye concentration of 2% showed the best fatigue resistance up to 36hr.

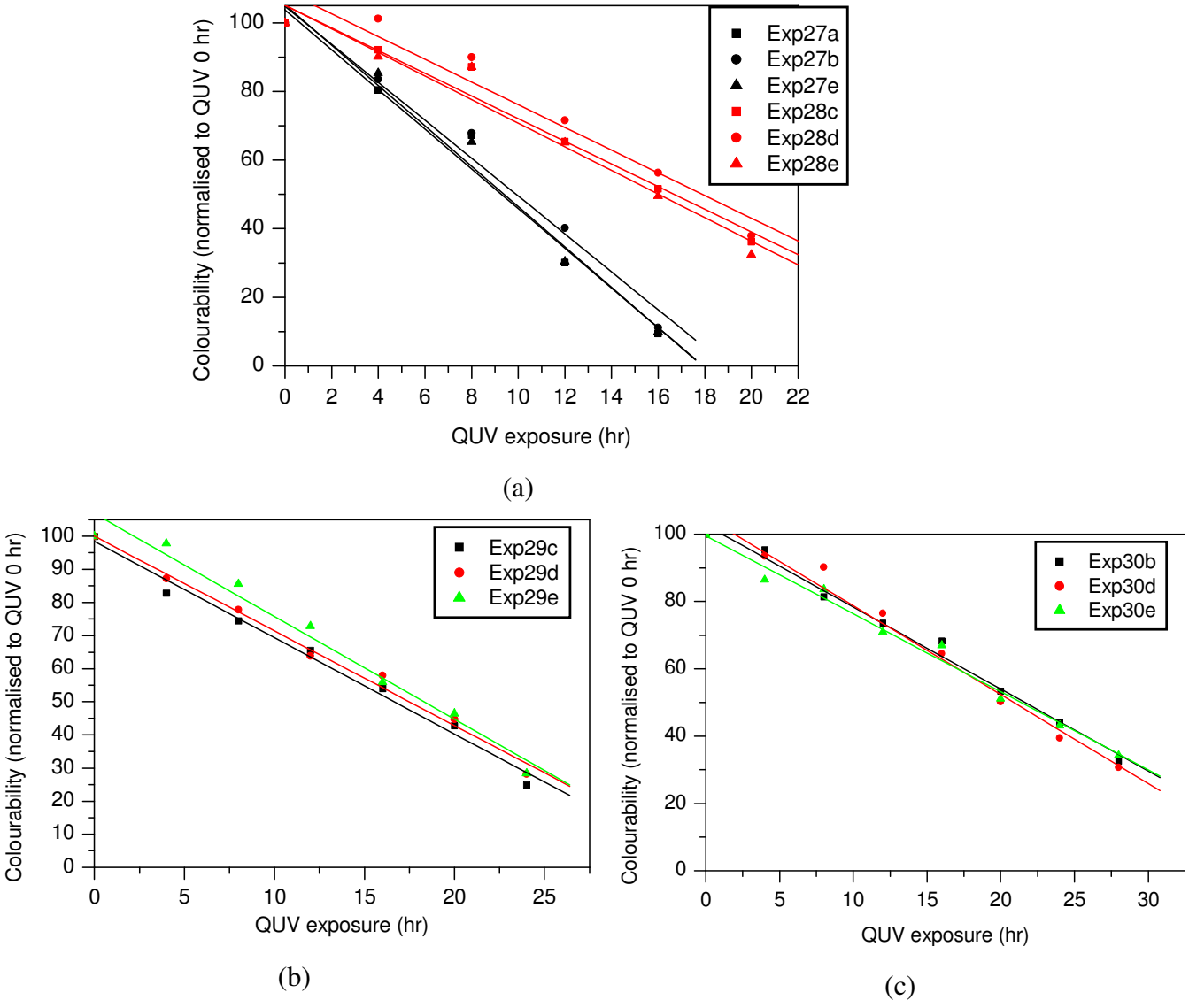

Figure 4.22. Fatigue resistance of (a) Exp 27 (no TInuvin)-Exp28 (0.5% Tinuvin) and (b) Exp 29 (1% Tinuvin) and (c) Exp 30 (2% Tinuvin)

Table 4.11. Exp 27–Exp 30: Linear fit to fatigue resistance data

Sample no	R	SD	M
Exp 27 (no Tinuvin 292)			
A	-0.9881	6.5675	-5.7851
B	-0.9892	5.9794	-5.5252
E	-0.9902	6.0680	-5.8786
Exp 28 (0.5% Tinuvin 292)			
C	-0.9829	5.1850	-3.3034
D	-0.9698	6.9685	-3.3109
E	-0.9799	5.8557	-3.4415
Exp 29 (1% Tinuvin 292)			
C	-0.9938	3.0880	-2.9078
D	-0.9956	2.5450	-2.8590
E	-0.9883	4.5314	-3.1013
Exp 30 (2% Tinuvin 292)			
B	-0.9948	2.6284	-2.4347
D	-0.9907	3.8296	-2.6405
E	-0.9935	2.8142	-2.3161

4.9 Discussion and conclusions

An experimental design was performed on a BMA miniemulsion formulation in which the TSC, surfactant concentration (SDS) and the initiator concentration (AIBN) were varied. The smallest PS miniemulsion was obtained at low TSC (15%) and high surfactant concentration (2%). The rate of conversion increased as the surfactant concentration increased. The PS of the BMA miniemulsion increased as the initiator concentration decreased. For a 30% TSC BMA miniemulsion, a minimum concentration of 0.36% w/w AIBN on total formulation was required to reach full conversion. Below 0.36% AIBN the rate of conversion was much lower. From the experimental design a BMA miniemulsion of 30% TSC, 2% SDS and 0.36% AIBN was used for further experiments. This miniemulsion had a manageable viscosity, a small PS, and a fast conversion rate.

During polymerisation to entrap the PC dyes in the BMA miniemulsion a small fraction of the dye converted to its open coloured form. This reaction could be thermally reversed when films produced from the miniemulsions were drawn on glass panels and placed in an oven. Entrapment of the PC dye caused a slight increase in PS of the miniemulsion but did not have any effect on the conversion rate or miniemulsion particles' morphology. Films of the PP dye entrapped in the BMA miniemulsion showed higher colourability, and faster

activation and deactivation kinetics, than films of the entrapped PT dye in the BMA miniemulsion. Colourability of the PP miniemulsion films increased non-linearly as the concentration of the dye increased, indicating a possible saturation point of entrapment versus colourability. The fatigue resistance of the PT dye was better than that of the PP dye entrapped at similar concentrations. At higher dye concentrations in the BMA miniemulsions the fatigue resistance of the PP dye increased.

When HALS was added to the BMA miniemulsion the PS increased. As the concentrations of the HALS and PC dye increased, the PS decreased. The incorporation of the HALS did not affect the conversion rate of the polymerisation or the morphology of the BMA miniemulsion particles. An increase in the HALS concentration increased the activation and deactivation kinetics of the PP dye. The entrapment of the HALS caused a slight improvement in the fatigue resistance of films of a 1% PP miniemulsion. At concentrations of 0.5–2% HALS on polymer solids there was however not a significant improvement, but only a slight delay in the onset of degradation. It is possible that much higher HALS concentrations are required to achieve a significant improvement in fatigue resistance of PC miniemulsions since it has a thermal history.

Films of the PP dye dispersed into a BMA solution polymer at 1% w/w gave similar values in colourability and activation kinetics to films of the PP dye entrapped in a BMA miniemulsion at 1% w/w. The half-lives of the PC solution polymer films were shorter than those of the PC miniemulsion films. Higher chain mobility in low MW solution polymers allowed faster deactivation kinetics compared to the higher MW miniemulsion polymers. Fatigue resistance of the PP dye was much better when entrapped in the BMA miniemulsion compared to when it was dispersed in a BMA solution polymer. The addition of the HALS had a much greater effect on the fatigue resistance of the PC solution polymer films compared to the PC miniemulsion films since it did not have a thermal history.

References

(1) Han, M.; Lee, E.; Kim, E. *Optical Materials* **2002**, 579.
(2) Such, G.; Evans, R. E.; Yee, L. H.; Davis, T. P. *Journal of Macromolecular Science* **2003**, *C43*, 547.
(3) de Arbina, L. L.; Asua, J. M. *Polymer* **1992**, *33*, 4832.
(4) Antonietti, M.; Landfester, K. *Progress in Polymer Science* **2002**, *27*, 689.
(5) Bechthold, N.; Tiarks, F.; Willert, M.; Landfester, K.; Antonietti, M. *Macromolecular Symposia* **2000**, *151*, 549.
(6) Autran, C.; delaCal, J. C.; Asua, J. M. *Macromolecules* **2007**, *40*, 6233.
(7) Chern, C.; Liou, Y.-C. *Journal of Polymer Science Part A: Polymer Chemistry* **1999**, *37*, 2537.
(8) Steiert, N.; Landfester, K. *Macromolecular Materials and Engineering* **2007**, *292*, 1111.
(9) Sandler, S. R.; Karo, W. *Polymer Synthesis*; Academic Press: California, 1974.

5 Summary, conclusions and recommendations

5.1 Introduction

The interest in smart materials in the coatings industry led to the original proposal for this thesis, namely the synthesis and investigation of smart nanoparticles. The requirements for coatings technology to move from solvent based to water based encouraged the entrapment of PC dyes in miniemulsions which are otherwise not compatible with aqueous systems. Discussion related to, and conclusions drawn for the objectives in Chapter 1 now follow.

5.2 Discussion and conclusions

5.2.1 Objective 1

Organic PC dyes were identified to provide the widest colour range. A literature review revealed that SO compounds are the most widely used due to their good fatigue resistance, compared to other organic PC dyes. SO compounds are however photodegraded via oxidation and radical attack. Hence the focus of this study was to entrap the PC dyes in a miniemulsion to impart improved fatigue resistance. Entrapment will reduce the presence of oxygen and incorporating additives in the miniemulsion system can reduce photodegradation by radical attack.

5.2.2 Objective 2

The actual syntheses of PC miniemulsions were preceded by first determining suitable sample preparation methods, instrument set-up and measurement reproducibility (in Chapter 3). The use of a cubic drawdown bar was identified to give the most uniform films, the homogeneity of which was measured with a film thickness gauge.

Activation and deactivation light sources were tested outside a standard UV-Vis instrument and then mounted to irradiate samples inside the sample chamber of the instrument. Due to time delays and the inability to measure activation profiles when irradiating the sample outside of the UV-Vis instrument, an in-situ measurement was preferred. A UV LED was identified as the best activation light source as it could be mounted within the UV-Vis

instrument sample holder, allowing the instrument to be closed (as usual) during operation to minimise the entrance of stray light. The UV LED did not have the highest intensity of the light sources considered but it provided the most stable irradiation source, with practically no warm-up time required and with very low heat dissipation. The UV LED can be switched on and off repeatedly without damaging the irradiation source. It has a long life-span and a narrow spectral output, which made it suitable for quantitative spectroscopic analysis. Depending on the deactivation kinetics of the PC dye, either thermal deactivation or forced deactivation via a tungsten lamp with a filter was used.

When considering improving the reproducibility of PC data, film thickness and homogeneity were identified as critical factors. Films with a maximum thickness variation of 4µm across the sample were used. Films with a maximum of 2µm difference between their mean film thicknesses should be used to keep the percentage deviation in colourability of five measurements of a single sample below 5%. The reproducibility of fading kinetics was better for samples with short half-lives (approximately 30s) than for samples with longer half-lives, (beyond 100s). Cyclability was confirmed to be of no concern for the PC systems evaluated. After fifty cycles of activation and deactivation the difference in colourability values was still within the experimental deviation for this measurement. Fatigue resistance was evaluated after exposing PC films to cycles of UV irradiation of four hours each. Triplicate analysis of each sample gave results that were adequately reproducible to be able to draw conclusions regarding fatigue resistance from the linear fit data imposed on it. Colourability data of the two PC dyes at a concentration of 1% on polymer solids was evaluated for conformance to the Beer-Lambert Law. Data of samples with a film thickness variation of less than 4µm across the sample complied with the law.

In conclusion, drawdown of the miniemulsions with a cubic bar was established as the best means of sample preparation. Activation via a UV LED and thermal deactivation or forced deactivation using a tungsten lamp and filter was established as the appropriate technique to determine the properties of the PC compounds. Reproducibility of colourability data and the linear fits plotted to fatigue resistance data had a maximum standard deviation of below 10%.

5.2.3 Objective 3

A DOE was applied to a standard BMA miniemulsion formulation to establish a stable product. Three factors that play important roles in stability and polymerisation rate of the miniemulsion, namely TSC, concentration of surfactant and concentration of initiator, were evaluated. An increase in PS was observed as the TSC increased. The PS decreased with an increase in surfactant concentration. These results were in agreement with literature reports on miniemulsion systems. Conversion rates were higher for reactions with higher TSC and higher concentrations of surfactant. A minimum concentration of 0.36% AIBN was required to avoid long inhibition periods.

The identified formulation (30%BMA, 1% SDS and 0.36%AIBN) satisfied objective three to establish a stable miniemulsion formulation suitable for entrapment of PC dyes.

5.2.4 Objective 4

During the polymerisation reactions whereby the PC dyes were entrapped, activation of the dyes was evident from the colour of the solutions. Upon irradiating the samples with the activation light source, much higher colour intensities were observed. This suggested that only a small fraction of PC dye was permanently in the activated (open) form. The PS of the miniemulsions and the half-lives of the corresponding films of these samples decreased with an increase in the concentration of the entrapped PC dye. Colourability and fatigue resistance also increased. The higher mobility of the samples with a higher concentration of PC dye corresponded with shorter half-lives. The PP dye showed higher colour intensity at 0.5% w/w than the PT dye at 1.27% w/w; however the PT dye showed similar fatigue resistance at 1.27% w/w to the PP dye at 2% w/w. The PT dye could be pre-encapsulated, which enhanced its UV resistance.

Objective four was therefore successfully achieved by entrapping the selected PC dyes into the identified miniemulsion, and the PC properties of films prepared from the samples were evaluated.

5.2.5 Objective 5

The PS of the BMA miniemulsion increased from 92nm to 96 nm with the entrapment of the HALS stabiliser (Tinuvin 292). With an increase in Tinuvin 292 (2%) and PC dye (1%) concentrations the PS decreased to 90nm. The half-life of a BMA miniemulsion with 1% PP dye was approximately 28s, which decreased to about 20s with the incorporation of 2% Tinuvin 292. During polymerisation, the inclusion of Tinuvin 292 did not change the reaction kinetics. It is therefore considered to be active to protect the PC dyes from UV degradation although it has a thermal history. At the concentrations of Tinuvin 292 incorporated into the miniemulsion formulations (0.5–2% volume on polymer volume) no significant improvement in fatigue resistance was observed. At a concentration of 2% fatigue took slightly longer to commence (at about 16hr QUV irradiation), but after commencement reached similar half-lives (about 24hr QUV irradiation) as in the cases of lower concentrations.

Thus objective five, to investigate the use of light stabilising additives in the miniemulsions with PC compounds to improve the fatigue resistance of the dyes, was achieved with limited success. A minimum improvement in fatigue resistance with the incorporation of Tinuvin 292 at 0.5–2% was established.

5.2.6 Objective 6

When comparing results of the miniemulsion systems to results of conventional solution polymer samples, a significant improvement in fatigue resistance was observed. This can be ascribed to the higher MW and broader MWD polymer present in miniemulsion samples compared to solution polymer samples. The polymer chains produced using miniemulsion polymerisation are less mobile than the polymer chains produced via solution polymerisation and thus allow fewer interactions of molecules due to steric hindrance – in effect protecting the dyes from degradation. The miniemulsion systems also allow compatibility with aqueous systems, unlike the conventional solution polymer samples which can only be used in solvent based systems. The improved fatigue resistance was not accompanied by poorer colourability.

In the final conclusion to objective six, entrapment of PC dyes in the BMA miniemulsion gave much improved fatigue resistance over conventional dispersion of the dye into a solution polymer. However, the results of the incorporation of the HALS (Tinuvin 292) in the

conventional solution polymer system were more pronounced, in terms of improving the fatigue resistance of PC films, which could be attributed to it not having a thermal history.

5.3 Recommendations

This study proved the concept of improving fatigue resistance of PC dyes by entrapment in a miniemulsion. There are however some aspects that can be further investigated or improved on.

In the measurement technique of evaluating PC properties, forced activation and deactivation can be achieved by using a custom built instrument. Activation and deactivation can be made automatic to remove the necessity for human intervention. Using customised instrumentation, faster cyclisation measurements can be performed to evaluate the effect of hundreds of cycles rather than the fifty cycles that was feasible with the set-up used in this study.

In this study only one monomer and UV stabiliser combination was investigated. It is possible that different monomers or combinations of monomers could provide higher colourability with improved fatigue resistance. Higher levels of the selected UV stabiliser as well as the addition of other additives to prevent degradation are well worth investigating. Initial evaluations of the newly synthesised smart nanoparticles were only performed on the films of the miniemulsion systems alone. Further investigation into the compatibility of these miniemulsions, or miniemulsions with different chemical compositions, with conventional waterbased coating systems could be pursued. The effect of the different components in the coating system, such as pigments and extenders, should be evaluated to optimise a smart coating with the most desirable properties in terms of colour intensity and fatigue resistance.

An illustration of how efficiently the photochromic miniemulsion actually works.

Before exposure to sunshine

After exposure to sunshine
(a sunny spot indoors)

and it deactivates within a few minutes.

Appendix A

Film uniformities

Table A.1. Film thicknesses of spin-coated samples

Sample and spin coating rate	Position of cut on glass slide and film thickness measurements in nm		
18% TSC; 2000rpm	Top	Middle	Bottom
	316.7	501.6	437.1
	310.4	688.7	417.3
	312	580	501
	300	626.7	460.5
	343.4	532.3	470.5
	331.3	730.9	506.2
	319.1	703.2	509.5
	321.4	534.1	448.9
	328.4	490.1	528.4
	337	447.1	448.1
18% TSC; 4000rpm	Top	Middle	Bottom
	151.9	607.6	264.4
	144.7	652.2	277
	122.6	820.7	294.5
	166.7	785.1	272.2
	128.6	607.7	271
	126.5	444.6	269.1
	139.2	645	290.2
	161.3	469.3	289.5
	141.4	541	286.7
	138.6	646.2	265.9
18% TSC; 6000rpm	Top	Middle	Bottom
	231.7	442.4	221.9
	346.5	440.6	279.6
	210.1	473.9	301
	231.8	517.6	255.3
	306.1	439.1	252.5
	217.3	356.3	290.4
	265.4	399.3	272.3
	316	377.4	231
	143.8	431.4	312.4
	132.2	458.5	325.9

Table A.2. Film thickness and uniformity measurements of Exp 19 prepared with film applicators of different sizes

Film applicator gap size	Mean	Min	Max	Max-Min
60µm				
A	15	11	17	6
B	13	11	14	3
C	12	11	13	2
D	14	11	16	5
E	14	11	18	7
F	10	10	11	1
75µm				
A	19	17	20	3
B	15	14	17	3
C	16	15	17	2
D	16	15	17	2
E	15	13	16	3
F	18	17	18	1
G	20	19	21	2
H	18	18	19	1
I	19	18	20	2
J	20	18	22	4
K	20	19	23	4
100µm				
A	18	12	23	11
B	18	17	19	2
C	18	17	19	2
D	19	18	20	2
E	18	16	20	4
F	24	21	27	6
125µm				
A	26	25	26	1
B	29	28	30	2
C	32	31	33	2

Appendix B

Experimental formulations

Table B.1. Experimental formulations for Exp 1–Exp 8

	TSC variation					SDS content variation			
Formulation	**Exp 1**	**Exp 2***	**Exp 3a***	**Exp 3b**	**Exp 4**	**Exp 5**	**Exp 6***	**Exp 7**	**Exp 8**
AIBN	0.5400	0.5400	0.5400	0.5752	0.5499	0.5436	0.5400	0.5426	0.5440
n-BMA	66.0374	52.0000	45.0000	45.6510	22.5452	45.0163	45.0000	45.0223	45.2689
Hexadecane	0.6390	0.6200	0.6200	0.7090	0.6637	0.6646	0.6200	0.6305	0.6234
SDS	1.5041	1.5000	1.5000	1.5000	1.5048	0.3848	0.7500	2.2617	3.0504
Water[#]	87.34	94.84	102.34	102.34	124.83	103.92	103.08	101.55	100.84
Total (g)	156.06	150.00	150.00	150.78	150.09	150.53	150.00	150.01	150.33

*Note: Actual experimental mass used not recorded, only theoretical formulations.

[#]Note: The water was weighed out on a two decimal balance (not the four decimal balance).

Table B.2. Experimental formulations for Exp 9–Exp 16

	TSC/SDS variation				AIBN variation			
Formulation	**Exp 9**	**Exp 10**	**Exp 11**	**Exp 12**	**Exp 13**	**Exp 14**	**Exp 15**	**Exp 16**
AIBN	0.5454	0.5467	0.5466	0.5492	0.9737	0.7576	0.3338	0.1270
n-BMA	22.5204	22.0388	60.0204	60.4536	45.0914	45.1513	45.4739	45.0448
Hexadecane	0.6768	0.6427	0.6326	0.6371	0.6758	0.6344	0.6452	0.7272
SDS	0.3833	3.0014	0.4035	3.0080	1.5418	1.5040	1.5243	1.5150
Water	126.41	123.54	89.61	86.11	102.31	102.71	102.96	103.03
Total (g)	150.54	149.77	151.21	150.76	150.59	150.76	150.94	150.44

Table B.3. Experimental formulations for Exp 17–Exp 26

	Incorporation of PC dye at increasing levels				Incorporation of HALS without PC dye			Incorporation of HALS with PC dye		
Formulation	**Exp 17***	**Exp 18**	**Exp 19**	**Exp 20***	**Exp21**	**Exp22**	**Exp23**	**Exp24**	**Exp25**	**Exp26**
AIBN	0.3586	0.3659	0.3662	0.3600	0.3647	0.3651	0.3695	0.3610	0.3714	0.3645
n-BMA	29.886	30.0689	30.0022	30.0000	30.0624	29.7276	30.0767	30.0382	30.0533	29.3724
Tinuvin 292					0.1826	0.3445	0.6642	0.1781	0.3376	0.6722
PC dye[#]	0.3786	0.1572	0.3042	0.6000				0.3024	0.3016	0.2955
Hexadecane	0.4118	0.4385	0.4200	0.4200	0.4300	0.4255	0.4550	0.4558	0.4325	0.4483
SDS	0.9962	1.0087	1.0067	1.0000	1.0139	1.0127	1.0338	1.0119	1.0281	1.0219
Water	67.96	68.61	68.51	68.22	68.91	68.28	68.92	68.69	68.66	68.32
Total (g)	100.00	100.65	100.61	100.00	100.96	100.16	101.52	101.04	101.18	100.49

*Note: Actual experimental mass used not recorded only theoretical formulations.

[#] Note: For Exp 17 the PC dye is Photosol 7-106 and for all the other formulations the PC dye is Reversacol Palatinate Purple

Table B.4. Experimental formulations for Exp 27–Exp 30

Formulation	**Bulk BMA solution polymer***	**Exp27**	**Exp28**	**Exp29**	**Exp30**
AIBN	0.0541	0.0325	0.0091	0.0089	0.0055
n-BMA	45.0950	27.1150	7.5952	7.4536	4.5651
Tinuvin 292			0.0378	0.0754	0.0932
PHOTO		0.2670	0.0748	0.0734	0.0449
THF	105.10	63.20	17.70	17.37	10.64
Total (g)	150.25	90.61	25.42	24.98	15.35

*Note: A bulk sample of a BMA solution polymer was made to which Reversacol Palatinate purple was added to prepare Exp 27. Exp 27 was split into three and different amounts of Tinuvin 292 were incorporated for Exp 28–Exp 30. This ensured that all samples had 0.98% w/w PC dye on polymer solids. The level of Tinuvin 292 varied from 0.45; 0.92 to 1.85% v/v on polymer solids for Exp 28–Exp 30, respectively.

Appendix C

Fatigue kinetics

Table C.1. Exp 17–Exp 20: Absorbance values of fatigue resistance

Sample no.	Fatigue kinetics (Absorbance at … hr QUV exposure)										
	0	4	8	12	16	20	24	28	32	36	40
Photosol 7-106											
Exp 17											
B	0.2168	0.1890	0.1810	0.1735	0.1752	0.1541	0.1328	0.1125	0.0847	-	-
C	0.2028	0.1855	0.1740	0.1698	0.1660	0.1365	0.1216	0.1086	0.0873	-	-
D	0.2225	0.1951	0.2015	0.1880	0.1666	0.1506	0.1281	0.1128	0.0921	-	-
Reversacol Palatinate Purple											
Exp 18											
A	0.2835	0.2342	0.1873	0.0894	0.0183	0.2835	-	-	-	-	-
B	0.2769	0.2166	0.1655	0.0735	0.0190	0.2769	-	-	-	-	-
E	0.2746	0.2368	0.1899	0.0908	0.0194	0.2746	-	-	-	-	-
Exp 19											
A	0.5232	0.4633	0.4577	0.3875	0.3264	0.2638	0.1420	-	-	-	-
D	0.4451	0.4246	0.3758	0.3375	0.2612	0.2380	0.1151	-	-	-	-
E	0.4783	0.4562	0.4361	0.3977	0.2952	0.2021	0.0885	-	-	-	-
Exp 20											
A	0.5993	0.5347	0.5445	0.5625	0.5264	0.5091	0.4471	0.3972	x	x	x
C	0.6396	0.6164	0.6088	0.6488	0.5513	0.5009	0.4647	0.4302	0.3724	0.3302	0.2076
E	0.6566	0.6191	0.6095	0.6675	0.5706	0.5440	0.4798	0.4953	0.3904	0.3307	0.1952

Table C.2. Exp 17–Exp 20: Normalised fatigue resistance data

Sample no.	Fatigue kinetics (Absorbance normalised against 0hr QUV exposure)										
	0	**4**	**8**	**12**	**16**	**20**	**24**	**28**	**32**	**36**	**40**
Photosol 7-106											
Exp 17											
B	100	87.1771	83.4871	80.0277	80.8118	71.0793	61.2546	51.8911	39.0683	-	-
C	100	89.0970	83.5735	81.5562	79.7310	65.5620	58.4054	52.1614	41.9308	-	-
D	100	87.6854	90.5618	84.4944	74.8764	67.6854	57.5730	50.6966	41.3933	-	-
Reversacol Palatinate Purple											
Exp 18											
A	100	86.9632	71.8405	57.4540	27.4233	5.6135	-	-	-	-	-
B	100	91.9018	71.8885	54.9286	24.3943	6.3060	-	-	-	-	-
E	100	82.7607	71.3683	57.2333	27.3659	5.8469	-	-	-	-	-
Exp 19											
A	100	88.5512	87.4809	74.0635	62.3853	50.4205	27.1407				
D	100	95.3943	84.4305	75.8257	58.6834	53.4711	25.8594				
E	100	95.3795	91.1771	83.1487	61.7186	42.2538	18.5030				
Exp 20											
A	100	89.2208	90.8560	93.8595	87.8358	84.9491	74.6037	66.2773	x	x	x
C	100	96.3727	95.1845	101.4384	86.1945	78.3146	72.6548	67.2608	58.2239	51.6260	32.4578
E	100	94.2888	92.8267	101.6601	86.9022	82.8511	73.0734	75.4341	59.4578	50.3655	29.7289

x Note: After 32hr QUV the film broke and the data set could not be completed. Reproducibility on the duplicate set films was good enough to draw correlations from.

Table C.3. Exp 24–Exp 26: Absorbance values of fatigue resistance

Sample no.	Fatigue kinetics (Absorbance at … hr QUV exposure)								
	0	4	8	12	16	20	24	28	32
Exp 24									
A	0.4324	0.4379	0.3699	0.3440	0.3272	0.2950	0.2377	-	0.1087
B	0.4744	0.4660	0.4006	0.3894	0.3435	0.3011	0.2582	-	0.1077
D	0.3796	0.4239	0.3833	-	0.2983	0.2319	0.1468	0.0530	-
Exp 25									
C	0.4858	0.4501	0.4650	0.4205	0.3476	0.3436	0.2441	0.2075	-
D	0.4456	0.4405	0.4198	0.3591	0.3066	0.2958	0.1925	0.1420	-
E	0.4474	0.4008	0.3840	0.3386	0.3302	0.3133	0.2456	0.2025	-
Exp 26									
C	0.3118	0.3053	0.2996	0.2896	0.2796	0.2165	0.1568	-	0.0527
D	0.2830	0.2824	0.2788	0.2767	0.2676	0.2004	0.1553	-	0.0341
E	0.3254	0.2777	0.3037	0.2616	0.2495	0.1973	x	x	x

Table C.4. Exp 24–Exp 26: Normalised fatigue resistance data

Sample no.	Fatigue kinetics (Absorbance normalised against 0hr QUV exposure)								
	0	4	8	12	16	20	24	28	32
Exp 24									
A	100	101.2720	85.5458	79.5560	75.6707	68.2239	54.9689	-	25.1454
B	100	98.2293	84.4435	82.0826	72.4073	63.4630	54.4266	-	22.7024
D	100	111.6702	100.9747	-	78.5827	61.0906	38.6723	13.9621	-
Exp 25									
C	100	92.6513	95.7184	86.5583	71.5521	70.7287	50.2470	42.7131	-
D	100	98.8555	94.2101	80.5880	68.8061	66.3824	43.2002	31.8671	-
E	100	89.5843	85.8292	75.6817	73.8042	70.0268	54.8949	45.2615	-
Exp 26									
C	100	97.9153	96.0872	92.8801	89.6729	69.4355	50.3035	-	16.8856
D	100	99.7880	98.5160	97.7739	94.5580	70.8127	54.8666	-	12.0495
E	100	85.3411	93.3313	80.3934	76.6749	60.6331	x	x	x

x Note: After 32hr QUV the film was exposed to continuous irradiation and could not be used for further measurements. Reproducibility on the duplicate set films was good enough to draw correlations from.

Table C.5. Exp 27–Exp 30: Absorbance values of fatigue resistance

Sample no.	Fatigue kinetics (Absorbance at … hr QUV exposure)							
	0	4	8	12	16	20	24	28
Exp 27								
A	0.4178	0.3358	0.2807	0.1258	0.0394	-	-	-
B	0.4160	0.3475	0.2824	0.1673	0.0464	-	-	-
E	0.4164	0.3550	0.2716	0.1266	0.0411	-	-	-
Exp 28								
C	0.4104	0.3780	0.3579	0.2682	0.2119	0.1484	-	-
D	0.3753	0.3797	0.3376	0.2685	0.2112	0.1423	-	-
E	0.4002	0.3607	0.3490	0.2605	0.1983	0.1297	-	-
Exp 29								
C	0.4277	0.3545	0.3186	0.2805	0.2312	0.1834	0.1066	-
D	0.4156	0.3627	0.3236	0.2656	0.2409	0.1858	0.1175	-
E	0.4017	0.3931	0.3440	0.2928	0.2245	0.1866	0.1141	-
Exp 30								
B	0.4101	0.3914	0.3340	0.3018	0.2801	0.2188	0.1807	0.1338
D	0.3837	0.3591	0.3463	0.2934	0.2478	0.1929	0.1514	0.1180
E	0.4397	0.3802	0.3678	0.3123	0.2944	0.2246	0.1898	0.1508

Table C.6. Exp 27–Exp 30: Normalised fatigue resistance data

Sample no.	Fatigue kinetics (Absorbance normalised against 0hr QUV exposure)							
	0	4	8	12	16	20	24	28
Exp 27								
A	100	80.3734	67.1852	30.1101	9.4304	-	-	-
B	100	83.5337	67.8846	40.2164	11.1539	-	-	-
E	100	85.3365	65.2885	30.4327	9.8798	-	-	-
Exp 28								
C	100	92.1053	87.2076	65.3509	51.6326	36.1598	-	-
D	100	101.1724	89.9547	71.5428	56.2750	37.9163	-	-
E	100	90.1299	87.2064	65.0925	49.5502	32.4088	-	-
Exp 29								
C	100	82.8852	74.4915	65.5833	54.0566	42.8805	24.9240	-
D	100	87.2714	77.8633	63.9076	57.9644	44.7065	28.2724	-
E	100	97.8591	85.6361	72.8902	55.8875	46.4526	28.4043	-
Exp 30								
B	100	95.4401	81.4436	73.5918	68.3004	53.3528	44.0624	32.6262
D	100	93.5887	90.2528	76.4660	64.5817	50.2737	39.4579	30.7532
E	100	86.4681	83.6479	71.0257	66.9547	51.0803	43.1658	34.2961